UNIVERSIDADE DE COIMBRA

FACULDADE DE CIÊNCIAS E TECNOLOGIA

Regulation of the Ras Pathway by Neurofibromin in Dendritic Spines

Regulação da Via de Sinalização Ras pela Neurofibromina em Espículas Dendríticas

Ana Isabel Ferreira Martins de Oliveira

DOUTORAMENTO EM BIOLOGIA

(BIOLOGIA CELULAR)

2011

Dissertação apresentada à Faculdade de Ciências
e Tecnologia da Universidade de Coimbra para
prestação de provas de Doutoramento em Biologia,
na especialidade de Biologia Celular

Principal Advisor: Prof. Ryohei Yasuda
(Duke University Medical Center, Durham, U.S.A.)

Co-Advisor: Prof. Carlos B. Duarte
(Universidade de Coimbra, Coimbra, Portugal)

Ana Isabel Ferreira Martins de Oliveira
2011

Ao meu tio Vitorino

Acknowledgements

I completed this work under the guidance of Dr. Ryohei Yasuda, my supervisor. I am very grateful for his support, encouragement, guidance, training and patience with my project and me.

I am especially grateful to my co-supervisor, Dr. Carlos Duarte, who patiently and promptly answered my emails and questions and advised me throughout my project, in an extremely helpful, kind and generous manner. Also, thank you for being the person who first attracted me to do research and who gave me my first chance to rotate in biomedical research labs. More importantly, thank you for the immense motivation to do science and for the extremely valuable Neurobiology classes during College.

Thanks to all the Yasuda lab members, past and present (Jui-Yun Chang, Wei Leong Chew, Lesley Colgan, Yasmin Escobedo-Lozoya, Nathan Hedrick, Elizabeth Johnson, Rishabh Kasliwal, David Kloetzer, Seok-Jin Lee, Hideji Murakoshi, Jun Nishiyama, Michael Patterson, Rohit Ramnath, Mikihiro Shibata, Takashi Sugawara, Erzsebet Szatmari, Airong Wan, Hong Wang, Jie Wang, Shenyu Zhai and Tony Zimmermann), who provided assistance, guidance and support in my daily work environment. Thanks to the permanent technical assistance of Airong Wang.

Special thanks to Dr. Anne West and Kelli McDowell for valuable technical advice and their infinite friendship and patience.

I also would like to thank my invaluable friends Helena Coelho, João Duarte, Ester Gaya, Tim Hanson, Dush Jayawickreme, John Kim, Ioanna Manopoulou, Lisa Pokorny, Oliver Ratmann, Mariana Ricca, Carl Rothfels, and Ana Sousa for their permanent presence, support and dedicated friendship along my project.

I would like to thank to several members of my family. I am extremely grateful to my parents António Oliveira and Isabel Ferreira for their constant encouragement and support along the journey. Thank you also to my uncle Vitorino Oliveira for his infinite encouragement and friendship. And thank you to other members of the family, too, namely tia Lúzia and avô Vitorino, who always supported me.

Finally, I am very grateful to the Doctoral Program in Experimental Biology and Biomedicine, organized by the Center for Neuroscience and Cell Biology in Coimbra, Portugal, for the great opportunity of being a student in the Program. I would also like to thank the other students of 2004 for the excellent intellectual and social environment they provided.

Este trabalho foi financiado através de uma Bolsa de Doutoramento (SFRH / BD / 15226 / 2004) concedida à autora deste, pela Fundação para a Ciência e a Tecnologia, entre 2004 e 2008. O presente trabalho foi também co-financiado pela União Europeia através do POCI – Programa Operacional Ciência e Inovação 2010 e do FSE – Fundo Social Europeu.

FCT Fundação para a Ciência e a Tecnologia
MINISTÉRIO DA EDUCAÇÃO E CIÊNCIA

Ciência.Inovação 2010 Programa Operacional Ciência e Inovação 2010
MINISTÉRIO DA CIÊNCIA, TECNOLOGIA E ENSINO SUPERIOR

FUNDO SOCIAL EUROPEU

This work was also funded by a predoctoral Young Investigator Award (YIA # 2009-01-014) granted to the author of this dissertation by the Children's Tumor Foundation, between 2009 and 2011.

Table of Contents

Abbreviations

AC	adenylate cyclase
ACSF	artificial cerebrospinal fluid
AMPAR	α-amino-3-hydroxy-5-methyl-4-isoxazole-propionic acid receptor
ANOVA	analysis of variance
AP5	2-amino-5-phosphonopentanoate
BDNF	brain-derived neurotrophic factor
BLA	basolateral amygdala
BTK	Bruton tyrosine kinase
CA	constitutively active
CA1	Cornu Ammonis 1
Ca^{2+}	calcium
CA3	Cornu Ammonis 3
CalDAG-GEF2	Ca^{2+} and diacylglycerol-regulated GEF2
CaM	calmodulin
CaMKII	Ca^{2+}/Calmodulin-dependent kinase II
cAMP	cyclic adenosine monophosphate
CAPRI	Ca^{2+}-promoted Ras inactivator
CASK	calcium/calmodulin-dependent serine protein kinase
cDNA	complementary deoxyribonucleic acid
CMV	cytomegalovirus
CNS	central nervous system
CRE	cAMP response element
CREB	cAMP response element-binding protein
Cs	cesium
CSRD	cysteine-serine rich domain
DG	dentate gyrus
DIV	days in vitro
DMEM	Dubelco's modified eagle medium
DN	dominant negative
DPT	days post-transfection
DRK	downstream of receptor kinase
EGF	epidermal growth factor
EGTA	ethylene glycol tetraacetic acid
ER	endoplasmic reticulum

ERK	extracellular-signal regulated kinase
FBS	fetal bovine serum
FLIM	fluorescence lifetime imaging microscopy
FRET	fluorescence resonance energy transfer
FTase	farnesyltransferase
FXS	Fragile X syndrome
GABA	gamma-aminobutyric acid
GAP	guanosine nucleotide activating protein
GDP	guanosine diphosphate
GEF	guanosine nucleotide exchange factor
GFAP	glial fibrillary acidic protein
GPCRs	G-protein coupled receptors
GRD	GAP-related domain
GTP	guanosine triphosphate
HFS	high frequency stimulation
HRP	horseradish peroxidase
HVR	hypervariable domain
IEGs	immediate early genes
KSR	kinase suppressor of Ras
lcmt	isoprenylcysteine carboxyl methyltransferase
l-DOPA	L-3,4-dihydroxyphenylalanine
LFS	low frequency stimulation
LSD	least significant difference
LTD	long-term depression
LTM	long-term memory
LTP	long-term potentiation
MAPK	mitogen-activated protein kinase
mEGFP	monomeric enhanced green fluorescent protein
MEK	mitogen-activated protein kinase kinase
mEPSC	miniature excitatory postsynaptic current
Mg^{2+}	magnesium
mGluR	metabotropic glutamate receptor
MNI-L-glutamate	4-methoxy-7-nitroindolinyl-caged-L-glutamate
MPNSTs	malignant peripheral-nerve sheath tumors
mRFP	monomeric red fluorescent protein
mTOR	mammalian target of rapamycin
mTORC	mammalian target of rapamycin complex

NA	numerical aperture
Na^+	sodium
NBQX	2,3-dihydroxy-6-nitro-7-sulfamoyl-benzo[f]quinoxaline-2,3-dione
NF1	Neurofibromatosis Type I
NLS	nuclear localization sequence
NMDAR	N-methyl D-aspartate receptor
PCR	polymerase chain reaction
PH	pleckstrin homology
PI3K	phosphatidylinositol 3-kinase
PIP2	phosphatidylinositol (4,5)-biphosphate
PIP3	phosphatidylinositol (3,4,5)-triphosphate
PKA	protein kinase A
PKC	protein kinase C
PKMζ	protein kinase M zeta
PMT	photomultiplier tube
PNS	peripheral nervous system
PP1	protein phosphatase 1
PPF	paired-pulse facilitation
PSD	postsynaptic density
PSD95	postsynaptic density protein 95
PTX	picrotoxin
PVDF	polyvinylidene fluoride
RBD	Ras binding domain
RPT	palmitoyltransferase
RSKs	ribosomal S6 kinases
RTKs	receptor tyrosine kinases
Ser	serine
SH2	Src homology 2
Shank3	SH3 and multiple ankyrin repeat domains 3
shRNA	short hairpin RNA
siRNA	small interfering RNA
Sos	son of sevenless
SRE	serum response element
STDP	spike timing dependent plasticity
SVs	synaptic vesicles
SynGAP	synaptic Ras GTPase activating protein
TBS	theta burst stimulation

Thr	threonine
TPA	12-O-tetradecanoyl-phorbol-13-acetate
TPFLIM	two-photon fluorescence lifetime imaging
TPLSM	two-photon laser scanning microscope
TTX	tetrodotoxin
uEPSC	uncaging-evoked excitatory postsynaptic current
VGCC	voltage-gated calcium channel
WT	wild type

Resumo

Diversas evidências experimentais têm sugerido que a plasticidade sináptica desempenha um papel importante na formação de memórias e na aprendizagem. A via de sinalização da Ras é um elemento importante em muitas formas de plasticidade sináptica, incluindo a potenciação sináptica de longa duração (LTP) e a morfogénese das espículas dendríticas. Em consonância com a função da Ras na plasticidade sináptica, muitas doenças mentais que causam défices de aprendizagem estão associadas com o funcionamento anormal desta via de sinalização. A Neurofibromatose Tipo I (NF1) é uma dessas doenças, sendo causada por mutações que resultam na perda de função do gene *Nf1*, que codifica a neurofibromina, uma proteína inactivadora da Ras. Entre outros sintomas, 40 a 60% dos pacientes têm problemas de aprendizagem e memória. Apesar de já ter sido demonstrado que a neurofibromina está presente nas espículas dendríticas dos neurónios do hipocampo, a função da neurofibromina nas espículas dendríticas ainda não está bem estudada.

Neste trabalho, investigámos o papel da neurofibromina na estabilidade de longa duração das espículas dendríticas, e a contribuição da Ras neste processo. A diminuição da expressão proteica da neurofibromina com “short-hairpin RNA” (NF1 shRNA) reduziu a densidade das espículas dendríticas nos neurónios piramidais da região CA1, em culturas organotípicas do hipocampo, sem perturbar outros aspectos da morfologia das espículas dendríticas. Este fenótipo resultou de um mecanismo dependente da sinalização pela Ras, uma vez que a co-expressão do domínio GAP (GRD; domínio inactivador da Ras) da neurofibromina juntamente com NF1 shRNA foi suficiente para restaurar a densidade normal de espículas dendríticas. Este fenótipo depende ainda da actividade neuronal, uma vez que não foi observada qualquer alteração na densidade das espículas quando a actividade neuronal foi suprimida nas preparações. O NF1 shRNA também diminuiu a frequência das “mini excitatory post-sinaptic currents” (mEPSCs), sugerindo que a neurofibromina é necessária para a manutenção da função normal das sinapses excitatórias.

A manutenção da densidade normal de espículas dendríticas depende também da existência de mecanismos de plasticidade estrutural. Para determinar se a neurofibromina é necessária para a

plasticidade estrutural das espículas dendríticas, analisámos o crescimento das espículas dendríticas associado com a LTP em neurónios onde a expressão proteica da neurofibromina foi reduzida com shRNA. Nestes ensaios, foi utilizada a estimulação "two-photon glutamate uncaging" numa única espícula dendrítica, um protocolo que induz um crescimento prolongado (~ 1 hora) das espículas dendríticas. Na presença do NF1 shRNA, este protocolo de estimulação induziu um efeito muito transitório no crescimento das espículas dendríticas. Este fenótipo foi abolido aquando da co-expressão do domínio GRD da neurofibromina, sugerindo a contribuição da sinalização pela Ras. A incubação da preparação com Mg^{2+} aboliu o fenótipo observado após a remoção de neurofibromina, indicando que o efeito desta proteína na plasticidade estrutural das espículas dendríticas é dependente da actividade neuronal.

Para investigar se a neurofibromina regula a actividade da Ras em espículas dendríticas durante a plasticidade estrutural, monitorizou-se a actividade da Ras em espículas dendríticas estimuladas de modo a exibirem plasticidade estrutural, e a actividade da neurofibromina foi manipulada usando NF1 shRNA. Nestes ensaios, a actividade da Ras foi medida utilizando a "fluorescence lifetime imaging" (FLIM) e a estimulação das espículas foi efectuada através de "two-photon glutamate uncaging". Observou-se que o declínio da activação da Ras foi muito mais lento em neurónios que expressavam NF1 shRNA. Pelo contrário, a sobre-expressão do domínio GRD da neurofibromina resultou num decréscimo da actividade basal da Ras, acompanhado por uma redução do pico da actividade durante a fase transitória da plasticidade estrutural, e acelerou a inactivação da Ras na resposta à estimulação de uma única espícula dendrítica. Estes resultados sugerem que a neurofibromina é uma das principais RasGAPs nas espículas dendríticas dos neurónios piramidais da região CA1 do hipocampo.

No seu conjunto, a menor densidade de espículas dendríticas, a redução da plasticidade estrutural e a activação persistente da Ras nos neurónios com baixos níveis de expressão proteica de neurofibromina sugerem que esta proteína desempenha um papel importante na região pós-sináptica no hipocampo. Estes resultados podem explicar, pelo menos em parte, os défices cognitivos observados nos pacientes com NF1 e no modelo animal de NF1, assim como a redução na plasticidade

sináptica observada no modelo animal de NF1. Além disso, o facto de os fenótipos observados nas espículas dendríticas serem abolidos quando a actividade da Ras é suprimida indica que a regulação rigorosa da via de sinalização da Ras é essencial para a estabilidade das espículas dendríticas e para a plasticidade estrutural, e poderá estar relacionada com o papel da neurofibromina na plasticidade sináptica, aprendizagem e memória. Por último, neste trabalho identificámos, pela primeira vez, uma proteína (neurofibromina) que actua como uma RasGAP nas espículas dendríticas e expandimos o conhecimento actual sobre a função da neurofibomina no cérebro.

Abstract

Synaptic plasticity is thought to underlie learning and memory formation. The Ras pathway plays critical roles in many forms of synaptic plasticity, including long-term potentiation (LTP) and morphogenesis of dendritic spines. Consistent with the important roles of Ras in synaptic plasticity, many mental diseases that cause learning deficits are associated with abnormal Ras signaling. Neurofibromatosis Type I (NF1) is one of such diseases, being caused by loss-of-function mutations of the *Nf1* gene, which encodes neurofibromin, a Ras inactivator protein. Among other symptoms, 40-60% of the patients show learning and memory disabilities. While it has been shown that neurofibromin is localized in dendritic spines of hippocampal neurons, the function of neurofibromin in dendritic spines is not well understood.

Here, we show that neurofibromin-dependent Ras regulation has an important role in the long-term stability of dendritic spines. We found that downregulation of neurofibromin by short-hairpin RNA (NF1 shRNA) decreased the density of dendritic spines in CA1 pyramidal neurons, in organotypic slice cultures of the hippocampus, leaving other aspects of spine morphology unaffected. This phenotype was Ras-dependent, since co-expression of the GAP-related domain (GRD; Ras inactivator domain) of neurofibromin together with NF1 shRNA was sufficient to restore the normal spine density. Additionally, this phenotype was activity-dependent: when neurons were cultured under suppressed neuronal activity, NF1 shRNA did not decrease the spine density. NF1 shRNA also decreased the frequency of mini excitatory postsynaptic currents (mEPSCs), suggesting that neurofibromin is required for the maintenance of normal function of excitatory synapses.

Normal spine structural plasticity is required to maintain spine density. To examine if neurofibromin is required for normal spine structural plasticity, we imaged spine enlargement associated with LTP in neurons in which neurofibromin was downregulated with shRNA. Previous studies showed that two-photon glutamate uncaging at single dendritic spines causes long-lasting (~ 1 hour) enlargement of dendritic spines. We found that dendritic spines of neurons expressing NF1 shRNA display a transient enlargement following stimulation, which decays rapidly. This phenotype was rescued

when co-expressing the GRD domain of neurofibromin, suggesting that it is a consequence of increased Ras signaling. Also, incubation with Mg^{2+} abolished the phenotype, indicating that the effects of neurofibromin on spine structural plasticity are activity-dependent.

To study whether neurofibromin regulates Ras activity in dendritic spines during spine structural plasticity, Ras activity was monitored in single dendritic spines undergoing structural plasticity in neurons in which neurofibromin activity was manipulated. Using a combination of fluorescence lifetime imaging (FLIM) and 2-photon glutamate uncaging, we observed that the decay of Ras activation was much slower in neurons expressing NF1 shRNA. In contrast, overexpression of GRD reduced the basal Ras activity, decreased the peak Ras activation during the transient phase of structural plasticity and accelerated Ras inactivation following single spine stimulation. Hence, these data suggest that neurofibromin is a major RasGAP in the dendritic spines of CA1 pyramidal neurons of the hippocampus.

Taken together, the observed lower spine density, impaired structural plasticity and persistent Ras activation in the dendritic spines of neurons with reduced neurofibromin expression levels provide strong evidence for a role of neurofibromin at postsynaptic sites in the hippocampus and may explain, at least in part, the cognitive deficits observed in NF1 patients and in the NF1 animal model, as well as the synaptic plasticity impairments in NF1 animal models. Moreover, the fact that the dendritic spine phenotypes observed here under low levels of neurofibromin expression are rescued when Ras activity is decreased indicates that a precise regulation of the Ras pathway is essential for proper structural plasticity and spine stability, which might explain, at least in part, the effect of neurofibromin-dependent regulation of the Ras pathway in synaptic plasticity, learning and memory. Lastly, we identified, for the first time, a protein (neurofibromin) that acts as a major RasGAP in dendritic spines and extended the current knowledge on the neurofibromin function in the brain.

CHAPTER I

General introduction

Chapter I. General introduction

Synaptic Plasticity in the Hippocampus

The adult human brain contains over 100 billion neurons, with each interconnected by thousands of synapses. Experiences can modify synapses, favoring some neuronal pathways and weakening others (Kessels and Malinow 2009). Synaptic plasticity can be defined by persistent changes in synaptic efficacy, namely long-term potentiation (LTP) and long-term depression (LTD), which are induced by specific temporal patterns of activity. LTP results from a persistent increase in the efficacy of synaptic transmission. In contrast, LTD arises from persistent reduction in synaptic strength. The strength of most excitatory synapses can be bidirectionally modified by activity, such that synapses express both LTP and LTD (Bliss, Collingridge et al. 2003). Here, we will focus on LTP.

Anatomy of the Hippocampus

The hippocampus is a brain structure localized to the temporal lobe, known to be crucial for spatial and associative learning and memory (Stubley-Weatherly, Harding et al. 1996; Sziklas, Lebel et al. 1998). It has an organized structure composed of several functionally distinct subareas, namely the dentate gyrus (DG), Cornu Ammonis 3 (CA3), Cornu Ammonis 1 (CA1) and subiculum (**Figure 1.1**) (Lopes da Silva and Arnolds 1978; Kerchner and Nicoll 2008). The hippocampus receives input from the entorhinal cortex (Heinemann, Schmitz et al. 2000), which forms direct connections with granule neurons of the dentate gyrus and pyramidal neurons in CA3 via the perforant path (**Figure 1.1.**) (Hjorth-Simonsen 1972; Lopes da Silva and Arnolds 1978). From the dentate gyrus, granule cells relay information onto CA3 pyramidal neurons via the mossy fiber pathway (Gaarskjaer 1978). The axons of CA3 pyramidal neurons project to ipsilateral and contralateral CA1 pyramidal neurons through the Schaffer collateral and

the associational commissural pathway, respectively (**Figure 1.1.**). Besides the CA3 region, CA1 neurons also receive input from the entorhinal cortex via the perforant path (Hjorth-Simonsen and Jeune 1972). The axons of CA1 pyramidal neurons project to the entorhinal cortex, completing the loop, or to the subiculum. From here on, we will primarily focus on CA1 pyramidal neurons, where our research was performed.

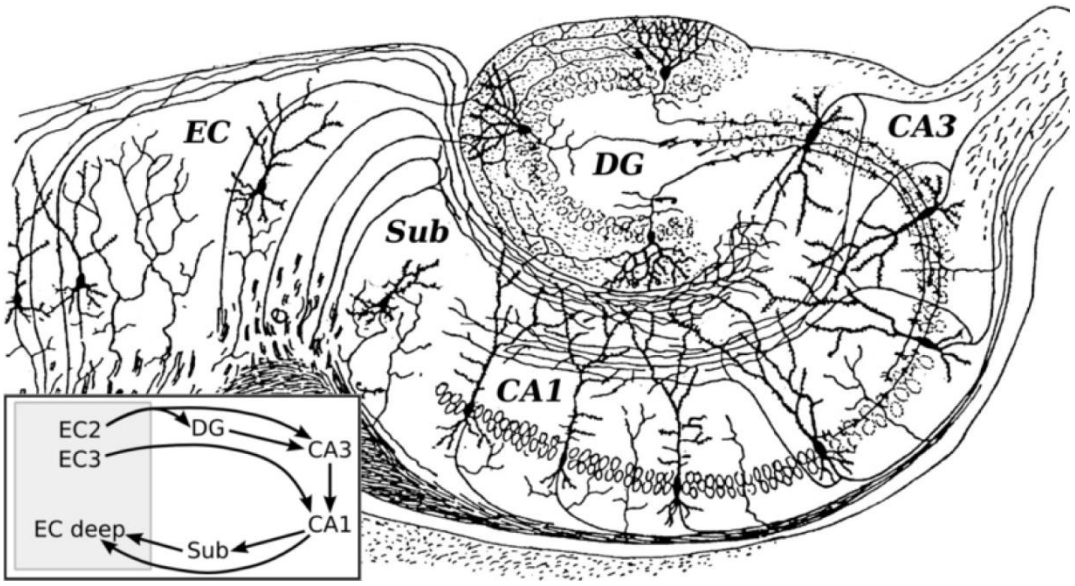

Figure 1.1. Diagram of the hippocampus viewed in the sagittal plane. EC, enthorhinal cortex; DG, dentate gyrus; CA3, Cornu Ammonis 3; CA1, Cornu Ammonis 1; Sub, Subiculum. *Adapted from Kerchner and Nicoll 2008.*

CA1 Pyramidal Neurons Morphology

CA1 pyramidal neurons are composed of a cell soma, one axon, basal dendrites and apical dendrites (**Figure 1.2.**). They are polarized cells covered with about ~10,000 dendritic spines (Kennedy, Beale et al. 2005; Sheng and Hoogenraad 2007). Most of the dendritic spines receive excitatory synaptic input. The soma and the first 100μm of apical dendrite are almost completely devoid of dendritic spines. The next 150μm of apical dendrite has a very low spine density, but the final 150μm of apical dendrite has a very high spine density.

In the present work, we use CA1 pyramidal neurons to address the postsynaptic function of neurofibromin, a protein that has been documented to participate in learning, memory, and in LTP in the Schaffer collateral pathway, whose postsynaptic elements reside on CA1 pyramidal neurons, mostly in dendritic spines.

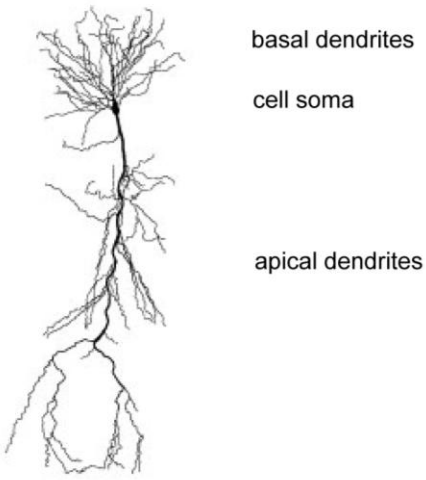

Figure 1.2. Schematic representation of the morphology of a CA1 pyramidal neuron. *Adapted from Spruston 2008.*

LTP

LTP is a fundamental property of the majority of excitatory synapses in the mammalian brain. The fact that LTP can be most reliably generated in brain regions involved in learning and memory is often used as an evidence for its functional relevance in cognitive processes. Particularly, in the hippocampus, LTP is the leading experimental model for learning and memory (Bliss and Collingridge 1993; Malenka and Nicoll 1999).

Coordinated activity of the presynaptic terminal and the postsynaptic cell can increase the synaptic strength (Hebbian plasticity). Activity can also modify the properties of synaptic plasticity *per se* (metaplasticity). Here, we will focus on Hebbian plasticity.

Several forms of LTP have been described based on the specific type of synapse (and brain area) and the induction paradigm. LTP has been best studied at the Schaffer collateral pathway of the hippocampus. Here, we will focus on this particular form of synaptic plasticity.

LTP Induction

During normal synaptic transmission glutamate is released from the presynaptic bouton and acts on both AMPA receptors (AMPARs) and NMDA receptors (NMDARs), though it activates only AMPARs. At resting potentials, the NMDA ion channel is blocked by the binding of extracellular Mg^{2+} in the ion pore (Herron, Lester et al. 1985). This block is released when the postsynaptic membrane is strongly depolarized (**Figure 1.3.**) (Herron, Lester et al. 1985). Thus, NMDARs act as coincidence detectors for presynaptic activity (glutamate release) and postsynaptic activity (depolarization).

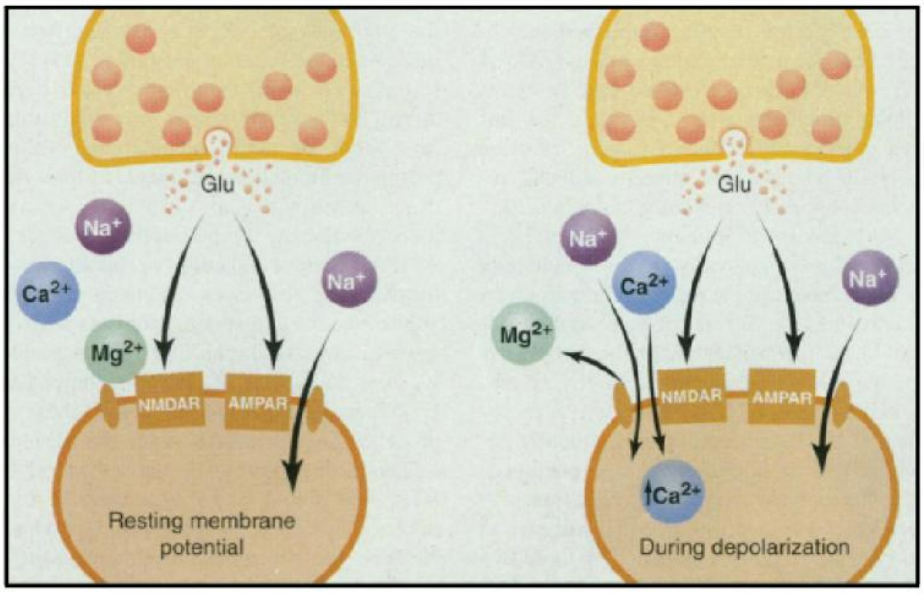

Figure 1.3. Model for the induction of LTP. During normal synaptic transmission, glutamate is released from the presynaptic bouton and acts on both AMPARs and NMDARs. However, Na^+ flows only through the AMPAR, but not the NMDAR, because Mg^{2+} blocks the channel of the NMDAR. Depolarization of the postsynaptic cell relieves the Mg^{2+} block of the NMDAR channel, allowing Na^+ and Ca^{2+} to flow into the dendritic spine by means of the NMDAR. The resultant rise in Ca^{2+} within the dendritic spine is the critical trigger for LTP. *Adapted from Malenka and Nicoll 1999*.

At the Schaffer collateral pathway of the hippocampus, LTP induction requires synaptic activation of postsynaptic NMDARs (Malenka and Nicoll 1999). LTP can be induced by different patterns of neuronal activity, all requiring postsynaptic depolarization. For example, LTP can be induced by tetanic stimulation, a short-period of presynaptic high-frequency stimulation (HFS) (Bliss and Lomo 1973). Also, pairing postsynaptic depolarization with presynaptic low-frequency stimulation induces LTP. Alternatively, LTP can be induced by presynaptic stimulation followed within milliseconds by postsynaptic back-propagating action potentials (spike-timing dependent plasticity, STDP) (Markram, Lubke et al. 1997; Bi and Poo 1998). Theta burst stimulation (TBS), which is a more physiological stimulus consisting of axonal stimulation at frequencies and patterns comparable to those exhibited by hippocampal neurons in behaving animals (each burst 4 pulses at 100Hz spaced by 200ms intervals or less), also induces LTP (Douglas and Goddard 1975; Larson, Wong et al. 1986). Chemical LTP protocols, namely the brief application of glycine (a co-agonist of NMDARs), have also proved successful at inducing LTP (Park, Penick et al. 2004). More recently, the pairing of focal two-photon MNI-L-glutamate uncaging with either low Mg^{2+} concentration or postsynaptic depolarization caused spine enlargements and enhanced AMPAR-mediated synaptic currents or insertion (Matsuzaki, Honkura et al. 2004; Makino and Malinow 2009; Patterson, Szatmari et al. 2010). Although LTP is triggered within seconds, it can last for hours in *in vitro* preparations and days *in vivo* (Malenka and Nicoll 1999).

Following NMDAR activation, the consequent rise of intracellular Ca^{2+} is the critical trigger for LTP (Malenka and Nicoll 1999; Bredt and Nicoll 2003; Malenka and Bear 2004). Consistently, preventing Ca^{2+} rise in the postsynaptic cell with Ca^{2+} chelators blocks LTP induction (Lynch, Larson et al. 1983) and injection and photolysis of a caged Ca^{2+} chelator (which releases Ca^{2+}) in the postsynaptic cell is sufficient to mimic LTP (Malenka, Kauer et al. 1988). Also, Ca^{2+} imaging techniques have shown that tetanic stimulation elevates Ca^{2+} within dendrites and dendritic spines (Regehr and Tank 1990; Müller and Connor 1991). According to the "Ca^{2+} hypothesis", rapid and large influxes of Ca^{2+} into the spine produce LTP (Kennedy, Beale et al. 2005), preferentially activating protein kinases (Malenka and Nicoll 1998), which are crucial for LTP. Importantly, the Ca^{2+} signal is restricted to the vicinity of the activated spines, due to compartmentalization and diffusion restriction granted by spine morphology (Yuste, Majewska et al. 2000; Noguchi, Matsuzaki et al. 2005). Some studies have suggested that the Ca^{2+} signal is amplified

by release from intracellular stores, given that thapsigargin, which depletes Ca^{2+} intracellular stores, inhibited the induction of LTP (Obenaus, Mody et al. 1989; Harvey and Collingridge 1992; Bliss and Collingridge 1993; Bortolotto and Collingridge 1993; Matias, Dionísio et al. 2002). However, the contribution of Ca^{2+} from intracellular stores to LTP remains controversial.

Ca^{2+} flowing through the NMDAR channel can bind to several effectors inside the spine, namely calmodulin (CaM), a ubiquitous Ca^{2+}-binding regulatory protein (Kennedy, Beale et al. 2005). In turn, the complex of Ca^{2+}/CaM activates Ca^{2+}/Calmodulin-dependent kinase II (CaMKII), which is critically involved in the induction of LTP. Accordingly, postsynaptic injection of inhibitors of CaMKII or genetic deletion of a critical CaMKII subunit blocked the ability to induce LTP (Malinow, Schulman et al. 1989; Silva, Stevens et al. 1992). Furthermore, a constitutively active (CA) form of CaMKII occluded LTP and increased synaptic transmission in CA1 neurons (Pettit, Perlman et al. 1994). Protein kinase A (PKA) is another Ca^{2+} sensor important for LTP induction. Elevation of cAMP levels activate PKA, leading to inhibition of protein phosphatase1 (PP1), which is involved in LTD (Mulkey, Endo et al. 1994). Conversely, pharmacological blockade of PKA blocks LTP (Otmakhova, Otmakhov et al. 2000). Protein kinase C (PKC) is also involved in LTP (Hu, Hvalby et al. 1987), particularly the form protein kinase M zeta (PKMζ) (Sacktor, Osten et al. 1993; Ling, Bernardo et al. 2002). Among other types of evidence, PKC inhibitors blocked LTP (Lovinger, Wong et al. 1987). The mitogen-activated protein kinase (MAPK) cascade that activates extracellular-signal regulated kinases (ERKs) has been implicated in LTP and in some forms of learning and memory (English and Sweatt 1997; Atkins, Selcher et al. 1998). Additionally, phosphoinositide 3-kinase (PI3K) participates in a form of LTP that involves the trafficking of AMPARs to synapses, whereas Src, a tyrosine kinase, may enhance the NMDAR function during LTP induction (Man, Wang et al. 2003; Thornton, Yaka et al. 2003).

LTP Expression

The question of whether LTP is expressed presynaptically or postsynaptically has been pursued for over 20 years and much debate and controversy remains. A number of experiments yielding contradictory results have been carried out over the years, some supporting a presynaptic locus, some

supporting a postsynaptic locus and others supporting both a pre- and postsynaptic locus for the expression of LTP.

The presynaptic hypothesis has been supported by studies demonstrating an increase in presynaptic vesicle release following LTP induction (Bliss and Collingridge 1993; Lisman 2009) or studies showing that synaptic failure rate decreases upon LTP (Nicoll 2003; Lauri, Palmer et al. 2007).

In the past 10-15 years, the postsynaptic hypothesis of LTP at hippocampal CA1 synapses has been somewhat prevalent. The postsynaptic hypothesis is supported by studies that found a selective increase in AMPAR EPSCs and little change in NMDAR EPSCs following LTP (Malenka and Nicoll 1999; Bredt and Nicoll 2003). According to this hypothesis, following LTP induction, CaMKII (and PKC) phosphorylates the GluA1 subunit of AMPARs on Ser^{831} (Roche, O'Brien et al. 1996; Barria, Derkach et al. 1997), causing the regulated insertion of AMPARs to the postsynaptic membrane (Hayashi, Shi et al. 2000; Lu, Man et al. 2001) or increase in AMPAR permeability (Derkach, Barria et al. 1999). This makes the synapse more powerful and underlies activity-induced changes in synaptic transmission, with no significant role for presynaptic changes (Malenka and Nicoll 1999; Malinow and Malenka 2002; Bredt and Nicoll 2003; Newpher and Ehlers 2008; Kessels and Malinow 2009; Lisman 2009). In line with these findings, a double phosphomutant mouse for Ser^{831} and Ser^{845} shows reduced LTP and memory retention in a spatial memory task, but no learning deficits (Lee, Takamiya et al. 2003). Activation of the small GTPase Ras downstream the NMDAR has also been shown required for the insertion of GluA1-containing AMPARs following LTP induction (Zhu, Qin et al. 2002; Patterson, Szatmari et al. 2010). Also, older experiments showing that paired-pulse facilitation (PPF) is not altered following LTP induction constitute an evidence for a postsynaptic modification in LTP (Muller and Lynch 1989), assuming that PPF change reports modifications in presynaptic release probability (Malenka and Nicoll 1999).

Technical advances over the last few years made it possible to study postsynaptic and presynaptic events with remarkable precision, providing strong evidence for **both** presynaptic and postsynaptic changes (Lisman 2009). In line with presynaptic locus for LTP expression, Enoki and collaborators (2009) used a sharp microelectrode injected in a CA1 neuron and demonstrated that LTP, induced at single synapses, is due to increased release of vesicles from the presynaptic terminal, without

change in the average amplitude of successful responses, there being no significant postsynaptic changes (Enoki, Hu et al. 2009). Additionally, a different study provides evidence for a molecular mechanism by which LTP could enhance the release of vesicles through measurements with FM1-43 dye (Ahmed and Siegelbaum 2009). On the other hand, recent work using two-photon glutamate uncaging (Matsuzaki, Honkura et al. 2004) provided evidence that all machinery needed for LTP is on the postsynaptic side. This technique makes use of two-photon laser pulses that are used to supply glutamate to a submicron region near an identified dendritic spine. With this method, if uncaging pulses are given together with postsynaptic depolarization or after Mg^{2+} removal, it is possible to induce LTP and to potentiate AMPAR-uEPSCs in a NMDAR- and CaMKII-dependent manner, at the stimulated synapse only (Matsuzaki, Honkura et al. 2004). Hence, the presynaptic element of the synapse is left out.

Structural and Functional Plasticity of Dendritic Spines

The formation of long-term synaptic plasticity and long-term memory (LTM) is closely associated with the remodeling of synaptic structure (Engert and Bonhoeffer 1999; Xu, Yu et al. 2009). Learning experiences that give rise to LTM have been found to induce increases in the number of presynaptic varicosities (Bailey and Chen 1988), as well as increases in the postsynaptic spine volume and density (Moser, Trommald et al. 1997). Mental retardation is often associated with synapse retraction and elimination (Fiala, Spacek et al. 2002). Structural plasticity of dendritic spines is considered to be tightly coupled with functional plasticity, and thus a physical basis for learning and memory (Matsuzaki, Ellis-Davies et al. 2001; Matsuzaki, Honkura et al. 2004; Bourne and Harris 2008; Lee, Escobedo-Lozoya et al. 2009; Patterson, Szatmari et al. 2010).

Dendritic Spines

The human brain contains more than 10^{13} spines (Nimchinsky, Sabatini et al. 2002). Dendritic spines were first described by Ramón y Cajal, in 1888, as a series of small protrusions extending from the dendrites of chicken Purkinje cells, as visualized by the Golgi method (Bonhoeffer and Yuste 2002; Bhatt, Zhang et al. 2009; Holtmaat and Svoboda 2009). Because dendritic spines are the sites of most excitatory synapses on pyramidal neurons in the mammalian brain, spine number can be used as a reasonable measure of excitatory synapse density. Spines are highly variable in morphology (Kasai, Fukuda et al. 2010) and dendritic spines with different sizes and shapes occur on the same neuron and even on the same dendrite (Holtmaat and Svoboda 2009). Dendritic spines have diverse structures and a small average volume of ~ 0.1 femtoliter (Tada and Sheng 2006; Holtmaat and Svoboda 2009). Traditionally, spines are classified morphologically as stubby, thin or mushroom (**Figure 1.4.**) (Harris 1999). Thin spines are long, narrow protrusions terminating in a small, bulbous head. Stubby spines are small protrusions lacking a clearly distinguishable neck and head. Mushroom spines have a narrow neck and a large and bulbous head. Spine structure is not only diverse, but also dynamic and it may change in response to neurotransmitter receptor activation or environmental and hormonal signals.

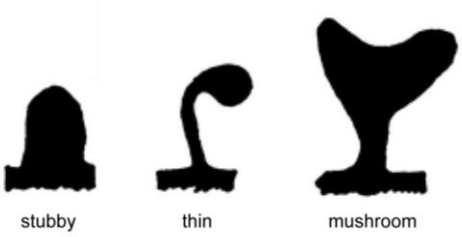

Figure 1.4. Sheme of different types of dendritic spines. Spines can be classified in stubby, thin or mushroom, depending on their morphology.

Regarding spinogenesis, dendrites of neonatal pyramidal cell are relatively smooth (Purpura 1975; Nimchinsky, Sabatini et al. 2002). The dendritic protrusions begin to increase in density during the first week of life, with dramatic increases of density during the second and third weeks, as the rate of

synaptogenesis reaches its peak (Nimchinsky, Sabatini et al. 2002). Spine morphology also changes with development (Harris, Jensen et al. 1992). The most abundant spine type early in development is the stubby spine (Nimchinsky, Sabatini et al. 2002). Filopodia are also frequently encountered (Papa, Bundman et al. 1995; Fiala, Feinberg et al. 1998; Nimchinsky, Sabatini et al. 2002) and were initially thought to be the precursors of dendritic spines. In the adult, thin or mushroom spines are more common, although many stubby spines are still present in the adult mouse and human cortex (Nimchinsky, Sabatini et al. 2002; Yuste and Bonhoeffer 2004; Sheng and Hoogenraad 2007). One report demonstrated that the stability of spines is correlated with their morphology, such that larger and stubby spines seem to be much more stable than longer, thinner ones (Trachtenberg, Chen et al. 2002). However, the correlation between structure and stability is not absolute: small spines can persist, and large spines can disappear (Holtmaat and Svoboda 2009). Furthermore, new dendritic spines are also generated on mature neurons, through the perforation and splitting of existing synapses (Harris 1999), but *de novo* spine formation can also occur (Kwon and Sabatini 2011).

Most spines contain a postsynaptic density (PSD) (Sheng and Hoogenraad 2007), an electron-dense thickening of the postsynaptic membrane, which is located adjacent to the presynaptic bouton associated with the spine (Harris, Jensen et al. 1992; Bourne and Harris 2008). The PSD is composed of hundreds of proteins (Kennedy, Beale et al. 2005; Sheng and Hoogenraad 2007). Many structural, receptor and signaling proteins are anchored in the PSD, representing several signaling pathways involved in synaptic plasticity (Nimchinsky, Sabatini et al. 2002; Kennedy, Beale et al. 2005; Sheng and Hoogenraad 2007; Bhatt, Zhang et al. 2009). Harris and Stevens (1989) demonstrated that the dimensions of the spine head are well correlated with the area of PSD and number of vesicles in the presynaptic axonal varicosity (Harris and Stevens 1989). Thus, in terms both of transmitter release and postsynaptic sensitivity, large spines are the site of strong synapses (Nimchinsky, Sabatini et al. 2002).

CA1 excitatory synapses use glutamate as a transmitter (Sheng and Hoogenraad 2007), and thus dendritic spines contain several types of glutamate receptors including ionotropic receptors - AMPA receptors (AMPARs), kainate receptors, and NMDA receptors (NMDARs) - and G-protein coupled metabotropic glutamate receptors (mGluRs) (Sheng and Kim 2002; Bourne and Harris 2008). NMDARs

occupy the center of the PSD, AMPARs are distributed more evenly throughout the PSD, whereas mGluRs are mostly at the periphery of the PSD (Sheng and Hoogenraad 2007).

Structural Plasticity of Dendritic Spines

Recent improvements in time-lapse imaging techniques have made it possible to observe changes of dendritic morphology and synaptic function at the level of single synapses (Yuste and Bonhoeffer 2001). Two-photon laser scanning microscopy (TPLSM) has become the tool of choice for high-resolution fluorescence imaging in highly scattering environments, such as the intact brain and the brain slice (Svoboda and Yasuda 2006). Compared with other optical techniques, TPLSM allows high-resolution imaging and efficient detection of a fluorescence signal with minimal photobleaching and phototoxicity (Svoboda and Yasuda 2006).

Dendritic spine structure is highly dynamic, particularly during postnatal development, when synaptic connections are rapidly being made (Kasai, Matsuzaki et al. 2003; Bhatt, Zhang et al. 2009): spines change their morphology, appear and disappear quickly, in both activity-dependent and activity-independent manners (Trachtenberg, Chen et al. 2002; Yasumatsu, Matsuzaki et al. 2008; Xu, Yu et al. 2009; Zito, Scheuss et al. 2009). As animals mature into adulthood, substantial changes in spine number and morphology may still occur during the learning process and under pathological conditions.

The link between synaptic plasticity and spine structure was first suggested by the finding that the size of the PSD is related to the size of the spine head and the number of AMPARs within it (Harris, Jensen et al. 1992; Nusser, Lujan et al. 1998; Matsuzaki, Ellis-Davies et al. 2001). Spine shrinkage and enlargement are associated with decreases and increases in synaptic AMPARs, which is one of the main mechanisms for LTD and LTP, respectively (Matsuzaki, Honkura et al. 2004; Park, Penick et al. 2004; Horne and Dell'Acqua 2007; Makino and Malinow 2009; Patterson, Szatmari et al. 2010). Hence, at the level of the dendritic spine, structural dynamics and receptor trafficking both contribute to functional plasticity (Kasai, Fukuda et al. 2010).

In brain slices, induction of LTP by pairing postsynaptic depolarization with presynaptic stimulation, TBS, or high frequency focal glutamate photolysis, can lead to a rapid outgrowth of dendritic protrusions (Engert and Bonhoeffer 1999; Maletic-Savatic, Malinow et al. 1999; Nagerl, Eberhorn et al. 2004; Kwon and Sabatini 2011). Conversely, induction of LTD and reduced neuronal activity cause shrinkage of existing dendritic spines and a net loss in spine number (Nagerl, Eberhorn et al. 2004; Zhou, Homma et al. 2004; Bhatt, Zhang et al. 2009). In other words, hippocampal neurons can undergo bidirectional morphological plasticity; spines are formed and eliminated in an activity-dependent way (Nagerl, Eberhorn et al. 2004). The first studies reported a relatively slow process of spine growth, taking about 30 minutes, making it unlikely that the growth of new spines can explain LTP (Engert and Bonhoeffer 1999). However, a recent report demonstrated that high frequency suprathreshold focal glutamate uncaging can rapidly (~ 10s) produce *de novo* spine growth in a NMDAR-dependent manner, in the vicinity of the stimulation point (Kwon and Sabatini 2011).

Functions of Dendritic Spines

Over one hundred years ago, Ramón y Cajal, who first described dendritic spines, proposed that spines increase and modify synaptic connections. In line with this idea, structural spine plasticity dramatically increases the memory storage capacity of the brain, because a wide range of synaptic connectivity patterns are attainable by spine or bouton growth (Holtmaat and Svoboda 2009). Several studies are consistent with a model in which activity-dependent spine-volume changes regulate new memory acquisition (by enlarging/stabilizing or eliminating the smallest spines) and existing-memory persistence (by changing volumes of spines). As such, activity-dependent plasticity selects memory content and modifies memory strength. In contrast, intrinsic fluctuations in spine volume may change the strength of a memory but rarely affect its content (Kasai, Fukuda et al. 2010). Additionally, as the late phase of LTP and long-term memory, maintenance of spine enlargement depends on protein synthesis (Tanaka, Horiike et al. 2008). Moreover, spine structures are stable for days in cultured hippocampal slices (De Roo, Klauser et al. 2008) and for years in the cortex *in vivo* (Grutzendler, Kasthuri et al. 2002;

Trachtenberg, Chen et al. 2002; Zuo, Lin et al. 2005). These data support the idea that structural plasticity is the basic cellular mechanism that underlies memory formation (Kasai, Fukuda et al. 2010).

Related to this, dendritic spine morphology has both chemical and electrical compartmentalization roles within individual synapses. In 1989, Harris and Stevens (1989) suggested that the constricted necks of hippocampal dendritic spines could reduce diffusion of activated molecules to neighboring spines, which was later confirmed (Harris and Stevens 1989; Svoboda and Tank 1996; Yuste and Majewska 2001; Bloodgood and Sabatini 2005; Noguchi, Matsuzaki et al. 2005). Accordingly, the degree to which NMDAR-mediated Ca^{2+} is elevated in the spine independently from the dendrite is influenced by spine shape, such that bigger spines with wider necks let more Ca^{2+} in the adjacent dendritic shaft, whereas smaller spines with narrower necks are more efficient at compartmentalizing Ca^{2+} within the activated spine (Noguchi, Matsuzaki et al. 2005). Because the level of postsynaptic Ca^{2+} elevation determines synaptic plasticity, spine neck geometry might explain why some groups observed that small thin spines are more susceptible to induction of LTP (Matsuzaki, Honkura et al. 2004). Because of signal compartmentalization, LTP and associated spine enlargement can be induced in single dendritic spines without affecting surrounding spines (Matsuzaki, Honkura et al. 2004; Yasuda and Murakoshi 2011). Hence, spine morphology might confer the input-specificity requisite of LTP.

Dendritic spine structure explains not only the input specificity characteristic of LTP, but also its associativity. A study by Harvey and Svoboda (2007), upon induction of a LTP stimulus in single dendritic spines by glutamate photolysis, showed that, within 5 minutes, a second weak subthreshold stimulation which usually does not produce plasticity, if applied to a second adjacent dendritic spine less than ~ 10μm away from the originally stimulated spine, can produce LTP and spine growth (Harvey and Svoboda 2007).

Abnormal Dendritic Spine Morphology in Mental Disorders

Abnormalities of spine morphology, density and dynamics are associated with disrupted synaptic, neuronal, and higher-order brain functions. Spine structure and plasticity abnormalities have been found

in many pathological conditions, including mental illnesses and age-related neurodegenerative diseases (Newey, Velamoor et al. 2005). For example, in fragile X syndrome (FXS), which is the most common form of inheritable mental retardation, spines are found in much higher density and display a more immature, long, and thin form (Rudelli, Brown et al. 1985; Hinton, Brown et al. 1991; Irwin, Patel et al. 2001; McKinney, Grossman et al. 2005; Grossman, Elisseou et al. 2006). Also, people with trisomy 21 (Down's syndrome) show decreased spine density in both the neocortex and hippocampus, as well as increased incidence of abnormally long and short spines (Marin-Padilla 1972; Suetsugu and Mehraein 1980; Ferrer and Gullotta 1990).

Schizophrenia can also be linked to abnormalities in spine size. Postmortem studies on the brains of schizophrenic patients demonstrate decreased spine density in neocortical pyramidal neurons, as a consequence of a reduced generation relative to elimination of synapses (Garey, Ong et al. 1998). Besides, several lines of evidence point to links between schizophrenia and abnormal activity-dependent plasticity (Lewis and Gonzalez-Burgos 2008; Kasai, Fukuda et al. 2010). Spine abnormalities have also been reported in tuberous sclerosis type I (Huttenlocher and Heydemann 1984).

Ras

Numerous signaling pathways have been implicated as playing crucial roles in hippocampal synaptic plasticity and hippocampus-dependent memory formation (Sweatt 2004). There is substantial interplay between these signaling pathways, increasing the level of complexity and implying a great degree of integration and coordination for signal transduction in hippocampal LTP induction. Among the multiple signaling pathways studied in the context of the cognitive processes, the NMDAR-Ras-MAPK-ERK pathway is clearly important in synaptic plasticity and memory formation in general, across many species, brain areas and types of synapses (Manabe, Aiba et al. 2000).

Ras Isoforms, Structure and Expression

Small G proteins constitute a large family of proteins that bind to and hydrolyze guanosine triphosphate (GTP) into guanosine diphosphate (GDP); therefore they are also named small GTPases (Ye and Carew 2010). Small GTPases are monomeric proteins, ubiquitously expressed, typically between 20-25KDa in size (Ye and Carew 2010). They are membrane-associated proteins, important for converting a wide range of extracellular signals from membrane receptors to intracellular signaling cascades (Raaijmakers and Bos 2009; Ye and Carew 2010). They regulate many cellular processes, including cell cycle progression, cell survival, actin cytoskeletal organization, cell polarity and movement, vesicular and nuclear transport (Raaijmakers and Bos 2009; Vigil, Cherfils et al. 2010).

In general, the activity of small GTPases is regulated by their GTP/GDP-binding state. When binding to GTP, they are in an active conformation and are able to bind downstream effectors, whereas binding to GDP returns them to the inactive state (Milburn, Tong et al. 1990; Vigil, Cherfils et al. 2010; Ye and Carew 2010).

The small GTPases superfamily includes many members, namely the Ras, Rho, Arf, Rab, and Ran families, some of particular importance to neuronal plasticity and memory (Takai, Sasaki et al. 2001; Ye and Carew 2010; Stornetta and Zhu 2011). Here, we will focus on the Ras family, which includes Ras (HRas, NRas, and KRas), Rap1 and Rap2 has major members. Specifically we will focus on Ras, which was the object of our study. *Ras* genes were first identified as oncogenes, as they play important roles in mediating cell proliferation, differentiation and survival during development. Mutations in *Ras* genes that result in constitutively active Ras family proteins are closely associated with tumorogenesis in humans (Ye and Carew 2010). Recently, a large number of reports also suggest that Ras family proteins are critical in memory formation. Furthermore, signaling of Ras proteins can modify neuronal function and structure, leading to changes in synaptic strength and neuronal firing rates (Ye and Carew 2010). At the membrane, Ras can interact with downstream effectors ultimately leading to short and long-term changes in neuronal function, namely synaptic plasticity, dendritic excitability, synapse formation, learning, and memory. Therefore, this pathway promotes an extensive amplification and divergence of signaling.

The different Ras isoforms generate distinct signal outputs, despite structural similarity and interaction with common activators and effectors (Hancock 2003). For example, KRas knockout is embryonic lethal, whereas HRas, NRas, and HRas-NRas double knockouts survive normally (Hancock 2003).These biological differences are probably caused by the carboxy-terminal (C terminal) 25 amino acids of the hypervariable domain (HVR), which is the only region that differs significantly in sequence between the otherwise highly homologous Ras isoforms.

Ras Membrane Localization

Ras proteins are synthesized as cytosolic precursors that undergo posttranslational processing to be able to associate with cell membranes (Hancock 2003; Wright and Philips 2006). They are targeted to membranes by a series of modifications of the C terminal. The HVR contains the protein sequences that are necessary for Ras to associate with the inner plasma membrane. The initial triplet of modifications is directed by the CAAX motif and is common to all Ras proteins. Accordingly, mutation of the CAAX motif in the HVR was shown to abolish plasma-membrane localization and signaling of Ras (Hancock 2003; Sung, Rodrigues et al. 2010). The first step of posttranslational modification is prenylation, which covalently attaches either farnesyl or geranylgeranyl isoprenoids to the conserved cysteine residue in the C terminal CAAX motif of Ras family proteins (C is cysteine, A is generally an aliphatic amino acid, and X can be a variety of amino acids) (Hancock 2003). This motif is farnesylated by farnesyltransferase (FTase) when the last amino acid is S, M, A, or Q. Second, the farnesylated CAAX sequence targets Ras to the cytosolic surface of the endoplasmic reticulum (ER). Here, the endopeptidase Rce1 removes the AAX tripeptide. Third, the C-terminal is methylated by isoprenylcysteine carboxyl methyltransferase (Icmt). This creates a hydrophobic domain that mediates membrane interactions (Hancock 2003; Wright and Philips 2006). Membrane anchoring of Ras family proteins is crucial for their signaling and cellular functions (Hancock 2003; Wright and Philips 2006). Inhibitors of prenylation have been designed as therapeutic tools for blocking oncogenesis (Li, Cui et al. 2005; Sousa, Fernandes et al. 2008; Agrawal and Somani 2009). After methylation, Ras proteins take one of two routes to the cell surface, which is controlled by a targeting signal that is located immediately amino-terminal (N terminal) to the farnesylated

cysteine. HRas and NRas undergo palmitoylation, by Ras palmitoyltransferase (RPT), on cysteine residues in their HVRs and enter the exocytic pathway, trafficking through the Golgi to the plasma membrane (Hancock 2003; Wright and Philips 2006; Arozarena, Calvo et al. 2011). KRas, which has a polylysine sequence instead of cysteine residues, bypasses the Golgi and reaches the plasma membrane (Hancock 2003; Wright and Philips 2006; Arozarena, Calvo et al. 2011). Interestingly, the interaction of Ras with the plasma membrane is highly dynamic. Ras is also present on endosomes and other intracellular membranes, such as the ER and Golgi (Hancock 2003; Wright and Philips 2006; Brown and Sacks 2009; Arozarena, Calvo et al. 2011).

Regulation of Ras Signaling Pathway by RasGEFs and RasGAPs

The activity state of Ras is determined by the balance of activating proteins GEFs (guanine nucleotide exchange factors) and of inactivating proteins GAPs (GTPase-activating proteins) (Thomas and Huganir 2004). Activation of GEFs promotes the dissociation of GDP from Ras family proteins, which facilitates the exchange of GDP for GTP (more abundant in the cytosol), and thus enhances the activity of Ras family proteins. Activation of GAPs enhances the rate of intrinsic GTP hydrolysis of Ras family proteins, which is normally slow, and reduces their activity. There is a wide array of GEFs and GAPs targeting different members of Ras family proteins and probably many more will be identified in the future (Cullen and Lockyer 2002; Raaijmakers and Bos 2009; Ye and Carew 2010).

It is important to note that GEFs and GAPs do more than simply turn on-off Ras family proteins. The activity of each GEF and GAP is under the regulation of distinct upstream signaling elements, such as cAMP, Ca^{2+}, and tyrosine kinases. Thus, each of them links specific upstream signaling elements to Ras family proteins. GEFs and GAPs are large, multidomain proteins, which interact with membrane lipids or other proteins that target them to specific intracellular compartments. Therefore, activation of a specific GAP or GEF protein can modify the activity of nearby Ras family proteins, thereby regulating specific downstream targets in restricted cellular compartments (Vigil, Cherfils et al. 2010; Ye and Carew 2010).

RasGEFs

RasGEFs link cell-surface receptors to Ras protein activation by catalyzing the dissociation of GDP from the inactive Ras proteins. GTP can then bind and induce a conformational change, allowing interaction with downstream effectors (Quilliam, Rebhun et al. 2002). They are blocked by dominant negative (DN) mutants of Ras (Quilliam, Rebhun et al. 2002), such as the 17N mutation (Feig 1999). To date, about 20 RasGEFs were described (Quilliam, Rebhun et al. 2002) and some of these have been shown to have important roles in synaptic plasticity, learning and memory (Ye and Carew 2010). Below, we briefly mention a few RasGEFs implicated in brain function.

Son of sevenless (Sos) was the first RasGEF identified in higher eukaryotes, downstream receptor tyrosine kinases, and, in mammals, it includes two closely related isoforms: Sos1 and Sos2 (Bowtell, Fu et al. 1992). Sos1 is ubiquitously expressed and it has been suggested that it might be the most commonly used RasGEF (Quilliam, Rebhun et al. 2002). Consistent with this hypothesis, a Sos1 knockout is embryonically lethal (Qian, Esteban et al. 2000). Interestingly, Sos proteins have been implicated in NMDAR-mediated ERK activation in neurons of young mice. A study in cortical neuronal cultures from $Sos2^{-/-}$ newborn mice ruled out the involvement of Sos2 in such phenomenons and indirectly implied that Sos1 is the major regulator of these well-known neuronal Sos functions (Arai, Li et al. 2009).

Ras-GRF1 is a neuron-specific RasGEF activated by increased intracellular Ca^{2+} concentration or G-protein coupled receptors (GPCRs). Although mice lacking Ras-GRF1 ($RasGRF^{-/-}$) show normal hippocampal function, as depicted from normal hippocampal LTP, spatial learning and memory, they are severely impaired in amygdala-dependent long-term synaptic plasticity and in memory amygdala-dependent tasks, such as inhibitory avoidance, contextual and cued fear conditioning (Brambilla, Gnesutta et al. 1997). However, a study by Giese and collaborators (2001) described opposite results with a different line of $RasGRF^{-/-}$ mice: these mice exhibited impairment in hippocampal-dependent memory tasks, but not in amygdala-dependent memory tasks (Giese, Friedman et al. 2001). $RasGRF^{-/-}$ also show higher basal synaptic activity at both amygdala and hippocampal synapses (Brambilla,

Gnesutta et al. 1997) and a posterior study demonstrated a role for Ras-GRF1 in neuronal excitability (Tonini, Franceschetti et al. 2001).

A recent report identified another brain specific RasGEF, v-KIND, expressed in developing mouse brain, predominantly in the cerebellar granule cells (Huang, Furuya et al. 2007). Whereas v-KIND overexpression suppressed dendritic extension and branching of hippocampal neurons and cerebellar granule cells, knockdown of endogenous v-KIND expression promoted dendrite growth, suggesting that v-KIND activates Ras signaling to control dendrite growth (Huang, Furuya et al. 2007).

Ca^{2+} and diacylglycerol-regulated GEF2 (CalDAG-GEF2), also known as RasGRP, is a RasGEF highly expressed in neurons throughout the forebrain (Toki, Kawasaki et al. 2001). Its function in the brain remains mostly obscure, but a recent report implicated CalDAG-GEF2 in striatum physiology. Namely, it has been suggested that CalDAG-GEF2 is involved in the expression of dyskinesias resulting from l-DOPA therapy in Parkinson's disease (Crittenden, Cantuti-Castelvetri et al. 2009). Thus, this protein could be a promising therapeutic target for limiting the motor complications arising from l-DOPA therapy.

RasGAPs

RasGAPs accelerate the very slow intrinsic GTP hydrolysis activity of Ras by several orders of magnitude. However, they have almost no effect on oncogenic Ras mutants (12V and 61L), which are constitutively activated (Hancock 2003). RasGAPs have a common ~ 250 amino acid RasGAP catalytic domain also named GAP-related domain (GRD), but otherwise show essentially no sequence similarity or domain architecture in the sequences that flank this RasGAP domain (Mitin, Rossman et al. 2005; Vigil, Cherfils et al. 2010). Accumulating evidence suggests that these molecules are crucial transducers of extracellular stimuli that serve to maintain the homeostasis of cellular functions (Iwashita and Song 2008). In this section, we review several major GAPs expressed in neurons.

p120RasGAP was the first GAP to be discovered (Mitin, Rossman et al. 2005) and is widely expressed (Bernards and Settleman 2005). p120RasGAP is recruited to growth factor receptors (Bernards and Settleman 2005). In neurons, p120RasGAP has been reported to transduce EphB2 (a

receptor tyrosine kinase) signals to inhibit the Ras-MAPK pathway, leading to cytoskeletal organization and adhesion responses in neuronal growth cones, during development (Elowe, Holland et al. 2001). A different study also implicated p120RasGAP in the development of the central nervous system (CNS), but through the regulation of repulsive function via the inhibition of Ras-PI3K pathway (Endo and Yamashita 2009).

SynGAP is a member of the RasGAP family that shows a CNS-restricted expression, especially in CA1 and DG of the hippocampus, and is specifically localized within the PSD (Grewal, York et al. 1999), where it directly interacts with PSD95 and NMDARs in spines (Kim, Liao et al. 1998). SynGAP contains a Ca^{2+}-binding motif that is essential for turning on its GAP activity (Pena, Hothorn et al. 2008). SynGAP is dually specific for both Ras and Rap, but it has greater affinity for Rap *in vitro* (Krapivinsky, Medina et al. 2004). Studies involving genetic manipulations of SynGAP have established a role for this RasGAP in synaptic plasticity (Komiyama, Watabe et al. 2002; Kim, Lee et al. 2003), dendritic spine morphology (Vazquez, Chen et al. 2004), learning and memory (Komiyama, Watabe et al. 2002; Muhia, Yee et al. 2010).

The GAP1 family includes RasGAPs sharing a domain structure consisting of N terminal tandem C2 domains, a central GRD domain, and a C terminal PH domain with an associated Bruton tyrosine kinase (BTK) motif (Cullen and Lockyer 2002). Included in this family is Gap1m, the mammalian counterpart of Drosophila Gap1, which is expressed in brain, placenta, and kidney tissues, with only low levels of expression in other tissues (Maekawa, Li et al. 1994). Another member of this family is the mammalian GapIII, which has high homology with Gap1m (Baba, Fuss et al. 1995). GapIII mRNA expression was detected at highest levels in the brain, particularly in neurons and oligodendrocytes, increasing with development (Baba, Fuss et al. 1995). Therefore, GapIII might have an important function in the brain, yet to be investigated (Baba, Fuss et al. 1995). Ca^{2+}-promoted Ras inactivator (CAPRI) is a member of the GAP1 family that is ubiquitously expressed (Lockyer, Kupzig et al. 2001). Whereas CAPRI is an inactive cytosolic RasGAP under basal conditions, treatments that induce elevation in the intracellular Ca^{2+} promote the translocation of CAPRI to the plasma membrane and switch it on, inhibiting the Ras-MAPK pathway (Lockyer, Kupzig et al. 2001).

Among one of the most studied RasGAPs is neurofibromin, perhaps due to its involvement in a common single-gene disease: Neurofibromatosis Type I (NF1). Neurofibromin exhibits its highest expression in the brain, despite ubiquitous expression at very low levels in other tissues (Mazzucchelli and Brambilla 2000). Interestingly, the first evidence suggesting a role of Ras in learning and memory came from studies of NF1, which results from loss-of-function mutations that compromise the expression of neurofibromin. Among many other symptoms, 40-60% percent of children with NF1 have learning disabilities and other cognitive deficits. Heterozygous *Nf1* knockout (*Nf1*$^{+/-}$) mice were established as an animal model for NF1 disease by Jacks and collaborators (Jacks, Shih et al. 1994) and, since then, multiple studies have revealed that deficits in memory and synaptic plasticity associated with *Nf1* loss-of-function can be rescued by manipulations that decrease Ras activity (Costa, Fedorov et al. 2002; Li, Cui et al. 2005; Guilding, McNair et al. 2007; Cui, Costa et al. 2008). A more detailed description on neurofibromin function is available in the last section of this chapter.

Signaling Pathways Upstream Ras Activation

Ras proteins transmit signals from receptor tyrosine kinases (RTKs) to intracellular networks (Harding and Hancock 2008). In neurons, TrkB is activated in spines and dendrites by brain-derived neurotrophic factor (BDNF) that is released from neighboring neurons (Poo 2001; Huang and Reichardt 2003). TrkB can then activate Ras, Rap, or both (Kennedy, Beale et al. 2005). Ras can also be activated by recruitment of the adaptors Src homology 2 (SH2) domain-containing transforming protein C (Shc) and Sos to the plasma membrane following phosphorylation of Shc by Src (Kennedy, Beale et al. 2005).

Alternatively, Ras can be activated following NMDAR activation. An influx of Ca^{2+} through NMDARs leads to the activation of the small GTPase Ras. Several studies have demonstrated that the opening of synaptic NMDAR channels leads to CaMKII activation (Malinow, Schulman et al. 1989; Tan and Chen 1997; Lee, Escobedo-Lozoya et al. 2009), which regulates Ras signaling via RasGEFs and/or RasGAPs (Stornetta and Zhu 2011). RasGRF1 specifically activates several Ras isoforms. It binds to the

GluN2B subunit of NMDARs and has been shown to mediate 60-70% of the NMDAR-mediated activation of the Ras/Raf/ERK cascade in cultured hippocampal neurons (Kennedy, Beale et al. 2005).

Signaling Pathways Downstream of Ras

Ras activation initiates multiple intracellular signaling cascades (**Figure 1.5.**), eventually leading to gene transcription (Mazzucchelli and Brambilla 2000). The best characterized downstream signaling cascade of Ras family proteins is the MAPK cascade (**Figure 1.5.**) (Adams and Sweatt 2002; Thomas and Huganir 2004; Ye and Carew 2010). When activated, Ras family proteins directly bind to the regulatory domain of protein kinase Raf (Ras binding domain of Raf, RBD) with high affinity (Raaijmakers and Bos 2009; Wimmer and Baccarini 2010; Ye and Carew 2010), thereby exposing its catalytic domain, which is subsequently phosphorylated and dephosphorylated at multiple sites for full activation. Although not sufficient, Ras proteins are necessary for Raf activation by anchoring Raf to the membrane compartment where other cofactors are present, and by unfolding Raf to allow for further modifications. In this “open” conformation, the kinase domain is free to recruit and phosphorylate its substrates (Wimmer and Baccarini 2010; Ye and Carew 2010). Ras can activate either c-Raf (also named Raf-1) or b-Raf, both of which can, in turn, activate MEK1 and MEK2 by serine phosphorylation (Hancock 2003; Thomas and Huganir 2004; Ye and Carew 2010). MEK is a specific kinase whose only proven target is ERK (Wimmer and Baccarini 2010; Ye and Carew 2010). Once activated, MEK phosphorylates ERK at threonine and tyrosine residues. ERK dissociates from MEK between the first and second phosphorylation (Harding and Hancock 2008) and regulates a vast array of targets distributed in different subcellular locations, including metabolic enzymes, structural proteins and transcription factors. Tight spatiotemporal regulation is crucial for driving the ERK signal in the right direction and achieving appropriate biological outcomes (Hancock 2003; Brown and Sacks 2009; Wimmer and Baccarini 2010). Downstream ERK, ribosomal S6 kinases (RSKs) phosphorylate the cAMP response element (CRE)-binding factor CREB, which plays an essential role in inducing expression of many immediate-early genes (IEGs), such as Fos. In addition, MAPKs can phosphorylate and activate serum response element (SRE)-

binding proteins, such as Elk1, thus contributing to the control of gene transcription (Mazzucchelli and Brambilla 2000).

PI3K is another effector of Ras family proteins (**Figure 1.5.**) (Ye and Carew 2010). PI3Ks are heterodimeric proteins with a p110 catalytic and a p85 regulatory subunit. The p110 has a RBD that binds to Ras, facilitating membrane translocation and enhancing the activity of PI3K (Raaijmakers and Bos 2009), which in turn converts phosphatidylinositol 4,5-biphosphate (PIP2) into phosphatidylinositol 3,4,5-triphosphate (PIP3). This brings Akt and PDK1 into close proximity, allowing the latter to phosphorylate Akt. The mTOR-rictor complex (mTORC2) also phosphorylates Akt at a different residue, which is required for full Akt activity. Akt activates mTOR and also phosphorylates other downstream effectors (Markman, Dienstmann et al. 2010), which will not be discussed here.

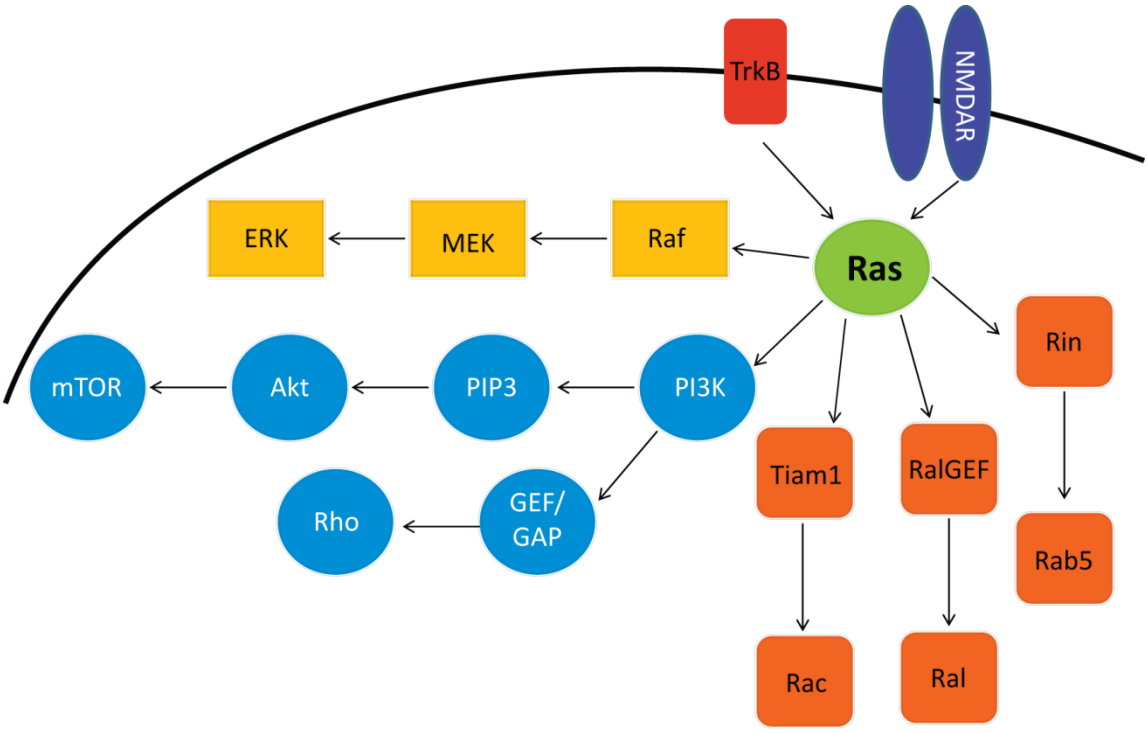

Figure 1.5. Schematics of the major signaling pathways downstream of Ras. *Adapted from Ye and Carew 2010*.

Ras family proteins also interact with other families of proteins in the small G protein superfamily (**Figure 1.5.**). Activated Ras can turn on the GEF activity of Tiam1, leading to activation of Rac, a member of Rho family proteins. Rac signaling mediates actin polymerization, therefore contributing to cell morphology (Heasman and Ridley 2008). In addition, Ras activation can lead to activation of RalGEF, which in turn activates Ral, a small G protein involved in exocytosis, and Rin, which activates Rab5, a small G protein involved in endocytosis (Ye and Carew 2010).

Dynamics in Ras Induced by Neuronal Activity

Neuronal activity can regulate Ras activity. For example, a study by Rosen and collaborators (1994) demonstrated that membrane depolarization of cultured cortical neurons by KCl induced rapid and transient Ras activation and subsequent activation of MEK and ERK, mediated by Ca^{2+} influx from voltage-gated calcium channels (VGCCs) (Rosen, Ginty et al. 1994). Another study by Yun and collaborators (1998) reported that Ras can also be activated following NMDAR activation (Yun, Gonzalez-Zulueta et al. 1998). Collectively, these studies suggest that neuronal activity activates Ras. Neuronal activity can also regulate the distribution of Ras. Fivaz and Meyer (2005) found that glutamate treatment can induce reversible translocation of KRas, but not HRas, from the plasma membrane to the perinuclear membrane compartments. This translocation required Ca^{2+} influx, activation of NMDARs and an interaction with CaM (Fivaz and Meyer 2005). Recently, Harvey et al. (2008) found that uncaging glutamate with a train of laser pulses induced robust Ras activation at the stimulated spine, the magnitude of which was correlated with spine enlargement. The activation of Ras was transient, peaking within 1 minute and returning to baseline by 10-15 minutes. Furthermore, they observed that the activated Ras spread over several micrometers and entered 10-20 neighboring spines (Harvey, Yasuda et al. 2008).

Ras in Synaptic Plasticity

Several studies have examined the role of Ras in synaptic plasticity by the local infusion of FTase inhibitors into specific brain regions. FTase inhibitors disrupt the attachment of Ras to membranes and, therefore, prevent its activation. O'Kane and collaborators (2004) showed that FTase inhibitors disrupt LTP in the CA1 hippocampal region (O'Kane, Stone et al. 2004). Murray and O'Connor (2004) showed that FTase inhibitors attenuate LTD in the hippocampal DG (Murray and O'Connor 2004). HRas fused with TAT, a cell permeant Ras, significantly reduced LTP in hippocampal Schaffer collateral synapses (Thornton, Yaka et al. 2003). Genetic manipulations were also used to investigate the role of Ras in synaptic plasticity. Ohno and collaborators (2001) reported that a KRas heterozygous knockout mouse (*KRas*$^{+/-}$) showed normal hippocampal LTP. However, a subthreshold dose of a MEK inhibitor, which did not affect LTP in WT mice, blocked LTP in the heterozygous KRas knockout mouse, suggesting the involvement of KRas in LTP induction (Ohno, Frankland et al. 2001). A different study by Kushner and collaborators (2005) examined mice expressing a constitutively active form of HRas (HRas^{12V}) in forebrain postnatal neurons and observed that HRas^{12V} is predominantly localized in axon terminals in CA1 pyramidal neurons. Increased ERK-dependent phosphorylation of Synapsin 1 (a protein involved in neurotransmitter release) was detected in the terminals of these mice, with resulting increased density of docked vesicles in glutamatergic terminals, larger miniature excitatory postsynaptic currents (mEPSCs) and enhanced PPF. These mice showed enhanced potentiation, even in the presence of NMDAR blockers. These effects were reversed by knockout of Synapsin 1, suggesting that HRas can mediate presynaptic facilitation (Kushner, Elgersma et al. 2005). Another report by Manabe and collaborators (2000) demonstrated that hippocampal LTP induced by HFS was larger in *HRas*$^{-/-}$ mice, suggesting that HRas can restrain LTP induction (Manabe, Aiba et al. 2000). In contrast, when using a pairing protocol, another group found that LTP was normal in *HRas*$^{-/-}$ mice, suggesting that the participation of HRas in LTP is sensitive to the stimulation pattern (Komiyama, Watabe et al. 2002). Collectively, these studies indicate that the two Ras isoforms, KRas and HRas, are involved in synaptic plasticity.

Studies involving genetic manipulation of Ras regulators, such as RasGAPs and RasGEFs, have also provided strong evidence on a role of the Ras pathway in synaptic transmission. Namely, a

RasGRF1 knockout mouse has abnormal LTP in the basolateral amygdala (BLA), despite normal NMDAR-dependent LTP in the hippocampus (Brambilla, Gnesutta et al. 1997; Mazzucchelli and Brambilla 2000). Also, neurofibromin heterozygous knockout mice exhibit deficits in hippocampal LTP, which can be compensated by reducing KRas expression either pharmacologically or genetically (Costa, Fedorov et al. 2002). Similarly, SynGAP heterozygous knockout mice also display impaired hippocampal LTP (Komiyama, Watabe et al. 2002; Kim, Lee et al. 2003), despite increased synaptic transmission (Rumbaugh, Adams et al. 2006).

Studies involving genetic manipulation of Ras scaffolds have also provided evidence for the involvement of Ras in synaptic plasticity. Scaffolding proteins can bring a subset of molecular elements into physical proximity, allowing specific interactions to occur. For example, Kinase Suppressor of Ras 1 (KSR) is a scaffolding protein for the Ras-ERK cascade, which is highly expressed in the adult brain, especially in the hippocampus. Hippocampal LTP is lost in *KSR*$^{-/-}$ mice (Shalin, Hernandez et al. 2006).

Regulation of Postsynaptic AMPA Receptors

Changes in AMPAR trafficking are important components of synaptic plasticity, and they have been implicated in multiple forms of adaptive behavior, including learning and memory (Kessels and Malinow 2009). A study by Zhu and collaborators (2002) established a role of Ras activation in AMPAR trafficking during LTP induction. Using transfected hippocampal CA1 pyramidal neurons, they observed that overexpression of WT- or CA-HRas enhanced whole-cell responses mediated by AMPARs at the basal state, whereas DN-HRas reduced the responses. Accordingly, DN-HRas inhibited synaptic insertion of AMPARs containing GluA2L, whereas CA-HRas promoted insertion of GluA1-containing receptors. In this study, when inducing LTP by pairing presynaptic stimulation with postsynaptic depolarization, they observed that Ras activation and subsequent ERK activation were required for LTP AMPAR current (Zhu, Qin et al. 2002).

Another report showed that SynGAP plays a critical role in AMPAR trafficking in hippocampal and cortical cultured neurons (Rumbaugh, Adams et al. 2006). Accordingly, overexpression of SynGAP in

neurons results in a remarkable depression of AMPAR-mediated mEPSCs, a significant reduction in synaptic AMPAR surface expression, and a decrease in the insertion of AMPARs into the plasma membrane (Rumbaugh, Adams et al. 2006).

Strong synaptic activity and experience-dependent activity stimulate additional Ras signaling and activate the Ras-PI3K-Akt pathway, which leads to phosphorylation of Ser^{831} of GluA1. Whereas Ser^{841} phosphorylation of GluA2L is sufficient to drive GluA2L-containing AMPARs into synapses (Qin, Zhu et al. 2005), phosphorylation of both Ser^{845} and Ser^{831} of GluA1 is required for the synaptic delivery of GluA1-containing AMPARs (Lee, Barbarosie et al. 2000). However, these findings contradict a number of other reports. For example, Manabe et al. (2000) found that enhanced LTP in HRas knockout mice was unrelated to AMPARs (Manabe, Aiba et al. 2000).

Regulation of Postsynaptic NMDA Receptors

Although changes in the activity of Ras family proteins do not affect NMDARs during spontaneous activity (Zhu, Qin et al. 2002), several studies suggest that HRas signaling can regulate the function of NMDARs during the induction of long-lasting synaptic plasticity. Treatment of brain slices with TAT-HRas led to the conclusion that HRas activation is able to reduce surface retention of GluN2A-containing NMDARs by inhibiting its Src-mediated phosphorylation (Thornton, Yaka et al. 2003). This was in line with findings by Manabe and collaborators (2000), who reported that HRas knockout mice ($HRas^{-/-}$) showed increased tyrosine phosphorylation of GluN2A and GluN2B subunits of the NMDAR in hippocampus and larger NMDAR synaptic responses induced by HFS (Manabe, Aiba et al. 2000).

Regulation of Presynaptic Neurotransmitter Release

In addition to modifications of postsynaptic receptors, changes in synaptic strength can also be achieved by regulating neurotransmitter release in presynaptic terminals. For example, the C terminal of Synapsin 1, which is a protein associated with the surface of synaptic vesicles (SVs), contains consensus sites for phosphorylation by ERK, a major downstream effector of Ras family proteins. Neurofibromin

restricts GABA release from inhibitory neurons by regulating ERK activation and Synapsin 1 phosphorylation, which was shown to be important for memory formation (Cui, Costa et al. 2008). A contradictory study by Kushner et al. (2005) reported that CA-HRas expression enhances synaptic potentiation and memory formation by facilitating vesicle docking and release in excitatory neurons (Kushner, Elgersma et al. 2005).

Ras in Structural Plasticity

Ras family proteins have long been found to regulate neuronal morphology during development by mediating the signaling of growth factors (Borasio, John et al. 1989). A study by Wu and collaborators (2001) demonstrated that the activation of the Ras-MAPK pathway by multiple spaced membrane depolarizations leads to filopodia formation, which can be reversed by a MEK inhibitor (Wu, Deisseroth et al. 2001). The SynRas mouse, a transgenic mouse expressing CA-HRas ($HRas^{12V}$) in postmitotic neurons (Heumann, Goemans et al. 2000), displayed an increase in neuronal structural complexity correlated with an increase in efficacy in synaptic transmission (Alpár, Palm et al. 2003; Gärtner, Alpár et al. 2004; Gärtner, Alpár et al. 2005; Seeger, Gärtner et al. 2005). Particularly, these mutant mice exhibited increased spine density in cortical pyramidal neurons (Gärtner, Alpár et al. 2005). Neurons from mice lacking SynGAP exhibited accelerated spine development and larger spines than those of WT mice (Vazquez, Chen et al. 2004), consistent with SynGAP playing an inhibitory role in Ras signaling (Chen, Rojas-Soto et al. 1998; Kim, Liao et al. 1998), spine and synapse morphogenesis (Vazquez, Chen et al. 2004).

More recently, several studies suggested that Ras also contributes to structural plasticity associated with the formation of long-term synaptic and behavioral plasticity (Ye and Carew 2010). Among these, Harvey and collaborators (2008) showed that Ras is activated in single dendritic spines following a LTP-inducing stimulus that leads to spine enlargements. Moreover, the same authors showed that a MEK inhibitor was sufficient to abolish the sustained phase of spine structural plasticity, indicating that Ras is crucial in structural plasticity (Harvey, Yasuda et al. 2008).

Ras in Learning and Memory

A number of studies have examined the role of Ras in memory formation by local infusion of FTase inhibitors into specific brain regions during different stages of memory processing. Among these studies, pretraining infusion of a FTase inhibitor into the BLA disrupted LTM for contextual and cued fear conditioning (Merino and Maren 2006). Additionally, genetic manipulations have been used to examine the role of specific Ras isoforms in memory formation. For example, despite robust memory for contextual fear conditioning in a KRas heterozygous knockout mouse, a subthreshold dose of a MEK inhibitor, which did not affect WT mice, blocked memory formation in the heterozygous KRas knockout mouse, suggesting the involvement of KRas in memory formation (Ohno, Frankland et al. 2001). Moreover, Kushner and collaborators (2005) reported that mice expressing $HRas^{12V}$ in forebrain postnatal neurons exhibited enhanced acquisition of spatial memory in the Morris water maze task, and enhanced short-term and long-term conditioned responses in contextual fear conditioning (Kushner, Elgersma et al. 2005). Taken together, these studies suggest that KRas and HRas are involved in memory formation.

Also, mice lacking RasGRF exhibited impaired memory consolidation, as revealed by emotional conditioning tasks that require the function of the amygdala, while normal performance was displayed in spatial learning tasks that require hippocampal function (Brambilla, Gnesutta et al. 1997; Mazzucchelli and Brambilla 2000). Additionally, hyperactivation of the Ras-MAPK-ERK signaling pathway in the neurofibromin heterozygous knockout mouse ($Nf1^{+/-}$) led to deficits in spatial learning and memory retention (Costa, Fedorov et al. 2002; Li, Cui et al. 2005).

Studies involving genetic manipulation of Ras scaffolds have provided additional support for the involvement of Ras in memory formation. A recent study by Shalin et al. (2006) using KSR knockout mice ($KSR^{-/-}$) suggested that KSR specifically links mGluR/PKC-Ras-ERK-Kv4.2 signaling cascade, which is essential for memory formation (Shalin, Hernandez et al. 2006). A recent study by Moressis et al. (2009), using a Downstream of Receptor Kinase (DRK) heterozygous loss-of-function mutant fly, suggested that scaffolding signaling of RTK-Ras-Raf is important for the acquisition of olfactory aversive conditioning in Drosophila, since these flies exhibited impaired acquisition and consolidation of olfactory aversive conditioning (Moressis, Friedrich et al. 2009).

Precise Regulation of Ras and Rasopathies

To date, innumerous reports provide evidence that synaptic AMPAR trafficking mediated by Ras signaling plays a key role in experience-dependent synaptic plasticity, as well as many forms of learning and memory. Studies involving diverse strategies to manipulate Ras activity suggest that precise spatiotemporal regulation of Ras signaling sustains the optimal synaptic load of distinct populations of AMPARs, which is essential for maintaining the highest capacity of plasticity, learning and memory (Thomas and Huganir 2004; Tidyman and Rauen 2009; Stornetta and Zhu 2011). Direct manipulation of Ras demonstrated that both hypo- and hyperactivation of Ras signaling impair synaptic AMPAR trafficking and synaptic plasticity (**Figure 1.6.**) (Zhu, Qin et al. 2002), providing a cellular and molecular base for this theory.

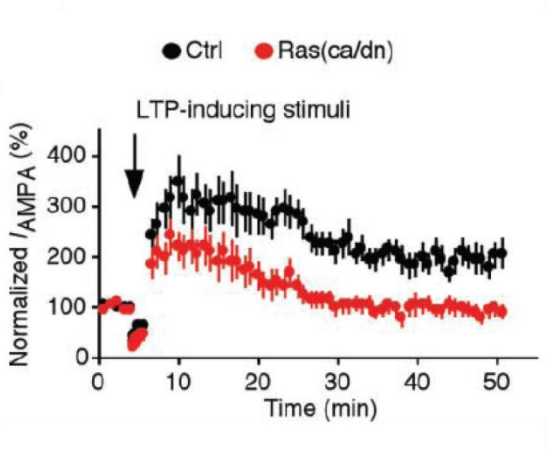

Figure 1.6. Time course of AMPAR trafficking during LTP. Synaptic AMPAR-mediated response amplitudes in CA1 pyramidal neurons expressing CA-Ras-GFP or DN-Ras-GFP and neighboring non-expressing control neurons before and after LTP-inducing stimuli. *Adapted from Stornetta and Zhu 2011.*

Importantly, disease-linked mutations of many genes relate to various signaling molecules along the Ras pathway, driving the Ras signaling either too high or too low and impairing the signal transduction dynamics. The fact that Ras signaling is undoubtedly involved in development and cancer explains a few common characteristics often shared by mental diseases besides learning disabilities, including cardiac defects, facial dysmorphism, and increased risk of cancer (Stornetta and Zhu 2011). On the other hand,

mutations affecting distinct signaling molecules in the Ras pathway determine unique phenotypes in different mental disorders (Tidyman and Rauen 2009; Stornetta and Zhu 2011). Among these mental disorders associated with learning disability due to dysregulated Ras signaling are: autism (Stornetta and Zhu 2011), cardio-facio-cutaneous syndrome (Stornetta and Zhu 2011), Coffin-Lowry syndrome (Thomas and Huganir 2004; Stornetta and Zhu 2011), Costello syndrome (Rauen 2007; Tidyman and Rauen 2009; Stornetta and Zhu 2011), FXS (Nimchinsky, Oberlander et al. 2001; Newey, Velamoor et al. 2005; Stornetta and Zhu 2011), NF1 (Costa, Fedorov et al. 2002; Shilyansky, Lee et al. 2010), Legius syndrome (Denayer, Ahmed et al. 2008; Tidyman and Rauen 2009), Noonan syndrome (Tidyman and Rauen 2009; Stornetta and Zhu 2011), Leopard syndrome (Tidyman and Rauen 2009), schizophrenia (Stornetta and Zhu 2011), and tuberous sclerosis (Qin, Zhu et al. 2005; Tavazoie, Alvarez et al. 2005; Vigil, Cherfils et al. 2010). All these “RASopathies” underscore the requirement for the precise regulation of Ras signaling in development and behavior.

Neurofibromin

Neurofibromin, the product of the *Nf1* gene, is a 250KDa protein, composed of 2818 amino acids (Marchuk, Saulino et al. 1991; Costa and Silva 2003), which is most well-known for being a major GAP for Ras proteins (Mazzucchelli and Brambilla 2000). The GRD of neurofibromin consists of a 360-amino acid region with 25% sequence homology to the catalytic domain of GAP and represents only a small portion (~12%) of the protein. Besides the GRD in the central portion of the protein (**Figure 1.7.**), neurofibromin also includes other biochemical domains, namely a PKA signaling domain close to the C terminal of the protein (**Figure 1.7.**), a PH domain and a Sec14-homology domain located in between the GRD domain and the C terminal (**Figure 1.7.**). Additionally, a regulatory domain with multiple phosphorylation sites (cysteine-serine rich domain, CSRD) has been described upstream the GRD domain (**Figure 1.7.**) and it

was demonstrated that phosphorylation of this region can regulate the RasGAP activity of neurofibromin (Mangoura, Sun et al. 2006; Larizza, Gervasini et al. 2009). The GRD domain is responsible for the negative regulation of Ras signaling (Xu, Lin et al. 1990), whereas the C terminal region contributes for PKA activation (The, Hannigan et al. 1997). Also, neurofibromin interacts with microtubules (McClatchey 2007; Shilyansky, Lee et al. 2010).

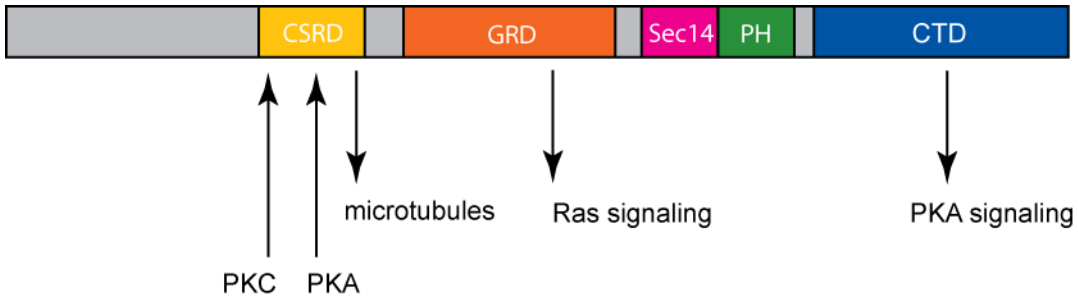

Figure 1.7. Schematic representation of neurofibromin biochemical domains, signaling and regulation. *Adapted from Larizza, Gervasini et al. 2009.*

Neurofibromin Expression and Distribution

Western blot and immunocytochemistry studies by Daston and Ratner (1992) demonstrated that neurofibromin is ubiquitously expressed in embryonic rats and is down-regulated in non-neuronal tissue during late fetal and early postnatal development (Daston and Ratner 1992). As a consequence, in the adult, neurofibromin is mainly expressed in the nervous system, despite its ubiquitous expression at very low levels (Mazzucchelli and Brambilla 2000). Within the brain, neurofibromin is predominantly expressed in neurons, non-myelinating Schwann cells, and oligodendrocytes (Danglot, Régnier et al. 1995). Within neurons, neurofibromin is expressed in many neuronal cell types, irrespective of neurotransmitter expression, neuronal pathway, or brain region (Daston, Scrable et al. 1992; Gutmann and Collins 1993). At the subcellular level, neurofibromin is very hydrophilic and has no transmembrane domains or other common protein motifs, therefore it is estimated that neurofibromin is a cytosolic protein. More specifically, neurofibromin was shown to distribute in the cytoplasm in a fibrillar array coincident with the

localization of the microtubules (Gutmann, Boguski et al. 1993). However, some reports claim that neurofibromin could also be located in the nucleus (Li, Cheng et al. 2001; Vandenbroucke 2004; Leondaritis, Petrikkos et al. 2009). Interestingly, a proteomic study by Husi and collaborators (2000) revealed that, in the mouse brain, neurofibromin associates with the NMDAR complex (Husi, Ward et al. 2000). Furthermore, another study reported that, in immature cultured cortical neurons, neurofibromin localizes to axons, neurites and the cell soma. In mature cultures, neurofibromin had a more diffuse pattern in the cell soma and a punctate distribution coincident with the distribution of a postsynaptic marker (Ethell and Yamaguchi 1999; Hsueh, Roberts et al. 2001). Moreover, subcellular fractionation of the adult brain revealed that neurofibromin is present, but not concentrated, at the PSD (Hsueh, Roberts et al. 2001).

Neurofibromin Signaling

Upstream Signaling

To date, the activators of neurofibromin in adult neurons have not been identified. However, neurofibromin is quickly regulated by PKC in response to growth factors that utilize tyrosine kinase receptors (Mangoura, Sun et al. 2006), and by ubiquitin-dependent proteolysis in response to both G-protein and tyrosine receptor signaling ligands (Cichowski, Santiago et al. 2003; Shilyansky, Lee et al. 2010; Vigil, Cherfils et al. 2010). In embryonic neuronal cultures, the Ca^{2+}-sensitive PKCα isoform phosphorylates neurofibromin in its N terminal, increasing its association with actin and maximizing its activity (Mangoura, Sun et al. 2006). Additionally, neurofibromin C tail serine phosphorylation, probably at Ser^{2808}, by PKC, following phorbol ester 12-O-tetradecanoyl-phorbol-13-acetate (TPA) stimulation, leads to neurofibromin translocation from the nucleus to the cytoplasm and increases its RasGAP activity (Leondaritis, Petrikkos et al. 2009). Thus, neurofibromin RasGAP activity might be activity-dependent. Growth factors can also quickly, but transiently, induce ubiquitin-dependent proteolysis of neurofibromin in an activity-dependent manner (Cichowski, Santiago et al. 2003). Nevertheless, it remains to be confirmed whether similar regulation of neurofibromin occurs in adult neuronal networks. Another possible

upstream regulator is the NMDAR. Notably, neurofibromin is part of the NMDAR complex in the mouse forebrain (Husi, Ward et al. 2000). The NMDAR interacts with intracellular signaling cascades through its C terminal, in a manner that is independent of Ca^{2+} influx (Bannerman, Niewoehner et al. 2008). Together, these suggest that neurofibromin could play a role in NMDAR-dependent regulation of Ras signaling.

Downstream Signaling

Neurofibromin has multiple biochemical roles. Neurofibromin is a RasGAP, negatively regulating Ras signaling and its downstream targets (**Figure 1.8.**) (Xu, Lin et al. 1990). Hence, in neurons, loss of neurofibromin leads to constitutive increases in intracellular Ras activity and its downstream signaling (Guilding, McNair et al. 2007). Also, inhibition of Ras by neurofibromin regulates the PI3K-Akt-mTOR pathway, as evidenced by studies that suggest that *Nf1* deficiency results in elevated activity of mTOR (Dasgupta, Yi et al. 2005; Johannessen, Reczek et al. 2005). Further, neurofibromin loss-of-function can allow Ras signaling to become decoupled from extracellular triggers, such as growth factors. Thus, following growth factor release or other signals, neurofibromin could act to limit and narrow the time window for Ras activation.

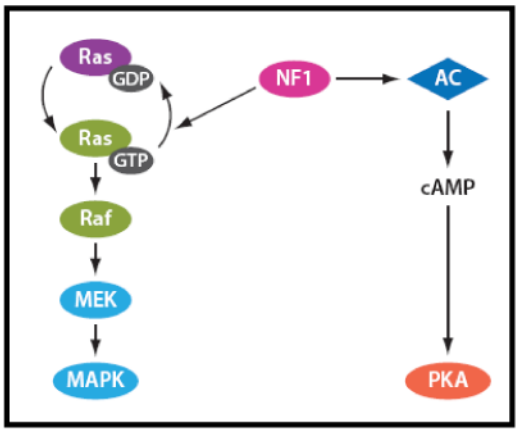

Figure 1.8. Simplified neurofibromin signaling. Neurofibromin functions as a negative regulator of the Ras-MAPK signaling cascade. Neurofibromin is also an activator of AC. *Adapted from Shilyansky et al. 2010*.

In addition to its role as a RasGAP, neurofibromin acts as an activator of adenylate cyclase (AC) (**Figure 1.8.**) (Tong, Hannan et al. 2002). Interestingly, neurofibromin can increase the AC activity in a Ras-dependent manner, flowing growth factor activation. Neurofibromin can also increase directly AC activity in a Ras-independent manner through its C terminal domain (Hannan, Ho et al. 2006).

The *Nf1* Gene

The *Nf1* gene, which encodes neurofibromin, is located on the q11.2 region of chromosome 17 and is one of the largest in the genome (Xu, Lin et al. 1990; Marchuk, Saulino et al. 1991). The *Nf1* gene is evolutionary highly conserved, with homologues present in most eukariotic genomes. The mouse *Nf1*-encoded protein shares 98% amino acid identity with their cognate human proteins (McClatchey 2007). The transcriptional regulation and downstream targets of *Nf1* are also conserved across species (Shilyansky, Lee et al. 2010). The *Nf1* gene is ubiquitously expressed throughout the body (Danglot, Régnier et al. 1995; Shilyansky, Lee et al. 2010) and it is driven by a weak promoter which accounts for its low expression in most mammalian cells (Larizza, Gervasini et al. 2009). Within the CNS, *Nf1* transcription is seen in the brainstem, cerebellum, striatum, cortex, hippocampus, and substantia nigra. In the cortex and hippocampus, *Nf1* is expressed in pyramidal neurons, interneurons, and glia (Shilyansky, Lee et al. 2010).

Several alternatively spliced isoforms of the *Nf1* gene have been reported. Alternative splicing of *Nf1* in exon 9a gives rise to an isoform including an additional 30bp sequence, which leads to the insertion of 10 amino acids between residues 420 and 421 of neurofibromin, at the junction of exons 9 and 10a. This isoform is specifically expressed in the CNS, in neurons. Alternative splicing of exon 23a gives rise to isoforms I and II. Interestingly, exon 23a encodes a 63bp (21 amino acids) region within the GRD domain. Exclusion of exon 23a produces isoform I of neurofibromin, whereas inclusion results in isoform II. Isoform II has a greater affinity for Ras, but 10 times lower RasGAP activity as compared to isoform I (Yunoue, Tokuo et al. 2003). Isoform I is predominantly expressed in neurons, while isoform II is mostly expressed in glia (Gutmann, Geist et al. 1995). The transcripts including exon 23a are widely expressed in all tissues and are the most abundant form in adult tissues apart from the brain. Exon 48a is

located in the 3' region of the coding sequence and inserts 54 nucleotides in the *Nf1* mRNA. The resulting transcripts are highly expressed in muscle (cardiac, skeletal and smooth) and weakly in several other tissues. Another alternatively spliced exon removes exon 11, thereby generating a truncated transcript that lacks the GRD domain and whose function remains unknown (Danglot, Régnier et al. 1995; Shilyansky, Lee et al. 2010).

The *Nf1* gene is considered a tumor suppressor gene, since loss-of-function mutations have been associated with the occurrence of benign and malignant tumors in neural-crest derived tissues (Danglot, Régnier et al. 1995). Loss-of-function *Nf1* mutations result in decreased cycling from the active to inactive state of Ras, thus leading to Ras hyperactivity and increased cell proliferation (Mitin, Rossman et al. 2005). Interestingly, the calculated mutation rate for *Nf1* is 1:10000, which is about 100-fold higher than the usual mutation rate for a single locus (Marchuk, Saulino et al. 1991). Inactivation of the mouse *Nf1* gene revealed that, like most tumor suppressors, *Nf1* is required for normal embryonic development. Therefore, the complete loss of neurofibromin is lethal. Homozygous *Nf1* mutant mice display heart malformation, hyperplasia of sympathetic ganglia, and die embryonically around E13.5 (Jacks, Shih et al. 1994; McClatchey 2007). Heterozygous mice for the null mutation are viable, but show increased tumor incidence with age (Jacks, Shih et al. 1994).

Neurofibromatosis Type I

Neurofibromatosis Type I (NF1), or von Recklinghausen disease, was described in the late 1700s, but was first recognized as a disorder and characterized extensively in 1882 by von Recklinghausen (McClatchey 2007). NF1 is an autosomal dominant genetic disease that affects about 1 of 3500 individuals in all ethnic groups. NF1 is caused by loss-of-function mutations in the gene *Nf1* and primarily affects tissues that derive from the neural crest. NF1 is characterized by multiple symptoms and pathologies, but the hallmark of the disease is the development of cutaneous café-au-lait spots (hyperpigmentation of melanocytes), Lisch nodes (harmatomas of the iris) (**Figure 1.9.**) and multiple neurofibromas, which are found in > 90% of the patients (Jett and Friedman 2010). The presence of

multiple benign tumors in the CNS and in the peripheral nervous system (PNS), as well as generally all over the body (myeloid leukemias, phaeochromocytomas), is also frequent (Cichowski, Shih et al. 1999; Costa and Silva 2003). The benign neurofibromas can develop into malignant peripheral-nerve sheath tumors (MPNSTs) (Jett and Friedman 2010). Some NF1 patients may also show optic pathway gliomas and other neurological lesions (Zhu, Harada et al. 2005; Albers and Gutmann 2009). Furthermore, in the brain, *Nf1* mutations can result in astrogliosis and astrogliomas (Nordlund, Rizvi et al. 1995; Zhu, Romero et al. 2001), and in learning disabilities that occur in 40-60% of the NF1 patients (Jett and Friedman 2010). Additionally, there is a significant incidence of headaches and seizures (Jett and Friedman 2010). A minority of patients might also have renal hypertension and occasionally skeletal abnormalities (such as scoliosis, pseudoarthrosis, megalencephaly, and short stature) (Jett and Friedman 2010) or mental retardation (Marchuk, Saulino et al. 1991; Danglot, Régnier et al. 1995).

Not only the NF1-related symptoms are diverse, as their onset and severity are rather variable and age-dependent. This is true even among patients belonging to the same family and carrying the same mutation (Marchuk, Saulino et al. 1991; Gutmann and Collins 1993; McClatchey 2007). In spite of its familial nature, NF1 is also characterized by an incredible high incidence of new mutations, due to the peculiarly high mutation rate and large size of the *Nf1* gene. New mutations account for approximately 50% of NF1 cases, unrelated to a family history of the disease. Among the diversity of mutations reported in NF1 patients, small deletions, insertions, nonsense mutations, frameshift mutations, or truncating mutations that completely inactivate the gene have been detected. To bring even more complexity to the disease, genotype-phenotype correlations have been difficult to establish within the NF1 condition. Except for extremely severe cases, correlated with huge deletions in the *Nf1* gene, most patients show only some symptoms of NF1. Even though, the clinical display of symptoms extends from minimal to severe. Some reports have partially attributed such diversity of symptoms to the contribution of modifying genes (Gutmann and Collins 1993; Ward and Gutmann 2005; McClatchey 2007).

Due to the crucial role of Ras in growth and development, NF1-associated tumorogenesis is strongly related to the inability to downregulate Ras. Accordingly, NF1-mutant tumors exhibit elevated levels of Ras-GTP (McClatchey 2007). Particularly relevant evidence supporting this idea comes from a

report that identified a missense mutation in the *Nf1* gene, in a family with multi-symptomatic NF1. This mutation was found to specifically abolish the RasGAP activity of neurofibromin, without affecting its ability to bind Ras (Klose, Ahmadian et al. 1998), suggesting that the loss of RasGAP activity underlies the NF1 symptoms.

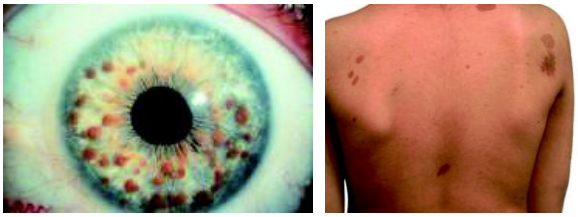

Figure 1.9. Examples of two of the most common symptoms of NF1. Lisch nodes (left) and café-au-lait spots (right). *Adapted from http://emedicine.medscape.com/article/1219222-overview and http://www.daviddarling.info/encyclopedia/B/birthmarks.html.*

Cognitive Deficits in NF1

NF1 does not cause global cognitive dysfunction, but specifically affects executive and other higher-order cognitive functions (Costa and Silva 2003; Hyman, Shores et al. 2005; Krab, Goorden et al. 2008). Specifically, NF1 affects planning, visuospatial function, reading/vocabulary, and motor coordination (Hofman, Harris et al. 1994; Costa and Silva 2003; Hyman, Shores et al. 2005). Additional deficits are seen in working memory, cognitive flexibility, and inhibitory control (Rowbotham, Pit-ten Cate et al. 2009). There is also a high correlation between NF1 and attention deficit disorder (Hofman, Harris et al. 1994; Kayl and Moore 2000; Koth, Cutting et al. 2000; North 2000; Costa and Silva 2003; Hyman, Shores et al. 2005). Overall, individuals with NF1 require special education (Krab, Goorden et al. 2008), which is able to compensate for the cognitive deficits.

Insights from Animal Models of NF1

Heterozygous *Nf1* knockout (*Nf1*$^{+/-}$) mice were established as an animal model for NF1 disease by Jacks and collaborators (1994). Like patients with NF1, this mouse is heterozygous for the *Nf1* loss-of-function mutation. The *Nf1*$^{+/-}$ mouse was made by inserting a neo gene in exon 31 of the *Nf1* gene, which leads to an unstable, quickly degraded transcript (Jacks, Shih et al. 1994). Based on the genetic, biochemical and behavioral parallels between the *Nf1*$^{+/-}$ mouse model and human NF1, it is thought that this mouse offers a useful model of the behavioral and cognitive symptoms associated with the disorder. The *Nf1*$^{+/-}$ mouse has, therefore, been utilized to identify physiological and molecular mechanisms that contribute critically to cognitive and behavioral changes associated with NF1 and important achievements were made in the past decade.

Nf1$^{+/-}$ mice are prone to developing some of the tumors seen in NF1 patients, notably pheochromocytoma and myeloid leukemia (Jacks, Shih et al. 1994). Furthermore, *Nf1*$^{+/-}$ mice also develop astrogliosis in several brain regions (Rizvi, Akunuru et al. 1999), including the hippocampus. Like most NF1 children, *Nf1*$^{+/-}$ mice are hyperactive and have attention problems, which can be rescued by Ras inhibitors (Li, Cui et al. 2005). At the cognitive level, *Nf1*$^{+/-}$ mice show spatial learning deficits in the hidden version of the Morris water maze (Silva, Frankland et al. 1997; Costa, Fedorov et al. 2002; Li, Cui et al. 2005; Cui, Costa et al. 2008), a task dependent on the hippocampal function. This suggests a role of neurofibromin in the hippocampus during memory processing. Probe trials given early on during water maze training revealed that *Nf1*$^{+/-}$ mice required more training trials than control animals to learn the position of the hidden platform. In other words, when searching for the missing platform in probe trials, the mutant mice spent less time in the appropriate quadrant compared to their WT littermates (Costa, Fedorov et al. 2002). Interestingly, *Nf1*$^{+/-}$ mice were able to overcome their performance deficit with extended training, which bypasses the requirement of the hippocampus (Packard and McGaugh 1996; Pouzet, Zhang et al. 2002). This sensitivity to overtraining is also a feature reported in NF1-associated learning disabilities in patients. *Nf1*$^{+/-}$ mice also show deficits in contextual conditioning, a test where mice associated a novel chamber with a mild foot shock (Cui, Costa et al. 2008). As with the Morris water maze, contextual conditioning has a spatial learning component and requires hippocampal function.

Interestingly, despite the finding by Nordlund and collaborators (1995) that neurofibromin is expressed in many brain regions (Nordlund, Rizvi et al. 1995), Silva and collaborators (1997) did not observe any memory deficit in *Nf1*$^{+/-}$ mice in cued fear conditioning, a form of amygdala-dependent and hippocampus-independent memory task, suggesting that neurofibromin does not affect amygdala-mediated memory (Silva, Frankland et al. 1997). Electrophysiological studies in the CA1 region of the hippocampus of *Nf1*$^{+/-}$ mutant mice demonstrated that LTP is impaired when induced with a TBS protocol (Costa, Fedorov et al. 2002). Interestingly, the same way that additional training rescues the learning impairments of the mutants, stronger synaptic stimulation (such as HFS) also rescues their LTP deficits (Costa, Fedorov et al. 2002). Therefore, the LTP deficits are thought to underlie the learning deficits seen in the *Nf1*$^{+/-}$ mice (Costa, Fedorov et al. 2002). Additionally, increased GABAergic inhibition was observed in these mice, compared to WT controls (Costa, Fedorov et al. 2002). Just as with the learning deficits, increased inhibition and synaptic plasticity impairments of the *Nf1*$^{+/-}$ mice were reversed by manipulations that decrease Ras activity (Costa, Fedorov et al. 2002; Li, Cui et al. 2005). *Nf1*$^{+/-}$ mice crossed to null Ras mutants (*KRas*$^{+/-}$ or *NRas*$^{-/-}$ mice) resulted in a double *Nf1*/*Ras* mutant that performed at the same level as the WT mice, even though each mutant individually showed deficits in this task (Costa, Fedorov et al. 2002). Equally, while LTP deficits were seen individually in each mutant, these were rescued in the double *Nf1*/*Ras* mutant (Costa, Fedorov et al. 2002). Also, pharmacological agents, such as FTase inhibitors, which inhibit Ras activity, were able to rescue the performance of the *Nf1*$^{+/-}$ mouse in the Morris water maze task and the LTP deficits (Costa, Fedorov et al. 2002; Li, Cui et al. 2005). Downstream the signaling pathway, Guilding et al. (2007) found that basal ERK phosphorylation and downstream CREB phosphorylation were elevated in the hippocampus of the *Nf1*$^{+/-}$ mice, while there was no change in the PI3K cascade. This suggests that neurofibromin specifically suppresses the ability of Ras to activate the Raf-MEK-ERK-CREB cascade. In this study, application of a subthreshold dose of a MEK inhibitor, which reversed the abnormal increase in ERK and CREB phosphorylation, reversed the LTP deficit in *Nf1*$^{+/-}$ mice (Guilding, McNair et al. 2007). Therefore, in *Nf1*$^{+/-}$ mice, both LTP and memory deficits are caused by increased Ras signaling due to loss of regulation by neurofibromin (Costa, Fedorov et al. 2002; Li, Cui et al. 2005; Cui, Costa et al. 2008).

The idea that modifying genes underlie the variability in the expression of NF1-related symptoms came from mouse studies, which indicated that background genetic modifiers alter the expression of *Nf1*$^{+/-}$-related phenotypes. For example, in the NF1 mouse model, the phenotypic effect of the *Nf1* mutations depends on the background strain on which that mutation is expressed (Silva, Frankland et al. 1997; Hawes, Tuskan et al. 2007). Since these strains are engineered with the same *Nf1* mutation, phenotypic differences across strains are attributed to differential expression of modifying genes across mouse strains. Silva and collaborators reported that, although the *GluN1*$^{+/-}$ mutation alone does not have a spatial learning phenotype, it exacerbates the spatial learning phenotype of the *Nf1*$^{+/-}$ mutant mice (Silva, Frankland et al. 1997).

Conditional mutants of the *Nf1* gene have also been extensively studied to identify the effects of *Nf1* deletion within specific neuronal types. Conditional mutants can be created in mice using the Cre-loxP system, a powerful tool widely used for restricting gene deletions to specific time frames, cell types, or areas. A mouse line was engineered with loxP sites flanking exons 31-32 of the *Nf1* gene (*Nf1* $^{flox/flox}$). The floxed *Nf1* gene acts like the WT allele prior to the expression of Cre recombinase. Mice carrying one floxed *Nf1* allele and one deleted *Nf1* allele (*Nf1*$^{+/floxed}$) show the same phenotypes as *Nf1*$^{+/-}$ mice (Zhu, Romero et al. 2001). Cui and collaborators (2008) used this strategy to cross *Nf1*$^{flox/flox}$ mouse with mice expressing Cre recombinase under the control of cell-type-specific promoters: Synapsin 1 promoter (for expression in neurons only), GFAP promoter (for expression in astrocytes only), αCaMKII promoter (for expression in pyramidal neurons only) and Dlx5/6 promoter (for expression in GABAergic neurons only) (Cui, Costa et al. 2008). They observed that *Nf1* deletion and increased Ras signaling has cell-type specific physiological effects that contribute to behavioral symptoms. Surprisingly, they reported that neurofibromin expression in hippocampal pyramidal neurons might not have such an essential role in hippocampal learning, in the strains of mice tested and tests performed. In contrast, neurofibromin expression in interneurons might be crucial for cognitive performance. In the Morris water maze, heterozygous deletion of *Nf1* from inhibitory neurons was sufficient to cause behavioral impairments, whereas deletion from pyramidal neurons or glia did not cause deficits in the conditions in which the task was performed. Thus, these authors reported that regulation of Ras signaling by *Nf1* is particularly critical in interneurons. In more detail, within the hippocampus of *Nf1*$^{+/-}$ mice, increased interneuronal Ras

signaling led to enhanced ERK phosphorylation, which therefore increased Synapsin 1 phosphorylation, a presynaptic protein involved in vesicle release. Consequently, *Nf1* deletion in interneurons caused enhanced activity-dependent GABA release, which, in turn, led to larger evoked inhibitory currents in CA1, shifting the balance between inhibitory and excitatory processes within the hippocampal networks of the mutant mice (Cui, Costa et al. 2008). As a result, LTP was impaired in the $Nf1^{+/-}$ mice, perhaps because the increased inhibition prevented sufficient depolarization of the NMDARs during learning (Costa, Fedorov et al. 2002; Cui, Costa et al. 2008). Both LTP and Morris water maze deficits were improved using picrotoxin (PTX), a $GABA_A$ receptor inhibitor, at concentrations that did not affect these phenomena in controls (Costa, Fedorov et al. 2002; Cui, Costa et al. 2008). Despite the fact that behavioral deficits occur as a result of a reversible increase in inhibition, it is important to also consider potential effects on development of neuronal networks, since most *Nf1* gene mutations in patients and mice are present from birth. Importantly, GABAergic inhibition plays an important role in the development patterning of neuronal networks, and so the *Nf1* mutation may cause development defects that correlate with symptoms of NF1 such as learning disabilities.

Finally, mouse models targeting specific biochemical domains of the *Nf1* gene have been examined to demonstrate the relative importance of the various regulatory functions of neurofibromin. Mice carrying a homozygous knockout of exon 23a of *Nf1* ($Nf1^{23a-/-}$), which encodes part of the GRD, showed no predisposition for tumor formation and developed normally. However, they exhibited impaired spatial learning and memory in the Morris water maze task (Costa, Yang et al. 2001). This study also underscores the importance of neurofibromin as a RasGAP in memory formation and revealed that the role of neurofibromin in memory and oncogenesis can be dissociated. Altered behavioral performance in these mutant mice is a direct function of their *Nf1* mutation, rather than a secondary effect of tumor formation.

The strongest support for functions of neurofibromin beyond Ras regulation comes from studies of *Drosophila melanogaster Nf1* mutants. Homozygous inactivation of Drosophila *Nf1* yields viable flies, but ones that are abnormally small and exhibit electrophysiological, learning, and circadian defects (Guo, The et al. 1997; The, Hannigan et al. 1997; Guo, Tong et al. 2000; Williams, Su et al. 2001). In an

aversive conditioning task, *Nf1*-deficient flies showed both a learning deficit immediately after one-cycle training and a long-term memory deficit 24 hours after spaced repeated-trial (Guo, Tong et al. 2000; Ho, Hannan et al. 2007). Interestingly, learning defects in *Nf1* null *Drosophila melanogaster* could be rescued by overexpression of a constitutively active form of PKA (Guo, Tong et al. 2000). These and other data suggested that the associative learning impairments in *Nf1* null flies are due to decreased activity of AC. Also, the mutant flies performed normally in memory tests after massed training, once again suggesting that extensive training might compensate for the cognitive deficits inherent to NF1. Ho et al. (2007) found that the C terminal of neurofibromin, which activated AC, was important for immediate memory, whereas its GAP activity was specifically required for the formation of LTM followed spaced training. Regulation of AC by neurofibromin has also been found in rodents (Tong, Hannan et al. 2002; Dasgupta, Dugan et al. 2003; Ho, Hannan et al. 2007; Lin, Lei et al. 2007; Brown, Diggs-Andrews et al. 2011). Particularly relevant for the context of this dissertation, a recent study by Lin et al. (2007) demonstrated that neurofibromin removal by shRNA resulted in PKA-dependent loss of dendritic spines in hippocampal cultured neurons (Lin, Lei et al. 2007).

Treatment of the Cognitive Effects

Cognitive defects are a challenging aspect of NF1 management, with nearly half of NF1 children exhibiting some type of learning disability. The key pathophysiologic mechanism underlying *Nf1* mutations in both mice and humans is increased Ras activity (Costa, Fedorov et al. 2002). Therefore, Ras has been the preferred therapeutical target for NF1. Since posttranslational farnesylation is required for the membrane localization and function of Ras, inhibition of farnesylation has been widely explored for NF1 pharmacotherapy. Indeed, pharmacological inhibitors of FTase downregulate Ras activity. Li et al. (2005) identified lovastatin, a FTase inhibitor, as a potent inhibitor of Ras/MAPK activity. Lovastatin decreased the enhanced brain Ras-MAPK activity of the $Nf1^{+/-}$ mice, rescued the LTP deficits, and reversed their spatial learning and attention impairments. Hence, lovastatin is currently the best drug candidate to ameliorate the cognitive deficits associated with NF1 (Li, Cui et al. 2005).

Aims

The general goal of this dissertation is to study the role of neurofibromin in Ras signaling and morphological plasticity of dendritic spines in CA1 pyramidal neurons. Abnormal Ras inactivation may account for the spatial learning and memory deficits, as well as LTP impairment, associated with neurofibromin loss-of-function mutants, as seen in NF1 patients and in animal models of the disease (*Nf1*$^{+/-}$ mice) (Silva, Frankland et al. 1997; Costa, Fedorov et al. 2002; Li, Cui et al. 2005). Because spatial learning and memory have been extensively described as being dependent on hippocampal function (Morris, Halliwell et al. 1989; Eichenbaum, Stewart et al. 1990), and because synaptic plasticity (which has been best studied in the Schaffer-collateral pathway of the hippocampus) is thought to underlie memory formation and learning (Morris, Davis et al. 1990; Silva, Elgersma et al. 2000) we focused our research in hippocampus. Furthermore, most of the excitatory synapses are made onto dendritic spines (Nimchinsky, Sabatini et al. 2002; Holtmaat and Svoboda 2009; Lee and Yasuda 2009) and LTP can be expressed in single dendritic spines (Matsuzaki, Honkura et al. 2004), making dendritic spines an attractive location to study a signaling pathway that regulates synaptic plasticity. The Ras signaling pathway has been reported to have a fundamental role in synaptic plasticity, learning and memory. Additionally, previous studies have demonstrated that Ras is important for postsynaptic structural plasticity (Wu, Deisseroth et al. 2001; Arendt, Gärtner et al. 2004; Harvey, Yasuda et al. 2008). Furthermore, neurofibromin has been shown to interact with the NMDAR complex (Husi, Ward et al. 2000) and to be present in dendritic spines of cultured neurons (Hsueh, Roberts et al. 2001). Hence, we hypothesize that the changes observed in dendritic spines upon neurofibromin loss-of-function are due to a dysfunction in the Ras signaling pathway.

The first specific aim of this dissertation was to understand the role of neurofibromin in regulating the spine density and morphology in mature neurons. In order to do this, hippocampal organotypic slice cultures were sparsely transfected with neurofibromin shRNA and GFP and imaged under a TPLSM. The dendritic spine density and morphology were analyzed and we investigated whether the observed phenotype was Ras-dependent and activity-dependent through either genetic or pharmacological

manipulations. Furthermore, we examined if neurofibromin is also capable of regulating the number of functional synapses in the hippocampus, by recording mEPSCs in the same type of preparation (**chapter III**).

We also examined if neurofibromin regulates the spine structural plasticity, the structural basis of synaptic plasticity. In order to pursue this question, we stimulated single dendritic spines of CA1 hippocampal neurons using the 2-photon glutamate uncaging technique and monitored the volume change of the stimulated spine for 30 minutes. Finally, we asked whether the observed effects were Ras-dependent and/or activity-dependent. We determined through pharmacological manipulations that a decrease in NMDAR function rescues the phenotype created by neurofibromin loss-of-function. We performed calcium imaging experiments in combination with 2-photon glutamate uncaging to examine if the NMDAR is regulated by neurofibromin signaling in dendritic spines of CA1 neurons (**chapter IV**).

Lastly, we proposed to examine to what degree neurofibromin inactivates Ras in dendritic spines during spine structural plasticity. We first developed an improved Ras sensor with good sensitivity to image Ras activation in single dendritic spines. Then, we monitored Ras activation using advanced techniques, namely two-photon glutamate uncaging and fluorescence lifetime imaging (FLIM), under genetic manipulations that affect neurofibromin function (**chapter V**).

CHAPTER II

Materials and methods

Chapter II. Materials and methods

Introduction

In this chapter, we describe in detail all materials and methods that we used in experiments described in the following chapters. Data are presented as mean ± standard error of the mean (s.e.m.) unless otherwise specified.

General Strategy

To study the function of neurofibromin, we transiently downregulated neurofibromin using shRNA. Overexpression of the GRD domain of neurofibromin (isoform I) (Costa, Yang et al. 2001) and of several modified Ras constructs, including dominant negative ($HRas^{17N}$) (Feig 1999) and constitutively active forms ($HRas^{12V}$) (Feig and Cooper 1988; Ehrhardt, Ehrhardt et al. 2002) was also used to study specifically the role of neurofibromin in Ras regulation.

We used two-photon fluorescence lifetime imaging microscopy (TPFLIM) to image signaling activity with high spatial and temporal resolution in slices (Svoboda and Yasuda 2006). We used organotypic slice cultures from the hippocampal brain region of rats (Stoppini, Buchs et al. 1991). Also, we used ballistic gene transfer, which results in sparse labeling of the hippocampal slice and, thus, makes single spine imaging possible (McAllister 2000). Electrophysiology studies were used to study a physiological function of several observations, or to confirm some morphological events.

DNA Constructs, Antibodies and Reagents

MNI-caged-L-glutamate, NBQX, AP5 and TTX were purchased from Tocris Cookson (Ballwin, MO).

The antibodies used for shRNA validation were the following: rabbit anti-neurofibromin (Santa Cruz Biotechnology, sc-68), mouse anti-alpha actinin (BD Biosciences, 612576), rabbit anti-pERK1/2 (Cell Signaling, 4377) and mouse anti-ERK1/2 (Cell Signaling, 9107).

As for cDNA constructs, we used a plasmid including shRNA targeted to rat neurofibromin and EGFP (SABiosciences). The plasmid consists of a dual promoter CMV-EGFP/U1-shRNA vector (pGeneClip), which ensures coexpression of green fluorescent protein (GFP) and shRNA. The sequences GCAGCTAGATGAAGTCAACTT (NF1 shRNA #1) and GCTGGCAGTTTCAAACGTAAT (NF1 shRNA #2) were tested. The sequence GGAATCTCATTCGATGCATAC was used as a negative control shRNA (scrambled shRNA, sc-shRNA) that does not knockdown neurofibromin. Further, in order to obtain neurofibromin shRNA constructs that do not express EGFP, SDS-PAGE purified cDNA oligonucleotides were designed and purchased from Integrated DNA Technologies (IDT):

- sc-shRNA sense
  TGGAATCTCATTCGATGCATACCTTCCTGTCAGTATGCATCGAATGAGATTCCTTTTTTC;
- sc-shRNA antisense
  TCGAGAAAAAAGGAATCTCATTCGATGCATACTCACAGGAAGGTATGCATCGAATGAGATTCCA;
- NF1 shRNA #2 sense
  TGCTGGCAGTTTCAAACGTAATCTTCCTGTCAATTACGTTTGAAACTGCCAGCTTTTTTC;
- NF1 shRNA #2 antisense
  TCGAGAAAAAAGCTGGCAGTTTCAAACGTAATTCACAGGAAGATTACGTTTGAAACTGCCAGCA.

These were cloned into the pLL3.8 vector (also a dual promotor vector CMV-EGFP/U6-shRNA) using the HpaI and XhoI restriction sites. EGFP was removed from the pLL3.8 vector using restriction sites NheI and EcoRI, followed by vector klenowing. The change of vector was justified by the fact that the initial vector pGeneClip has no convenient restriction sites for EGFP removal and to gain the possibility of producing lentivirus expressing neurofibromin shRNAs in the future, if needed.

The GRD domain from neurofibromin isoform I (NF1-GRD) was obtained from Fuyuhiko Tamanoi lab through Addgene in the pGBT9 vector. NF1-GRD cDNA was amplified by polymerase chain reaction (PCR) using the following primers: GGCCAGCTAGCGAATTCATGGAATTGATGGAAGCC (forward) and GCGCTGGTACCGCCCCTTTCGATTCTAGG (reverse); and then inserted onto the pCI vector and onto the pmEGFP-C1 vector using the restriction sites EcoRI and KpnI.

The constructs pCI-mEGFP-HRas, pCI-mEGFP-HRas^{12V}, pCI-mEGFP-HRas^{17N}, pCI-mRFP-RBD-mRFP and pCI-mRFP-RBD^{59A}-mRFP were previously described (Yasuda et al. 2006). Two point mutations were inserted in the original pCI-mRFP-RBD-mRFP to produce pCI-mRFP-RBD^{65E,108A}-mRFP. To insert the K108A mutation, a PCR was performed using the following primers:

- CTCCACGAACACAAAGGTGCAAAAGCACGCTTAGATTGG (forward);
- CCAATCTAAGCGTGCTTTTGCACCTTTGTGTTCGTGGAG (reverse).

To insert the mutation K65E, a second PCR was performed using the primers:

- GCAACACTATCCGTGTTTTCTTGCCGAACGAGCAAAGAACAGTGGTCAATGTGCGAAATGG (forward);
- CCATTTCGCACATTGACCACTGTTCTTTGCTCGTTCGGCAAGAAAACACGGATAGTGTTGC (reverse).

All primers were purchased from IDT.

Cell Culture and Transfection

HEK293T cells were cultured in 35mm dishes in Dubelco's modified eagle medium (DMEM) supplemented with 10% fetal bovine serum (FBS) at 37^{o}C in 5% CO_2, and transfected with plasmid DNA using Lipofectamine 2000 (Invitrogen), according to the manufacturer's instructions: 2µg of cDNA in 100µL Opti-MEM (Invitrogen) was mixed with 3µL of lipofectamine 2000 in 100µL Opti-MEM that was pre-incubated for 5 min at room temperature. The mixture was incubated for 20 min and added dropwise into the media. Cells were then incubated for 24 hours.

HEK293T cells were used to test for the different Ras sensors. Approximately 16-18 hours after transfection, the cells were deprived by a reduction of the FBS supplement in the DMEM from 10% to

0.5%. Eight hours after that, the cells were imaged in a solution containing HEPES (30mM, pH 7.3) buffered ACSF (130mM NaCl, 2.5mM KCl, 1mM $CaCl_2$, 1mM $MgCl_2$, 2mM $NaHCO_3$, 1.25mM NaH_2PO_4 and 25mM glucose) (Murakoshi, Lee et al. 2008).

For shRNA validation, hippocampal neuron cultures were prepared from E18 rat embryos and grown on 35mm dishes coated with poly-D-lysine as previously described (Liao, Zhang et al. 1999; Ehlers 2000). The hippocampal neuron cultures were kindly prepared by Carrie Marean-Reardon, in Dr. Michael Ehlers laboratory.

Lentivirus and Infection

Lentivirus packaged with pLL3.8 harboring either scrambled control shRNA or shRNA targeting neurofibromin and mEGFP were generated by the Duke Neurotransgenic Laboratory, supported, in part, with the funding from NIH-NINDS Center Core Grant 5P30NS061789. For the shRNA validation experiments, hippocampal neuron cultures were infected with the lentivirus mentioned in the previous paragraph at DIV 1-3. Cell lysates were collected 5-7 days later for immunoblot analysis.

Organotypic Hippocampal Slice Cultures and Transfection

Hippocampal slice cultures were prepared from postnatal day 6 or 7 rats (Stoppini, Buchs et al. 1991), in accordance with the animal care and use guidelines of the Duke University Medical Center. Pups were anesthetized using isofluorane, decapitated, and quickly placed in chilled dissection media containing: 1mM $CaCl_2$, 5mM $MgCl_2$, 10mM glucose, 4mM KCl, 26mM $NaHCO_3$ and 248mM sucrose. The hippocampuses were removed, transferred to a tissue chopper and sliced into 350 µm slices. Next, the slices were placed on a Millipore membrane (3 to 5 slices per membrane), with a 0.2µm pore size filter, and left to incubate in tissue media (pH 7.4 and mOsm 300) containing: 0.0084g/ml HEPES base MEM, 20% horse serum, 1mM L-glutamine, 1mM $CaCl_2$, 2mM $MgSO_4$, 12.9mM D-glucose, 5.2mM $NaHCO_3$, 30mM HEPES, 0.075% ascorbic acid, and 1µg/ml insulin. The organotypic slice cultures were incubated

at 35^{o}C, 97% O_2 and 3% CO_2. The culture medium was changed every 2-3 days. After 10-15 days in culture, the slices were ballistically transfected, using a Helius gene gun (Bio-Rad). Bullets were prepared using 8-11mg of 1.6μm gold particles (Bio-Rad) coated with a total of 50μg of plasmids containing cDNA. For the Ras sensor, a ratio of 1:1:3 was used between neurofibromin construct (sc-shRNA, NF1 shRNA or GRD1; 10μg), Ras sensor donor (mEGFP-HRas; 10μg) and Ras sensor acceptor (mRFP-RBD^{65E,108A}-mRFP; 30μg). For all pharmacological experiments, the respective drug ($MgCl_2$ or AP5) was added to the culture medium at the time of transfection and kept in the culture medium until the experiment was performed. Experiments were done 4-7 days later, to allow for full knockdown of the *Nf1* gene. At this time, hippocampal slices containing transfected CA1 neurons located between 15 to 100μm deep from the surface were used for imaging, at room temperature (~ 25^{o}C).

Western Blot

E18 hippocampal neurons were infected with lentivirus harboring shRNAs constructs directed against neurofibromin or scrambled control shRNA. Five to seven days later, the majority of the cells were verified to be infected by checking for green fluorescence in the culture. The neurons were lysed in TEENT lysis buffer (50mM Tris-HCl, 1mM EDTA, 1mM EGTA, 150mM NaCl, 1% Triton X-100, pH 7.4) containing a protease inhibitor cocktail (Roche) (Wang, Edwards et al. 2008). The lysates were cleared by centrifugation and protein concentrations were measured by BCA assays (Pierce). Samples containing equal amounts of protein were denatured in Laemli buffer and boiled for 5 minutes. The samples were then subjected to SDS-PAGE and immunoblotting. Briefly, the lysates were loaded on 7.5% acrylamide gels for protein separation and transferred to a PVDF membrane (pore size 0.45 μm, Millipore). Following blocking with 5% nonfat dry milk in 1x TBS containing 0.25% Tween-20, the PVDF membrane was incubated with primary antibodies, at 4^{o}C, overnight. The membrane was washed several times and then incubated with secondary antibodies conjugated with horseradish peroxidase (HRP) (Jackson Immunoresearch, West Grove, PA) diluted at 1:5000, for one hour, at room temperature. Signals were visualized with the enhanced chemiluminescence (ECL Plus) detection systems (GE Biosciences). Alpha-actinin, in the same sample, was used as a loading control. Primary antibodies used in the study include:

rabbit anti-neurofibromin 1:500 (Santa Cruz, sc-68), mouse anti-alpha actinin 1:5000 (BD Biosciences, 612576), rabbit anti-pERK1/2 1:1000 (Cell Signaling, 4377), and mouse anti-ERK1/2 1:1000 (Cell Signaling, 9107).

mEPSC Recording

mEPSC recording was performed as previously described (Shankar, Bloodgood et al. 2007). The hippocampal slices were placed in standard artificial cerebral spinal fluid (ACSF) containing: 130mM NaCl, 2.5mM KCl, 2mM $NaHCO_3$, 1.25mM NaH_2PO_4 and 25mM glucose aerated with 95% O_2 and 5% CO_2. The following pharmacological agents were added to the ACSF: 20μM bicuculline, 1μM TTX, 20μM mibefradil, 100μM PTX, 20μM nimodipine, 50μM AP5. This combination of antagonists, in combination with intracellular cesium, blocks many dendritic conductances, increases the resting input resistance, and improves the ability to detect mEPSCs.

Whole-cell voltage-clamp recordings were obtained at a holding potential of - 70 mV, from visually identified transfected CA1 pyramidal hippocampal neurons or their neighboring unstransfected pyramidal neurons, using pipettes (4-5MOhm) containing Cs-based internal solution: 100mM Cs methanesulfonate, 20mM CsCl, 10mM HEPES, 10mM EGTA, 4mM $MgCl_2$, 0.4mM NaGTP, 4mM MgATP, 10mM phosphocreatine.

Recordings were made using a Multiclamp 700B amplifier, filtered at 2kHz, digitized at 10kHz, and acquired during a 60s period. Five recordings were made and averaged per neuron.

mEPSCs were analyzed in MATLAB, using custom software with detection criteria that included an amplitude > 8 pA, a minimum rise rate of 5 pA/ms, and a decay constant between 1-12 ms.

Two-Photon Fluorescence Microscopy

A custom-built two-photon microscope with two Ti:sapphire pulsed lasers (MaiTai; Spectra-Physics, Fremont, CA) was used for imaging (**Figure 2.1.**). One of the lasers was tuned to 920nm for imaging of mEGFP- and mRFP-tagged constructs, the other one was tuned to 720nm for glutamate uncaging. The intensity of each laser beam was independently controlled with electro-optical modulators (350-80 LA; Conoptics, Danbury, CT). Two laser beams were combined using a beam-splitting cube and passed through the same set of galvano-scanning mirrors and objective (60X, 0.9 NA; Olympus, Melville, NY). Emitted fluorescence from mEGFP- and mRFP-tagged constructs was divided using a dichroic mirror (565nm; Chroma) and detected by wide aperture photomultiplier tubes (PMTs; R3896; Hamamatsu) for both red and green fluorescence after wavelength filters (HQ510/70-2p for green and HQ620/90-2p for red; Chroma Techonology, Brattleboro, VT). Fluorescence was detected by summing epifluorescence and transfluorescence signals, as previously described (Mainen, Maletic-Savatic et al. 1999). Fluorescence signal was acquired by ScanImage (Pologruto, Sabatini et al. 2003), using a data acquisition board (PCI-6110, National Instruments).

The only exception to this occurred during the excitation of the red fluorescence for the cell line experiments described in **chapter V**. For these experiments, the red fluorescence was acquired in a similar system, but using a mode-locked Ytterbium-doped laser with a fixed wavelength of 1030nm (Amplitude Systèmes, Bordeaux, France).

All two-photon based experiments were performed at a constant temperature of ~ 25^{o}C in Mg^{2+}-free ACSF containing the following: 4.0mM $CaCl_2$, 1µM TTX and 2.0mM 4-methoxy-7-nitroindolinyl (MNI)-caged-L-glutamate. ACSF was constantly bubbled with 95% O_2 and 5% CO_2 through the experiments.

Imaged and stimulated spines were located on secondary and tertiary apical dendrites within 50 to 150µm from the soma.

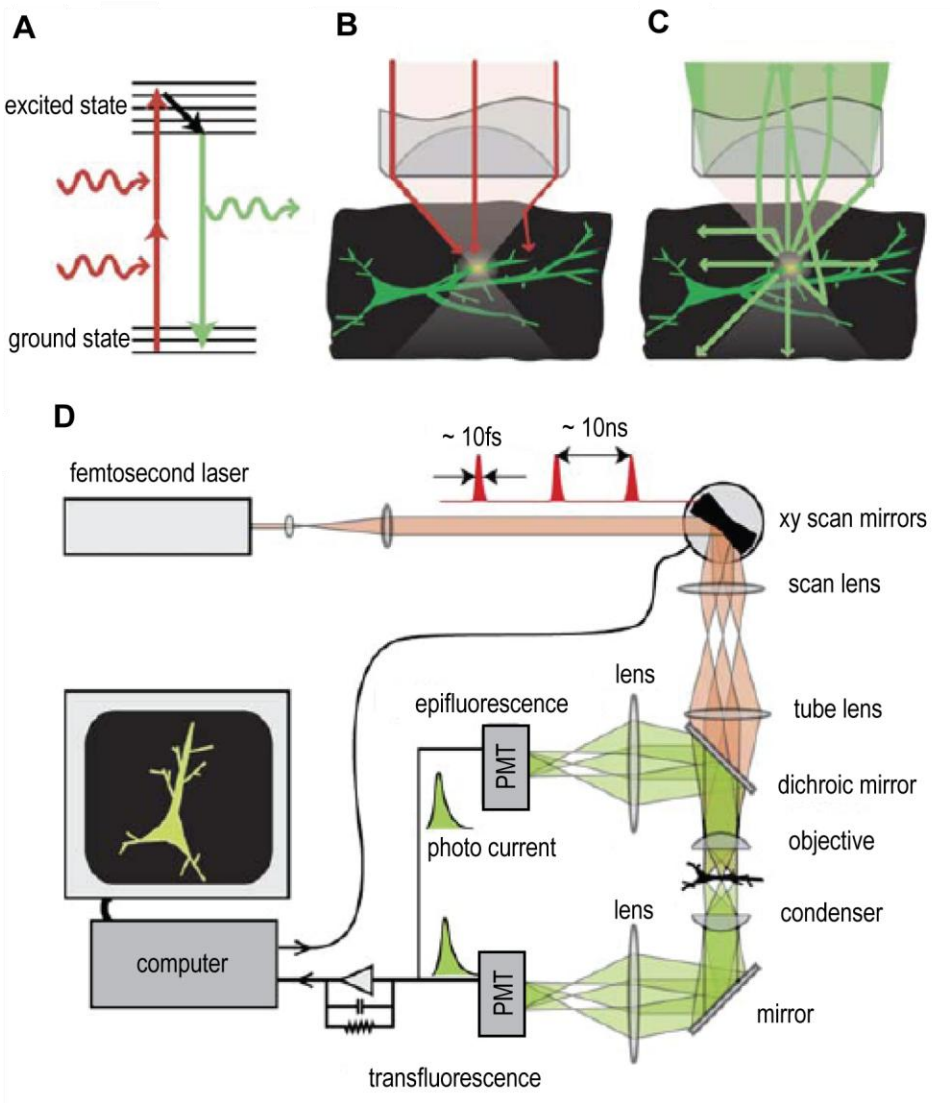

Figure 2.1. Two photon excitation microscopy. (A) Simplified Jablonski diagram of the two-photon excitation process. **(B)** Localization of excitation in a scattering medium (black). The excitation beam (red) is focused to a diffraction-limited spot by and objective where it excites green fluorescence in a dendritic branch, but not in a nearby branch. The paths of two ballistic photons and one scattered photon are shown (red lines). Scattered photons are too dilute to cause off-focus excitation. The intensity of the beam decreases with depth as an increasing number of excitation photons are scattered. **(C)** Fluorescence collection in a scattering medium. Fluorescence photons are emitted isotropically from the excitation volume (red lines). Even scattered fluorescence photons contribute to the signal if they are collected by the objective. Since the field of view for detection is larger than for excitation, the fluorescence light exiting the objective back-aperture will diverge substantially (green). **(D)** Schematic of a two-photon excitation microscope with epifluorescence and transfluorescence detection. *Adapted from Svoboda and Yasuda (2006).*

Morphometric Imaging

Transfected CA1 pyramidal neurons of the hippocampus were identified by green fluorescence and characteristic morphology 5-8 days after transfection. High resolution images (512 x 512) were acquired as z-stacks of several sections at 2µm spacing for the full neuron or 1µm spacing for apical dendrites. Each section was an average of three scans. First, one image of the entire cell was taken (x,y = 342µm x 369µm), followed by three to four images of apical dendrites (x,y = 70µm x 80µm). Morphometric analysis was performed using custom software written in MatLab (Mathworks, Natick, MA). Spines were counted, and the total number was divided by the length of dendrite in the field of view to calculate the density. The spine type was automatically categorized by the software and spine length was measured from the tip of the protrusion to the junction with the dendritic shaft. Spine volume was also calculated. For neurons chronically exposed to AP5, imaging was performed in the constant presence of the antagonist.

Two-Photon Glutamate Uncaging and Spine Enlargement

Five to seven days after transfection, local uncaging stimulation was delivered on the tips of spine heads (~ 0.5µm from the center of the spine in the direction away from the dendritic shaft), upon 4 basal acquisitions spaced by one minute interval, to stimulate the glutamate receptors (in particular, NMDARs, **Figure 2.2.**) in the spine. Only spines well separated from the parent dendrite and nearby spines were selected for experiments. For individual experiments, Z stacks were acquired 4 times before plasticity induction and then acquired once every minute after the uncaging protocol for 30 minutes. Images were acquired with a resolution of 128 x 128 pixel (x,y = 14µm x 17µm).

The uncaging protocol applied to induce structural plasticity consisted of 30 uncaging pulses with 6ms duration at 0.5Hz, in ACSF containing 4mM $CaCl_2$, 0mM $MgCl_2$, 1µM TTX and 2mM MNI-L-glutamate. Individual z-series were then collapsed into maximum projections and used to quantify the integrated fluorescence intensity of individual spines. For the experiments described in **chapter IV**, the GFP fluorescence intensity was used to measure the spine volume, whereas the mRFP signal from

mRFP-RBD^{65E,108A}-mRFP was used to measure the spine volume for the FLIM experiments described in **chapter V**. The changes in spine volume upon uncaging were quantified by the fractional change in fluorescence light intensity ([F-F0]/F0). The sustained volume change was calculated as the mean volume at 25 min to 30 min minus the mean baseline, normalized to the baseline volume. The transient volume change was calculated as the difference between the mean peak volume at ~ 1 min after uncaging and the sustained phase, normalized to the baseline volume. The volume increase caused by NMDAR activation could be overestimated for the FLIM experiments, because a population of mRFP-RBD^{65E,108A}-mRFP binds to activated Ras in the stimulated spine. However, since mRFP-RBD^{65E,108A}-mRFP is expressed at higher levels than mEGFP-Ras, this effect is likely small.

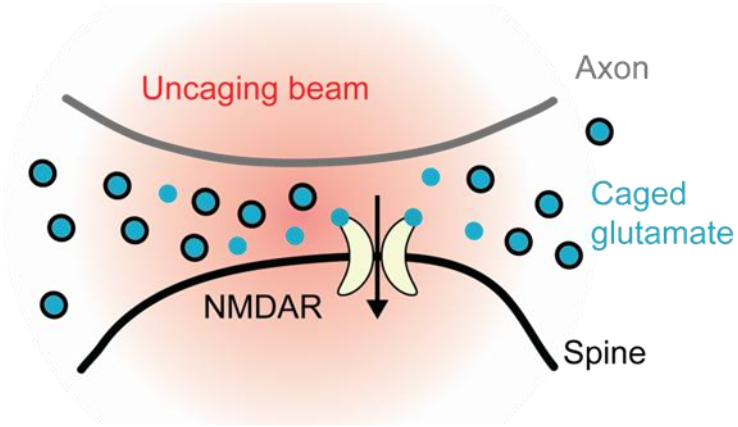

Figure 2.2. Schematic representation of a single spine stimulation by two-photon glutamate uncaging. 2mM MNI-L-glutamate is added in ACSF containing 4 mM Ca^{2+}, 0 mM Mg^{2+}, and 1 µM TTX. Uncaging laser beam at 720nm is focused on the tip of a spine head. Upon stimulation, MNI-L-glutamate is uncaged, becomes physiological L-glutamate and binds to the NMDARs located on the surface of the spine head. The NMDARs open, Ca^{2+} flows in and activate downstream signaling pathways, namely Ras. *Adapted from Harvey, Yasuda et al. (2008).*

Calcium Imaging and uEPSC Recording

Four to six days after transfection, CA1 pyramidal neurons transfected with NF1 shRNA were identified by their red fluorescence and typical morphology. Calcium imaging was performed simultaneous to glutamate uncaging and current recordings (Carter and Sabatini 2004; Sobczyk, Scheuss et al. 2005; Zito, Scheuss et al. 2009), using a pulsed Ti:sapphire laser (MaiTai, Spectra-Physics) tuned

to 920nm. Whole-cell voltage clamp was performed (V_{hold} = 0mV) on CA1 pyramidal hippocampal neurons in organotypic slice cultures with pipettes (4-5MOhm) containing Cs-based internal solution: 135 mM $CsMeSO_3$, 10 mM HEPES, 10 mM Na-phosphocreatine, 4mM $MgCl_2$, 4mM Na_2-ATP, 0.4mM Na-GTP, 3mM sodium-L-ascorbate. To this solution, we added a red Ca^{2+}-insensitive dye (300μM Alexa 594, Invitrogen) and a green Ca^{2+}-sensitive dye (500μM Oregon-Green-BAPTA 5N, Invitrogen). Recordings were made using a Multiclamp 700B amplifier, filtered at 2 kHz for voltage-clamp recordings, in ACSF containing: 127mM NaCl, 25mM $NaHCO_3$, 25mM D-glucose, 2.5mM KCl, 1.25mM NaH_2PO_4, 4mM $CaCl_2$, 0mM $MgCl_2$, 1μM TTX and 2mM MNI-caged-L-glutamate and 20μM NBQX. Upon breaking the membrane, 20 minutes were allowed for indicator loading into the cell via diffusional equilibration, when the red fluorescence intensity reached a steady state. Ca^{2+} imaging started at this moment and both dyes were excited at 920nm. Frame scans were acquired every 16ms. A typical trial starts with the measurement of the dark current of the photomultiplier (0 to 50ms) followed by shutter opening. After a short measurement of baseline fluorescence (60 to 120ms), MNI-L-glutamate uncaging (1 pulse, 6ms, 4-5mW) is evoked. Measurement of peak fluorescence is averaged over 3 to 20ms around the peak. For each spine, approximately 10 trials were collected and averaged, which has been reported to not cause rundown of two-photon uncaging-induced excitatory postsynaptic currents (uEPSCs) or spine calcium concentration signals by Zito and collaborators (Zito, Scheuss et al. 2009).

The change in [Ca^{2+}] was measured as follows (Yasuda, Nimchinsky et al. 2004):

$$\Delta[Ca^{2+}] = \frac{\left(\Delta G/R\right) \cdot K_d}{\left(G/R\right)_{saturated}} \qquad \text{Eq. (3)}$$

where $\left(G/R\right)_{saturated}$ is the ratio of green fluorescence intensity to red fluorescence intensity at saturating [Ca^{2+}] (10mM) measured in a pipette and K_d is 32μM for Oregon-Green-BAPTA-5N (Invitrogen).

Simultaneously, uEPSCs were recorded from the soma. The uEPSCs were averaged across the multiple trials (~ 10) for the same spine. Of note, given that we used a very potent AMPAR blocker (NBQX) in ACSF, the recorded current was uniquely representative of the NMDAR component. The I_{NMDAR} is typically recorded at + 40mV, not at a holding potential of 0mV. However, we observed that the

inward current at 0mV, under conditions that block I_{AMPAR}, was a potent method for specific activation of NMDARs (by MNI-L-glutamate uncaging).

Two-Photon Fluorescence Lifetime Imaging (TPFLIM)

To compare the sensitivity of the Ras GTPase fluorescence resonance energy transfer (FRET) sensors in cells, we transfected HEK293T cells with the different Ras GTPase FRET sensors described in **chapter V**, imaged under TPFLIM and acquired four basal (128 x 128 pixel; x,y = 87μm x 100μm) pictures. Next, we applied 100ng/ml epidermal growth factor (EGF) to stimulate Ras signaling and acquired more pictures. The fraction of mEGFP-HRas bound to the several versions of mRFP-RBD-mRFP was calculated from the fluorescence lifetime decay. Fluorescence lifetime was measured only from mEGFP-HRas and, thus, nonspecific binding of mRFP-RBD-mRFP should not affect our FRET measurements. The sensor that showed the best response and localization was selected for the following experiments.

To characterize the fluorescence lifetime of the newly developed Ras sensor in neurons, we sparsely transfected CA1 pyramidal neurons of organotypic hippocampal slices with the Ras sensor using ballistic gene transfer and imaged the fluorescence lifetime using TPFLIM 6 to 8 days after transfection. Images were acquired with 128 x 128 pixel resolution (x,y = 14μm x 17μm for **Figure 5.4.**; x,y = 17μm x 22μm for **Figure 5.5.**). NMDARs were activated with MNI-L-glutamate (2mM), through an uncaging protocol lasting 4 minutes and 32 seconds in the absence of extracellular Mg^{2+}. This method was sufficiently sensitive to visualize Ras activation in individual spines.

The newly developed acceptor for this sensor mRFP-RBD^{65E,108A}-mRFP distributes homogeneously all over the neurons, including soma, dendrites, spines and axons, and its mRFP signal is bright, similarly to the observations of Harvey and collaborators (2008) (**Figure 2.3.**). The donor was previously described (Yasuda, Harvey et al. 2006; Harvey, Yasuda et al. 2008) and localizes to the cell membrane, as the native HRas protein. RBD contains the K65E mutation to reduce the affinity GTP-bound Ras and RBD (from K_D 0.13 to 0.67) (Jaitner, Becker et al. 1997). RBD contains a second mutation

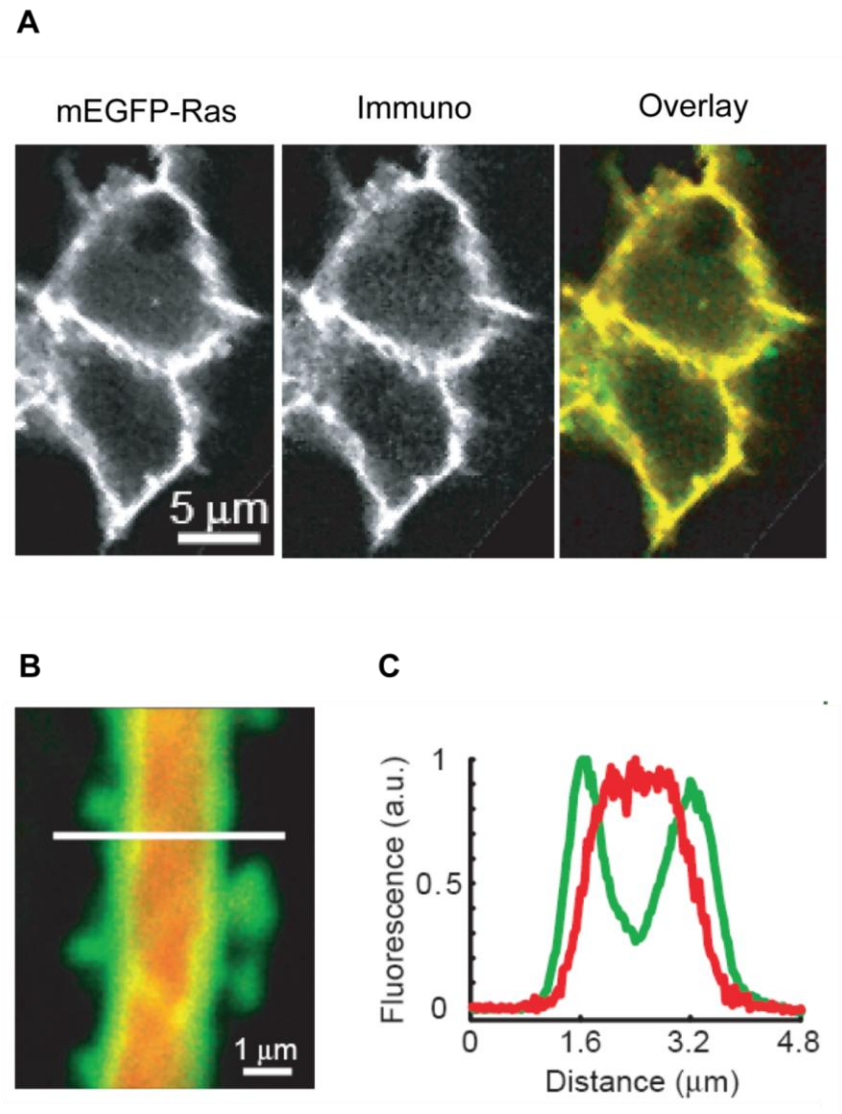

Figure 2.3. Membrane localization of mEGFP-Ras and cytosol distribution of mRFP-RBD^{59A}-mRFP. **(A)** GFP fluorescence and immunofluorescence images of HEK293T cells transfected with mEGFP-Ras. In the overlay image, the GFP fluorescence and immunofluorescence are pseudo-colored green and red respectively. **(B)** Green and red fluorescence image of the thick apical dendrite of a neuron transfected with FRas-F (mEGFP-Ras and mRFP-RBD^{59A}-mRFP). **(C)** Green and red fluorescence measured along the white line in (A). *Adapted from Harvey, Yasuda et al. (2008).*

(K108A) that abolishes a nuclear localization signal (NLS) present in the WT RBD. Spine structural plasticity in cells expressing the Ras sensor showed similar magnitudes and timecourses with GFP-transfected cells (data not shown), suggesting that the new Ras sensor did not perturb the signaling network in the spine, as seen by Harvey and collaborators (2008) for the FRas-F sensor (Harvey, Yasuda

et al. 2008). At the time of transfection with the Ras sensor, 8mM $MgCl_2$ (final concentration 10mM) was added to the culture medium to minimize the effects of Ras overexpression in synaptic efficacy (Yasuda, Harvey et al. 2006; Harvey, Yasuda et al. 2008).

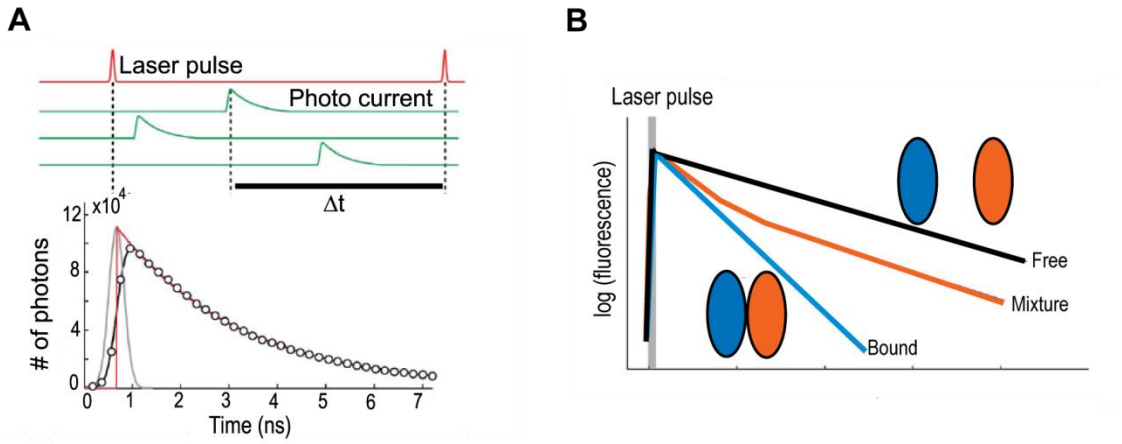

Figure 2.4. Two photon excitation fluorescence lifetime imaging. (A) Shematic illustrating the principle of time-correlated photon counting. The time between photons and the next laser pulse is measured. **(B)** Fluorescence lifetime curve of mEGFP. Measured histogram of photon arrival times (open circles). The curve can be decomposed into the true fluorescence decay curve (red) and a pulse response function (gray) that reflects the finite response time of the detector. **(C)** Schematics of the time domain fluorescence lifetime measurements. Fluorophores are excited with a short laser pulse. When the donor and acceptor do not interact, the fluorescence decays with a single exponential defined by the donor. When they do interact, the fluorescence decays with a double exponential, a combination of the decay of the free donor and the donor bound to the acceptor. *Adapted from Yasuda (2006), Svoboda and Yasuda (2006) and Yasuda, Harvey et al. (2006).*

Details of FRET imaging using a custom-built TPFLIM have been described previously (Yasuda, Harvey et al. 2006; Harvey, Yasuda et al. 2008) (**Figure 2.4.A-B**). For FLIM in the green channel, a PMT with low transfer time spread (H7422-40p, Hamamatsu) was used. A wide aperture PMT (R3896, Hamamatsu) was used for the red channel. Each pixel of a FLIM image represents the fluorescence lifetime of the donor fluorophore (mEGFP), which is defined as the average time between the fluorophore excitation and photon emission. The lifetime is obtained from the fluorescence decay curve (a histogram of the collection of single photons generated by a time-correlated single photon counting board (SPC-730; Becker-Hickl; **Figure 2.4.B**) controlled with a custom software (FLIMImage) integrated into ScanImage),

following pulsed excitation. A shorter lifetime implies higher FRET. Red signal was acquired using a separate data acquisition board (PCI-6110) and ScanImage software.

Fluorescence Lifetime Analysis

To quantify Ras activation, the fraction of mEGFP-Ras (donor) molecules bound to mRFP-RBD^{65E,108A}-mRFP (acceptor) molecules (binding fraction) was calculated. The binding fraction was calculated by direct fitting of the fluorescence decay curve, which is composed of two populations corresponding to free donors and donors bound to acceptors.

The fluorescence lifetime decay curve, *F*(*t*), was fitted with a single exponential function convolved with the Gaussian pulse response function of a microscope as follows (Yasuda, Harvey et al. 2006):

$$F(t) = F_0 \cdot H(t, t_0, \tau_D, \tau_G) = F_0 \frac{1}{2} exp\left(\frac{\tau_G^2}{2\tau_D} - \frac{t - t_0}{\tau_D}\right) erf\left(\frac{\tau_G^2 - \tau_D(t - t_0)}{\sqrt{2}\tau_D\tau_G}\right) \quad \text{Eq. (1)}$$

where *t* is photon arrival time for each collected photon by the PMT, t_0 is the offset time between the start of a laser pulse and the start of photon arrival, τ_D is the fluorescence lifetime of the free donor (2.6ns), τ_G is the standard deviation of the Gaussian pulse response function (0.12ns – 0.16ns), and F_0 is the peak fluorescence. To improve the stability of this fitting, all pixels in an image were summed and fitted with Eq. (1). Furthermore, τ_D and τ_G are pre-determined and these values are fixed for fitting. F_0 and t_0 are obtained by fitting.

The mean fluorescence lifetime, τ_m, of a fluorescence lifetime decay curve was then measured from the mean photon arrival time $\langle t \rangle$ as follows (Yasuda, Harvey et al. 2006):

$$\tau_m = \langle t \rangle - t_0 = \frac{\int dt \cdot tF(t)}{\int dt \cdot F(t)} - t_0 \quad \text{Eq. (2)}$$

Here *F*(*t*) was not fitted with Eq. (1), but is raw experimental data represented by a histogram of single photons collected by the time-correlated single photon counting board.

CHAPTER III

Neurofibromin maintains the density of dendritic spines and functional synapses in CA1 pyramidal neurons in the hippocampus

Chapter III. Neurofibromin maintains the density of dendritic spines and functional synapses in CA1 pyramidal neurons in the hippocampus

Introduction

Among multi-symptom disorders relevant to the neuroscience field, it is well established that 40-60% of the patients afflicted with NF1 exhibit cognitive impairment (Silva, Frankland et al. 1997; Costa, Fedorov et al. 2002; Costa and Silva 2003; Shilyansky, Lee et al. 2010). The NF1 mouse model, a heterozygous knockout of the *Nf1* gene, shows spatial learning and memory impairment and LTP impairment (Silva, Frankland et al. 1997; Costa, Fedorov et al. 2002; Li, Cui et al. 2005). These phenotypes were rescued when Ras activation was downregulated either by pharmacological approaches or by combining the heterozygous *Nf1* knockout with heterozygous *KRas* knockout. This suggests that the LTP deficits are related to excessive Ras activation (Costa, Fedorov et al. 2002).

As $Nf1^{+/-}$ mice were identified as a useful model for learning disabilities of NF1, the physiological properties of the $Nf1^{+/-}$ mice were extensively studied. It has been also found that inhibitory synapses are substantially potentiated in these mice (Costa and Silva 2002). Later, Cui and collaborators (2008) reported an excessive phosphorylation of Synapsin 1 in inhibitory neurons in the hippocampus, which results in increased presynaptic vesicle fusion and GABA release, leading to increased inhibitory transmission. This same study excludes a role of glia or excitatory neurons in the cellular abnormalities identified in the $Nf1^{+/-}$ mouse (Cui, Costa et al. 2008).

Besides the role in presynaptic function, a number of studies have reported that neurofibromin is also important for postsynaptic function. Hsueh and collaborators (2001) identified the presence of neurofibromin in dendritic spines of the hippocampus, where it associates with the adhesion molecule Syndecan-2. Additionally, they observed that neurofibromin is present at the PSD (Hsueh, Roberts et al. 2001). Recently, Lin and collaborators (2007) reported that neurofibromin removal by shRNA decreases

the density of dendritic spines in primary cultures of the hippocampus (Lin, Lei et al. 2007). Hence, these studies suggest a function of neurofibromin at postsynaptic sites.

Studies from Ras manipulation experiments have also provided evidence that Ras holds an important postsynaptic function. For example, at the functional level, Zhu and collaborators provided evidence for the crucial postsynaptic function of Ras. In this study, they infected hippocampal brain slices with virus harboring several HRas constructs and verified an increase in AMPAR-mediated transmission in neurons overexpressing WT-HRas or CA-HRas, whereas a decrease in AMPAR-mediated synaptic transmission was observed in neurons overexpressing a DN-HRas. The effects of WT-HRas and DN-HRas were blocked by a NMDAR antagonist (AP5) and by high concentration of Mg^{2+} (Zhu, Qin et al. 2002). Other studies have demonstrated that Ras is required for proper spine formation and maintenance. For example, using a Synapsin 1 promoter, Heumann et al. (2000) created a gain-of-function transgenic mouse model in which constitutively active $HRas^{12V}$ is expressed selectively in neurons (synRas mice). In this mouse, there is an up-regulation of ERK activity in the cortex, hippocampus and other brain regions. This group reported that dendritic spine density is increased in synRas mice, which correlated with a two-fold increase in synapse number (Heumann, Goemans et al. 2000). In another study by Biou and collaborators (2008), the expression of a constitutively active Ras (KRas or NRas) form destabilized spine morphology, producing filopodia on dendrites of mature (> 21DIV) hippocampal neurons, whereas a dominant negative Ras form did not affect spine morphology. Moreover, spine destabilization was rescued by co-expressing dominant negative Ras (Biou, Brinkhaus et al. 2008). In a study by Kumar and collaborators (2005), overexpression of a constitutively active Ras mutant, Ras^{61L}, resulted in prominent filopodia-like protrusions and decrease in spine density. Besides, they used a mutant $Ras^{61L,35S}$, which specifically activates the MAPK pathway, and when overexpressing it they observed a moderate but significant decrease in spine density. Such observation was not repeated when using the mutant $Ras^{61L,40C}$, which specifically activates the PI3K pathway (Kumar, Zhang et al. 2005). This study supported previous findings by Wu and collaborators (2001), who reported a simultaneous persistent activation of MAPK pathway (as detected by increased phosphorylation of ERK1/2 by immunocytochemistry in dissociated hippocampal neurons) and stable formation of filopodia-like structures in the dendrites of these neurons following multiple spaced membrane depolarizations with

a high concentration K^+ solution. Interestingly, the morphological changes induced by spaced depolarizations were reversed by a MEK inhibitor (U0126), confirming the involvement of the Ras-MAPK signaling pathway in these morphological changes (Wu, Deisseroth et al. 2001). Therefore, we hypothesized that Ras hyperactivation by neurofibromin loss-of-function could, similarly, affect the CA1 pyramidal neurons spine morphology.

Results

Neurofibromin shRNA Validation

To test the hypothesis that neurofibromin regulates the spine number and shape, we tested the efficiency of neurofibromin knockdown by two shRNA constructs directed against neurofibromin. Primary cultures from E18 rat hippocampus were prepared. The cultures were infected with lentivirus containing mEGFP and NF1 shRNA #1, NF1 shRNA #2, or a scrambled control shRNA at DIV1-3. Seven days later, we examined the green fluorescence for each viral infection under the microscope and verified that the majority of cells were infected. Western Blots were performed to screen for an efficient neurofibromin shRNA that is capable of removing the protein. Alpha-actinin was used as a loading control. **Figure 3.1.** shows the efficient neurofibromin knockdown by constructs NF1 shRNA # 1 and NF1 shRNA #2 in E18 hippocampal neurons.

Figure 3.1. also shows that phospho-ERK (p-ERK1/2) levels is increased in neurons expressing NF1 shRNA, suggesting that neurofibromin removal results in upregulation of the Ras-ERK pathway. Based on the experimental data from Western blot, NF1 shRNA #1 and NF1 shRNA #2 were selected for use in the following experiments.

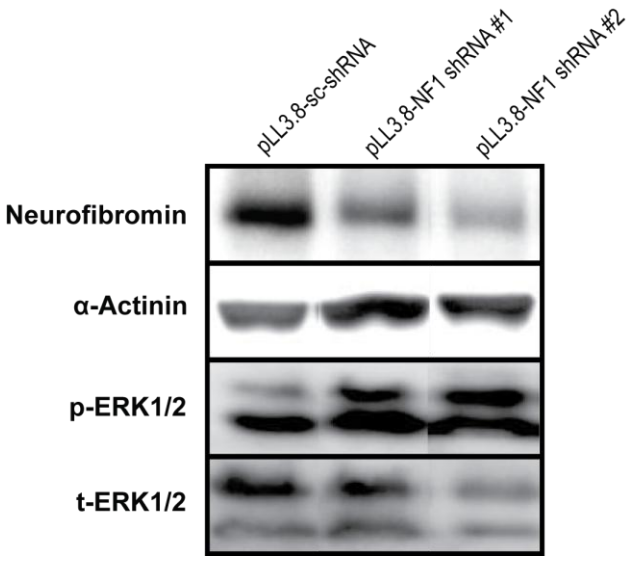

Figure 3.1. Neurofibromin shRNA validation. Knockdown of endogenous neurofibromin in E18 hippocampal neuronal primary cultures infected with lentivirus containing a scrambled shRNA or shRNA constructs directed against neurofibromin for 7 days. α-actinin was used as a loading control. Amounts of phospho-ERK1/2 and total ERK1/2 (t-ERK1/2) are also shown in the same samples. Total protein levels were measured by Western Blot.

Loss of Dendritic Spines in Neurofibromin Knockdown Neurons

To analyze the dendritic spine structure, we transfected organotypic slice cultures at DIV10-15 with shRNA constructs directed against neurofibromin for 5-7 days. Transfected neurons were identified by their green fluorescence. Then, using TPLSM, we acquired images of an entire CA1 pyramidal neuron (**Figure 3.2.A)**, followed by images of secondary and tertiary apical dendrites of that same neuron (**Figure 3.2.B**). Pyramidal neurons expressing both NF1 shRNA #1 and shRNA #2 showed reduced spine density 5-7 days post transfection (DPT) (68 ± 5.8 for control sc-shRNA neurons, 47 ± 1.9 for neurons expressing NF1 shRNA #1 and 36 ± 4.1 for neurons expressing NF1 shRNA #2; $p \leq 0.05$ ANOVA followed by post hoc least significant difference (LSD) tests; **Figures 3.2.B**-**C**).

Regarding the spine morphology, three spine categories were defined: mushroom, stubby and thin spines. Spines from control neurons and neurofibromin knockdown neurons (either transfected with NF1 shRNA #1 or NF1 shRNA #2) showed similar distribution among the three defined categories with no significant difference in their spine morphology (0.64 ± 0.02, 0.60 ±0.06 and 0.52 ± 0.01 for mushroom

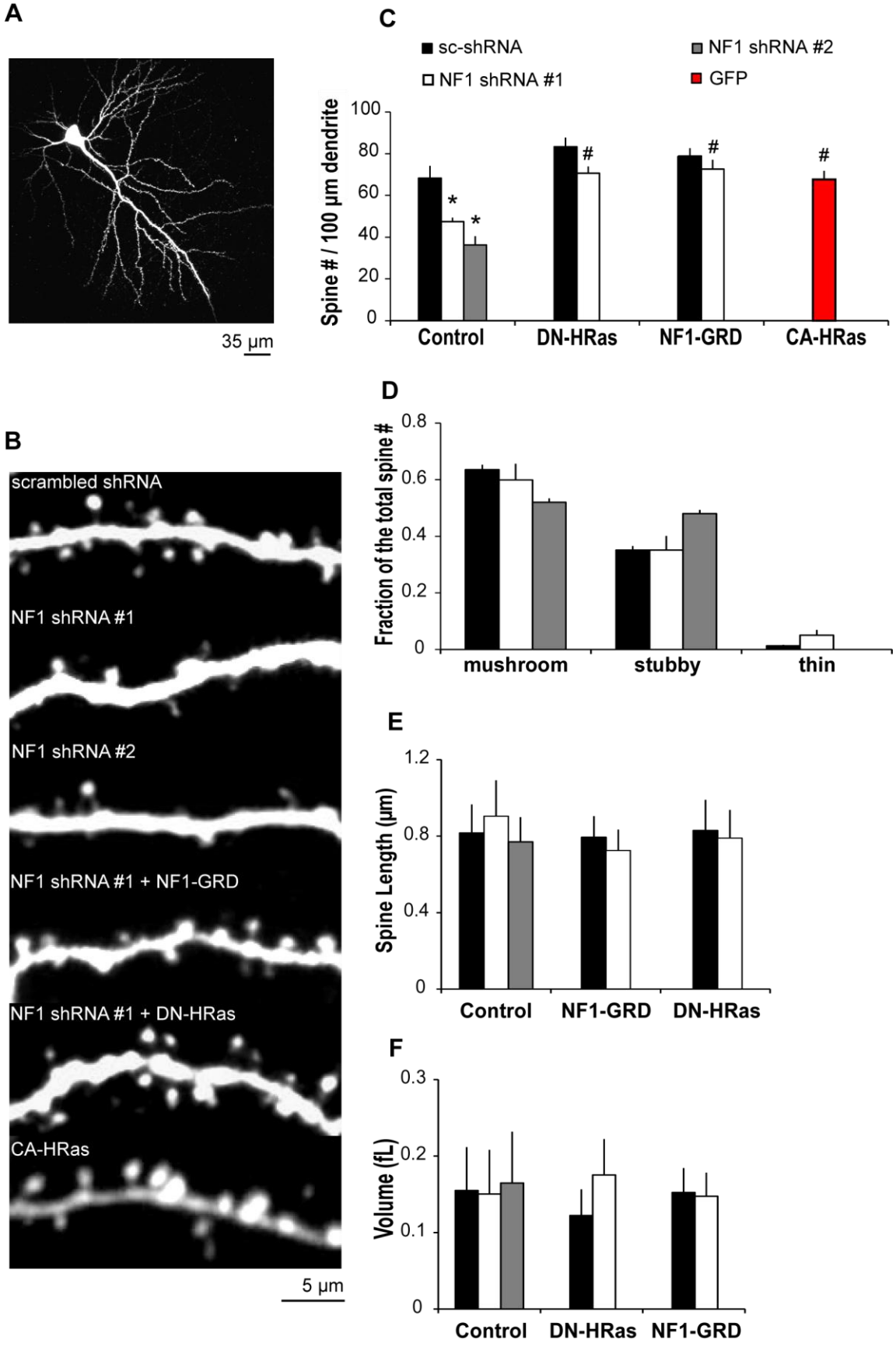
A
35 μm
B
scrambled shRNA
NF1 shRNA #1
NF1 shRNA #2
NF1 shRNA #1 + NF1-GRD
NF1 shRNA #1 + DN-HRas
CA-HRas
5 μm
C
sc-shRNA
NF1 shRNA #1
NF1 shRNA #2
GFP
Spine # / 100 μm dendrite
100
80
60
40
20
0
*
*
#
#
#
Control
DN-HRas
NF1-GRD
CA-HRas
D
Fraction of the total spine #
0.8
0.6
0.4
0.2
0
mushroom
stubby
thin
E
Spine Length (μm)
1.2
0.8
0.4
0
Control
NF1-GRD
DN-HRas
F
Volume (fL)
0.3
0.2
0.1
0
Control
DN-HRas
NF1-GRD

spines of control sc-shRNA neurons, NF1 shRNA #1 neurons and NF1 shRNA #2 neurons, respectively ($p = 0.37$); 0.35 ± 0.01, 0.35 ± 0.05 and 0.48 ±0.01 for stubby spines of control sc-shRNA neurons, NF1 shRNA #1 neurons and NF1 shRNA #2 neurons, respectively ($p = 0.18$); 0.01 ± 0.003, 0.05 ± 0.018 and zero for thin spines of control sc-shRNA neurons, NF1 shRNA #1 neurons and NF1 shRNA #2 neurons, respectively ($p = 0.062$); **Figure 3.2.D**).

At the same time, the spine length, which was measured from the top of the spine head center until the connection point with the dendrite, was the same between control sc-shRNA neurons (0.82 ± 0.01μm, n = 6), NF1 shRNA #1 expressing neurons (0.89 ± 0.06μm, n = 7) and NF1 shRNA #2 transfected neurons (0.76 ± 0.04μm, n = 8) (**Figure 3.2.E**, $p = 0.17$).

Also unchanged was the average spine volume between control sc-shRNA neurons and neurons where neurofibromin was knocked down (0.16 ± 0.07fL for control sc-shRNA neurons, n = 6; 0.14 ± 0.02fL for NF1 shRNA #1 expressing neurons, n = 7; and 0.16 ± 0.04fL for NF1 shRNA#2 expressing neurons, n = 8, $p = 0.93$; **Figure 3.2.F**).

In conclusion, our results indicate that downregulation of neurofibromin reduces the spine number in CA1 pyramidal neurons.

Figure 3.2. Neurofibromin regulates the spine morphology of CA1 pyramidal neurons in organotypic slice cultures, in a Ras-dependent manner. Organotypic hippocampal slice cultures were transfected and treated at DIV10-15 with shRNA constructs against neurofibromin or scrambled shRNA, DN-HRas, CA-HRas and the neurofibromin GRD domain. The slices were imaged 5-7 days later. Z-stacks were acquired and maximum projections were made from them. **(A)** Representative image of a CA1 pyramidal neuron in organotypic hippocampal slice cultures transfected. **(B)** Representative images of segments of apical secondary and tertiary dendrites transfected with shRNA constructs, or shRNA constructs and/or HRas constructs or neurofibromin GRD domain for 5-7days. **(C)** Quantification of the spine density in the apical dendrites of neurons shown in (B). * $p < 0.05$ compared with control for each condition. **(D)** Quantification of the types of spines analyzed. **(E)** Quantification of the spine length. **(F)** Plot of the spine volume.

Dendritic Spine Loss by Neurofibromin Removal Can Be Rescued by Manipulations that Decrease Ras Activity

Are the effects of neurofibromin removal in spine morphology due to increased Ras signaling? Given that it was previously established that the removal of one Ras copy is enough to correct for the deficits observed in both cognition and LTP in a mouse model of NF1 (Costa et al. 2002) and that Ras manipulations alter the spine number (Heumann et al. 2000, Kumar et al. 2005, Biou et al. 2008), we speculated that Ras hyperactivation might also be the signaling problem determining the observed morphological abnormalities. In order to test this hypothesis, we performed several genetic Ras manipulations to determine if they can rescue the spine number decrease seen in neurons expressing NF1 shRNA. Namely, we co-transfected both shRNA directed against neurofibromin and only the GRD domain (isoform I) of neurofibromin, or co-transfected NF1 shRNA #1 (we used this construct to test Ras manipulations rescue effect) with dominant negative HRas (DN-HRas, $HRas^{17N}$), or we overexpressed constitutively active HRas (CA-HRas, $HRas^{12V}$) alone. In our preparations, co-expressing the GRD domain (Ras inactivator domain) of neurofibromin rescued the spine number to control levels (47 ± 1.9 for neurons expressing NF1 shRNA, n = 7; 73 ± 4.4 for neurons expressing both NF1 shRNA and the GRD domain, n = 9; 68 ± 5.8 for control sc-shRNA neurons, n = 6; **Figures 3.2.B**-**C**). The same rescue effect on the spine number was observed when we co-transfected CA1 neurons in organotypic slice cultures from the hippocampus with both NF1 shRNA and a DN-HRas construct ($HRas^{17N}$) (68 ± 5.8 for control sc-shRNA neurons, n = 6; 71 ± 3 for neurons expressing both NF1 shRNA and DN-HRas, n =6; 47 ± 1.9 for neurons expressing NF1 shRNA #1, n = 7; **Figures 3.2.B**-**C**). These results suggest that Ras hyperactivation causes the spine elimination upon neurofibromin knockdown. The number of spines in neurons overexpressing scrambled shRNA only were similar with that in neurons overexpressing both scrambled shRNA and DN-HRas (68 ± 5.8 for control neurons, n = 6; 83 ± 4.3 for neurons overexpressing both scrambled shRNA and DN-HRas, n = 6; $p \geq 0.05$; **Figure 3.2.B**). Also, overexpression of the neurofibromin GRD domain together with scrambled shRNA did not alter the number of spines observed for neurons overexpressing sc-shRNA only (68 ± 5.8 for control sc-shRNA neurons, n = 6; 79 ± 3.7 for neurons overexpressing both sc-shRNA and the GRD domain of neurofibromin, n = 11; $p \geq 0.05$; **Figure 3.2.B**). However, when we transfected CA1 neurons with CA-HRas only, the spine number was

maintained as compared with control sc-shRNA neurons (68 ± 5.8 for control sc-shRNA neurons, n = 6; 68 ± 4.3 for neurons overexpressing CA-HRas, n = 10; $p \geq 0.05$; **Figure 3.2.B**). This apparent inconsistency may be because mechanisms other than Ras hyperactivation, for example PKA signaling (Lin, Lei et al. 2007), may contribute to this phenotype.

Dendritic Spine Loss by Neurofibromin Loss-of-Function is Activity-Dependent

To verify the impact of activity blockade in spine morphology upon neurofibromin loss-of-function, we transfected organotypic slice cultures of the hippocampus with shRNA directed against neurofibromin or the scrambled control shRNA and treated the transfected slices with a NMDAR antagonist (AP5, 100 μM) or with $MgCl_2$ (8mM additionally to the regular content in the tissue culture medium, making up to 10mM). We used NF1 shRNA #1 for the AP5 experiment and NF1 shRNA #2 for the $MgCl_2$ experiment. Five to seven days later, we imaged secondary and tertiary apical dendrites of the transfected neurons and analyzed the spine morphology of these neurons. In our preparations, AP5 treatment rescued the spine number to control levels (66 ± 3.9 for neurons expressing NF1 shRNA #1, n = 7; 68 ± 5.8 for control neurons expressing sc-shRNA, n = 6; **Figures 3.3.A-B**), indicating that the spine loss due to neurofibromin removal is activity-dependent.

When using NF1 shRNA #2 cloned into a different vector (pLL3.8), we observed dendritic spine loss, as expected, compared to the control pLL3.8-sc-shRNA. The spine density was measured to be 50 ± 5.4 spines for neurons expressing pLL3.8-NF1 shRNA #2 (n = 5), and 88 ± 6.9 for control neurons expressing pLL3.8-sc-shRNA (n = 5, $p \leq 0.05$; **Figures 3.3.C-D**). However, when we treated the slices transfected with pLL3.8-NF1 shRNA #2 with $MgCl_2$, the spine density was not significantly different from that of the neurons expressing a sc-shRNA (68 ± 7.5 for neurons expressing pLL3.8-NF1 shRNA #2 and treated with $MgCl_2$, n = 7; 88 ± 6.9 for control neurons expressing pLL3.8-sc-shRNA, n = 5; $p > 0.05$; **Figures 3.3.C-D**). Instead, we observed a partial rescue of the spine number, since there is no statistical difference between control neurons and neurons where neurofibromin was removed and that were also

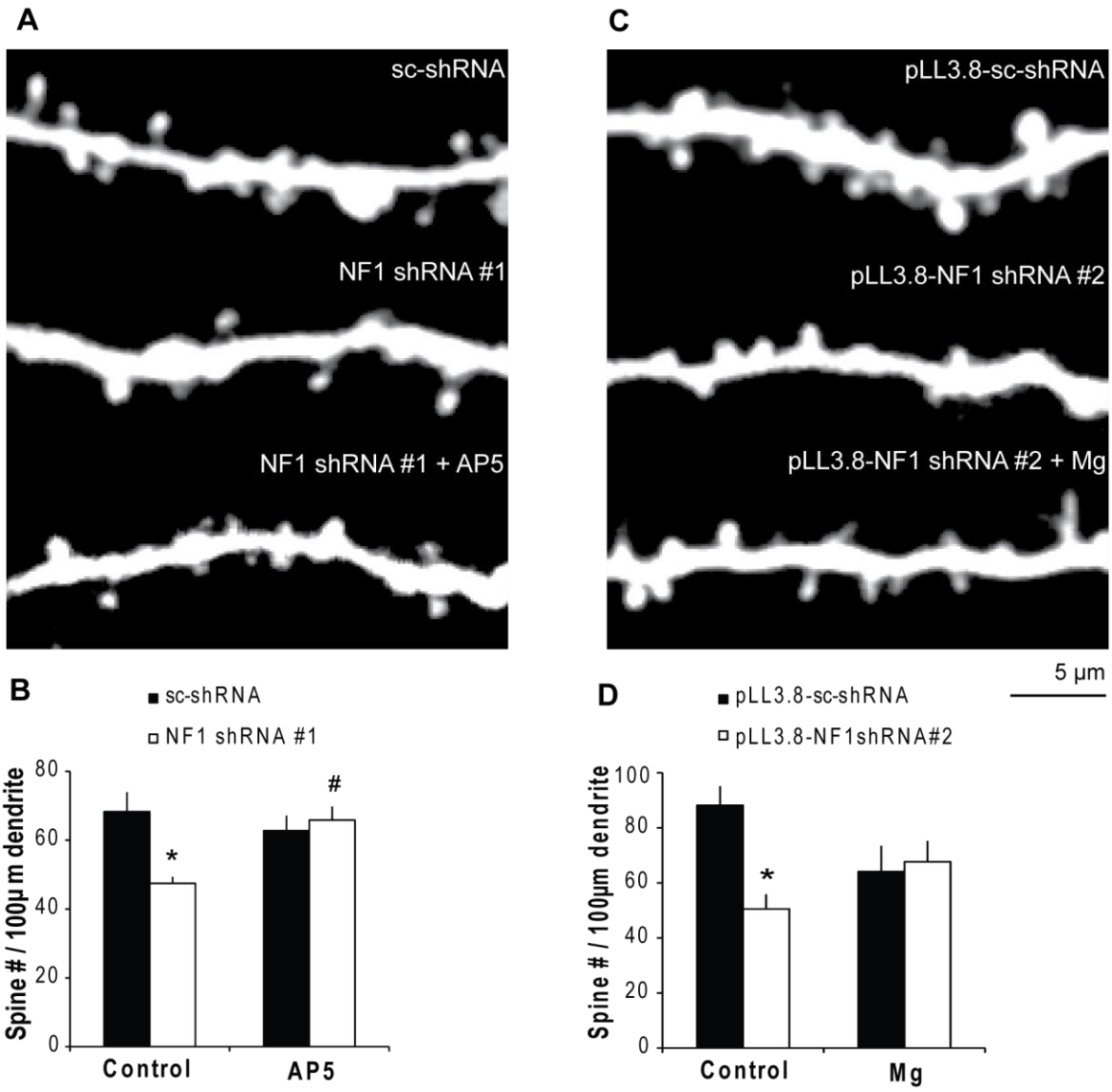

Figure 3.3. Neurofibromin regulates the spine morphology of CA1 pyramidal neurons in organotypic slice cultures, in an activity-dependent manner. Organotypic hippocampal slice cultures were transfected and treated at DIV10-15 with NF1 shRNA #1 or sc-shRNA and treated with 100µM AP5 from the moment of transfection until the end of the experiment; or slices were transfected with pLL3.8-sc-shRNA or pLL3.8-NF1 shRNA #2 and treated with an extra 8mM $MgCl_2$ from the moment of transfection and until the end of the experiment. The slices were imaged 5-7 days later. Z-stacks were acquired and maximum projections were made from them. **(A)** Representative images of segments of secondary and tertiary apical dendrite. **(B)** Quantification of the spine density in the apical dendrites of neurons shown in (A). * $p \leq 0.05$ compared with control, $^{\#}$ $p \leq 0.05$ compared with NF1 shRNA #1. **(C)** Representative images of segments of secondary and tertiary apical dendrites of CA1 pyramidal neurons in organotypic hippocampal slice cultures transfected. **(D)** Quantification of the spine density in the apical dendrites of neurons shown in (C).

treated with $MgCl_2$. The lack of total rescue of spine number by $MgCl_2$ could be related to the fact that $MgCl_2$ also seems to have a slight, yet non-significant, effect on the spine number of control neurons (88 ± 6.9 for control neurons expressing pLL3.8-sc-shRNA, n = 5; 64 ± 9.4 for neurons expressing pLL3.8-sc-shRNA and treated with $MgCl_2$, n = 4; **Figure 3.3.D**).

Loss of Excitatory Synapses in Neurofibromin Loss-of-Function Neurons

In hippocampal pyramidal neurons, each dendritic spine is normally associated with one and only one glutamatergic synapse and the vast majority of excitatory synapses form onto the heads of dendritic spines. Thus, changes in spine number are thought to reflect changes in the number of active synapses. Therefore, we speculated that the number of excitatory synapses is reduced in the absence of neurofibromin. In order to confirm that NF1 shRNA-induced spine loss reflects a loss of excitatory synapses, we transfected organotypic slice cultures of the hippocampus with NF1 shRNA #1 and scrambled shRNA for 6-8 days and then we performed whole-cell voltage-clamp recordings from CA1 neurons. Spontaneous activity, indicated by mEPSCs, was monitored in transfected neurons and their neighboring untransfected neurons for 60 seconds per trial, five trials per neuron (**Figure 3.4.A**). At 6-8 DPT, NF1 shRNA expressing neurons had moderately reduced membrane capacitance (C_m) (C_m = 157 ± 3pF and 139 ± 3pF for scrambled shRNA and NF1 shRNA neurons, respectively; n = 42-45), indicating decreased membrane area (data not shown). The input resistance (R_{in}) was similar between scrambled shRNA neurons and NF1 shRNA-expressing neurons (R_{in} = 174 ± 11 and 181 ± 9mOhm for scrambled shRNA and NF1 shRNA neurons, respectively; n = 42-45; data not shown). The mEPSC amplitude and frequency were averaged across trials and we observed that, indeed, neurons where neurofibromin was removed showed fewer events as seen by a lower mEPSC frequency (0.39 ± 0.05Hz for neurons expressing neurofibromin shRNA in contrast with 0.59 ± 0.09Hz in neurons expressing scrambled shRNA, p = 0.04; or 0.39 ± 0.05Hz for neurons expressing neurofibromin shRNA in contrast with 0.62 ± 0.07Hz in untransfected neurons, p = 0.009, **Figures 3.4.A**-**B**). We also compared the mEPSC frequency between untransfected neurons and neurons expressing scrambled shRNA and observed no differences between

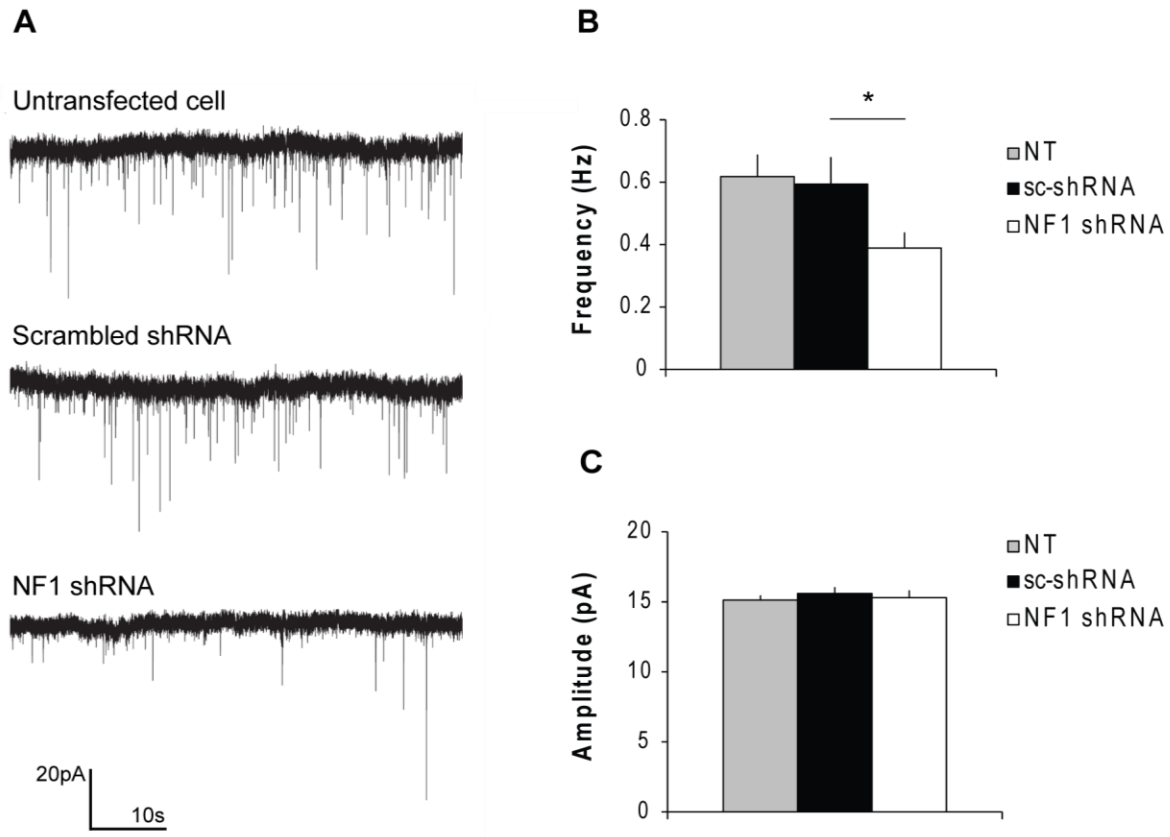

Figure 3.4. Neurofibromin regulates the number of functional excitatory synapses in CA1 pyramidal neurons, in organotypic slice cultures. Organotypic hippocampal slice cultures were transfected at DIV10-15 with shRNA constructs against neurofibromin or scrambled shRNA. Seven days later, whole cell voltage-clamp recordings were performed to access the mEPSCs. **(A)** Representative traces of mEPSCs recorded at a holding potential of -70mV for untransfected neurons (n = 53), scrambled shRNA (n = 42) and NF1 shRNA (n = 45). **(B)** Quantification of the frequency of the mEPSCs recorded. *p < 0.05. **(C)** Quantification of the amplitude of the mEPSCs recorded. Values are presented as average and error bars are SEM.

these two groups (0.62 ± 0.07Hz and 0.59 ± 0.09Hz for untransfected neurons and scrambled shRNA neurons, respectively; p = 0.83, **Figures 3.4.A**-**B**). Therefore, we conclude that there is a loss of excitatory synapses in neurofibromin knockdown neurons and, therefore, neurofibromin is required for the maintenance of functional excitatory synapses.

With respect to the mEPSC amplitude, we observed no differences between neurons where neurofibromin was knocked down and control neurons (15.6 ± 0.5pA in neurons expressing scrambled shRNA and 15.4 ± 0.5pA for neurons expressing neurofibromin shRNA, p = 0.72; or 15.4 ± 0.5pA for neurons expressing neurofibromin shRNA and 15.1 ± 0.3pA in untransfected neurons, p = 0.72, **Figures**

3.4.A,**C**), suggesting that the AMPAR content is similar between conditions and unaffected by neurofibromin removal. Also, there were no differences between the amplitude of the mEPSCs recorded from untransfected neurons and neurons expressing scrambled shRNA (15.1 ± 0.3pA and 15.6 ± 0.5pA for untransfected and scrambled shRNA neurons; p = 0.41, **Figures 3.4.A**,**C**). Thus, postsynaptic expression of neurofibromin is required for the maintenance of functional excitatory synapses, without affecting the AMPAR content.

Discussion

In this chapter, we asked whether neurofibromin has a role in dendritic spine morphology and used shRNA constructs directed against neurofibromin to answer this question. Under the conditions of our organotypic slice culture preparations, we observed that reduced levels of neurofibromin cause a decrease in dendritic spine density in the pyramidal neurons of the CA1 region of the hippocampus. In line with my observations, during the course of our project, Lin and collaborators (2007) reported the first evidence that neurofibromin is required for filopodia and dendritic spine formation in hippocampal cultured neurons. In this study, in young hippocampal neurons, the expression of neurofibromin shRNA impaired dendritic filopodia formation, and in mature hippocampal neurons, the expression of neurofibromin shRNA reduced the density of dendritic spines (Lin, Lei et al. 2007). This study provided evidence that neurofibromin regulates filopodia and dendritic spine formation through PKA activation and did not test whether the RasGAP function of neurofibromin was involved in the observations. Of note, we observed no further dendritic spine abnormalities besides the difference in density. The conclusions of the morphology data that we present in this dissertation are further supported by the conclusions achieved with mEPSCs recording in our hippocampal slices' preparation, which indicate that reduced levels of neurofibromin expression lead to a decreased number of functional excitatory synapses.

In the present study, we observed, by Western Blot, that the Ras-MAPK pathway is activated in neurons with reduced expression of neurofibromin, by means of increased phospho-ERK1/2 (a member of the Ras-MAPK pathway downstream Ras activation) expression, as compared to control neurons overexpressing a scrambled shRNA. ERK has recently been implicated as an important regulator of activity-dependent structural changes in hippocampal neurons. Specifically, formation and stabilization of dendritic spines involves ERK activation, a role likely to be involved in long-term information storage in the CNS (Goldin and Segal 2003). Therefore, precise Ras activation might be crucial for the stabilization of dendritic spines. Hence, since previous studies reported that synaptic plasticity and spine morphology is altered in transgenic mice holding Ras transgenes (Manabe, Aiba et al. 2000; Arendt, Gärtner et al. 2004), we asked if the reduction in spine density that we observed in our preparations were due to Ras hyperactivation. In order to answer this question, we overexpressed a DN-Ras form or the NF1-GRD domain together with NF1 shRNA in hippocampal slice cultures and analysed the dendritic spine density. Our data shows that these manipulations, which decrease Ras activity, were able to rescue the spine density phenotype to control levels, indicating that neurofibromin regulates the dendritic spine density in a Ras-dependent manner. In line with our data, Kumar and collaborators (2005) observed that overexpression of a constitutively active Ras mutant resulted in decrease in spine density. They further used a mutant $Ras^{61L,35S}$, which specifically activates the MAPK pathway, and when overexpressing it they also observed a moderate, but significant, decrease in spine density. In our experiments, a different constitutively active form ($HRas^{12V}$) was unable to cause a decrease in dendritic spine density, suggesting that, despite the role of Ras signaling regulation by neurofibromin in spine morphology, another signaling pathway might be involved in the observed phenotype. In line with this speculation, Lin et al. (2007) reported that dendritic spine removal by neurofibromin in mature cultured neurons resulted from increased PKA signaling. Therefore, we speculate that both Ras signaling and PKA signaling are required for proper spine numbers. Our results are also in line with a study by Biou and collaborators (2008), reporting that expression of constitutively active Ras destabilized spine morphology due to its interaction with debrin (a component of the actin cytoskeleton that competes with other actin-binding proteins to influence the spine morphology), whereas debrin-induced spine destabilization was rescued by co-expressing a dominant negative Ras. As seen by Kumar and collaborators (2005) and in our own

preparations (data not shown), constitutively active Ras often produced filopodia on dendrites of mature hippocampal neurons, whereas dominant negative Ras did not affect spine morphology. Thus, together with these reports, our data suggests that Ras hyperactivation causes a reduction in spine density. We speculate that spine removal under conditions of Ras hyperactivation is a homeostatic mechanism to overcome the effects of overstimulation of the Ras pathway, but further experiments must be performed in order to test this hypothesis.

However, in contrast with our data, Arendt et al. (2004) observed that dendritic spine density was increased and correlated with a two-fold increase in synapse number in a mouse overexpressing a constitutively active HRas form ($HRas^{12V}$) in neurons only (driven by the Synapsin 1 promoter). These data are equally in contrast with our data from mEPSCs, which reports that the number of excitatory functional synapses is decreased when neurofibromin expression levels are reduced. Instead, Arendt and collaborators (2004) reported that, in whole cell patch clamp preparations, the frequency of AMPAR-mediated spontaneous excitatory postsynaptic currents was increased by 39%, but the amplitude of the mEPSCs was unaffected when compared to WT littermates, which is in line with our data. These effects were seen in the cortex, whereas our observations were done in the hippocampus, which could potentially explain the discrepancies of the two studies.

Furthermore, we asked whether the effect of neurofibromin on spine density is activity-dependent. In order to test this hypothesis, we treated hippocampal slice cultures overexpressing NF1 shRNA constructs with Mg^{2+} or AP5 in order to block activity. Our data indicates that neurofibromin maintains spine density in an activity-dependent manner. This finding supports the speculation that the spine removal in conditions where neurofibromin expression is reduced might be a homeostatic mechanism to compensate for the Ras hyperactivation resulting from neurofibromin loss-of-function. Ras is activated by the NMDAR, among other stimulus, under normal conditions. If neurofibromin is removed, Ras will be hyperactivated upon NMDAR stimulation/activation. If NMDAR-mediated activity is blocked, Ras activation might occur with a smaller magnitude despite neurofibromin loss-of-function, removing the need for spine density decrease. This is, however, just one possible explanation that requires further verification.

CHAPTER IV

Neurofibromin is required for Ras-mediated dendritic spine structural plasticity in CA1 hippocampal neurons

Chapter IV. Neurofibromin is required for Ras-mediated dendritic spine structural plasticity in CA1 hippocampal neurons

Introduction

In the previous chapter, we demonstrated that neurofibromin is required to maintain the dendritic spine density. Normal spine structural plasticity is required to maintain spine density. Therefore, in the present chapter, we assess whether neurofibromin regulates structural plasticity in dendritic spines of CA1 pyramidal neurons.

Costa et al. (2002) reported that a mouse model of NF1, a heterozygous mouse for the *Nf1* gene, shows impaired LTP upon TBS in the Schaffer collateral pathway (Costa, Fedorov et al. 2002). Importantly, previous studies have correlated spine structural plasticity with LTP induction (Engert and Bonhoeffer 1999; Maletic-Savatic, Malinow et al. 1999). For example, Nagerl and collaborators (2004) have induced LTP in Schaffer collaterals and long-term imaging showed an increase of size in several spines in the CA1 area or even the formation of new spines (Nagerl, Eberhorn et al. 2004). Similarly, LTD induction, using low frequency stimulation (LFS), has proven efficient on promoting the removal of dendritic spines or decrease of their size in CA1 neurons, in hippocampal slices (Nagerl, Eberhorn et al. 2004; Zhou, Homma et al. 2004). Thus, despite the fact that it remains unclear whether structural plasticity is the morphological correlate of synaptic plasticity, several studies strongly support this idea. Furthermore, several studies have reported that learning and memorizing tasks lead to increased rates of spine formation and elimination, as well as spine remodeling with spine volume increases (Harms, Rioult-Pedotti et al. 2008; Xu, Yu et al. 2009). Therefore, one can speculate that the impairments in memory and learning, associated with reduced levels of neurofibromin expression, might be correlated with impairments in structural plasticity.

In line with our hypothesis, recent studies have reported a role of Ras in dendritic spine structural plasticity following LTP stimulus (Harvey, Yasuda et al. 2008; Patterson, Szatmari et al. 2010). Of note, Harvey et al. (2008) reported that a MEK inhibitor (a kinase downstream of Ras) (U0126) blocked the sustained phase of spine structural plasticity in CA1 pyramidal neurons, following single spine stimulation with LTP-inducing stimulus (Harvey, Yasuda et al. 2008). Similarly, a study by Patterson and collaborators (2010) has reproduced these results, supporting the idea that Ras is required for structural plasticity and AMPAR exocytosis (Patterson, Szatmari et al. 2010). However, to our knowledge, there are no studies addressing the effects of Ras hyperactivation in dendritic spine structural plasticity. In this chapter, we hypothesized that precise Ras regulation is crucial for structural plasticity, as previously suggested by other authors, who predict that precise Ras regulation is required for optimal capacity to induce LTP, learning and memory (Thomas and Huganir 2004; Stornetta and Zhu 2011). Thus, we predict that Ras hyperactivation, due to low expression levels of neurofibromin, will, like Ras hypoactivation, result in impaired structural plasticity. As a result of this prediction, we also predict that neurofibromin signaling regulates dendritic spine structural plasticity.

Results

Impaired Structural Plasticity in Neurofibromin Loss-of-Function Neurons

In order to test this hypothesis, we transfected organotypic slice cultures of the hippocampus with NF1 shRNA and scrambled shRNA for 5-7 days. We selected transfected CA1 pyramidal neurons based on their green fluorescence and imaged apical secondary and tertiary dendrites located 50 - 150μm from the soma, with a 60X, 0.9NA, Olympus objective in a TPLSM. Images with 128 x 128 pixel resolution were acquired every minute. The neurons were imaged in ACSF with 1μm TTX, 2mM MNI-L-caged-glutamate, 4mM $CaCl_2$ and 0mM $MgCl_2$. Four basal acquisitions were made with a Ti:Sapphire laser

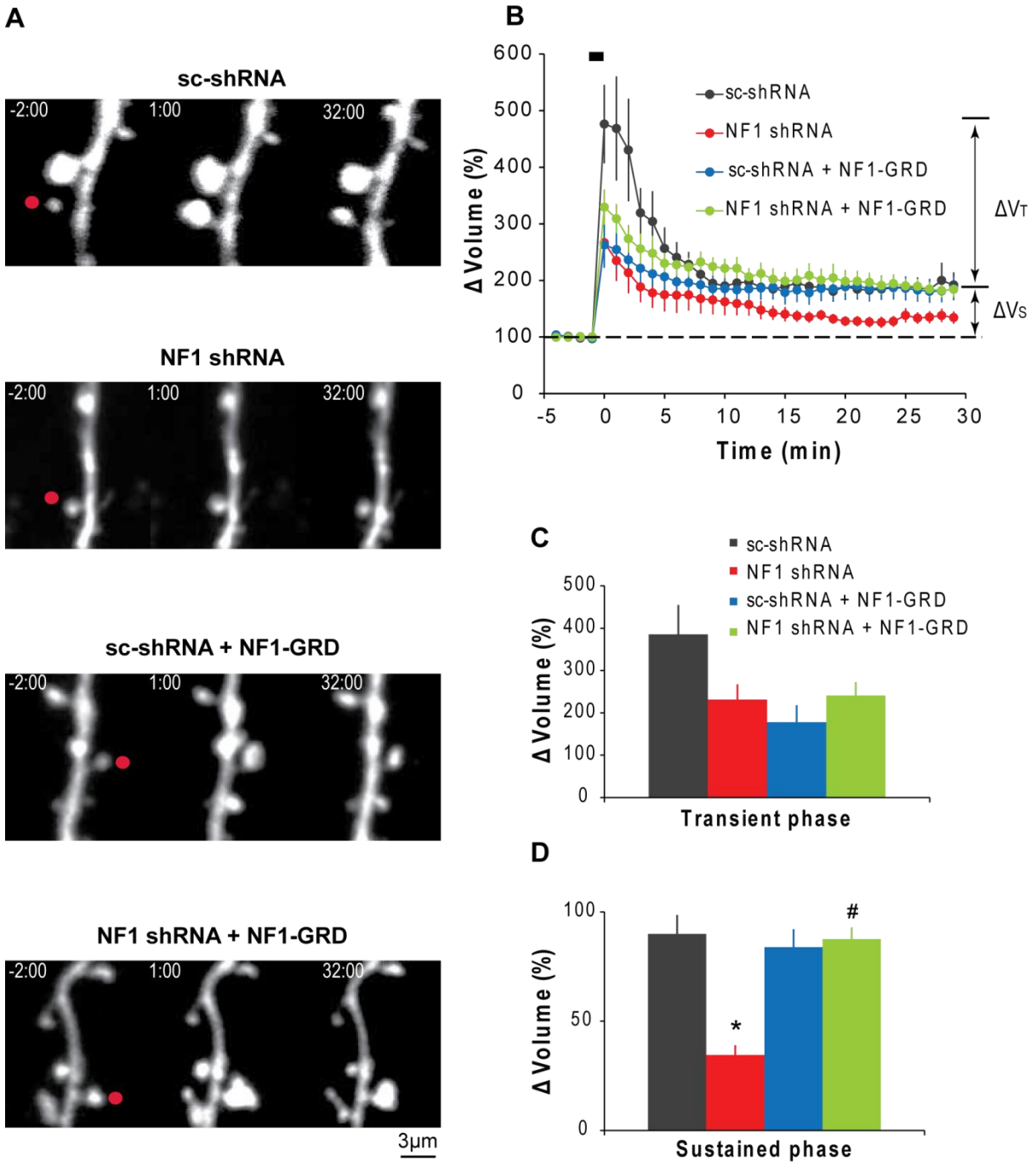

Figure 4.1. Neurofibromin impairs the transient phase of the spine structural plasticity in CA1 pyramidal neurons of the hippocampus, in a Ras-dependent manner. (A) Representative images of portions of secondary or tertiary dendrites of CA1 pyramidal neurons transfected with NF1 shRNA, scrambled shRNA, NF1 shRNA #1 and NF1-GRD domain or scrambled shRNA and NF1-GRD domain, for 5-7 days. The images were taken with a 60x, 0.9NA, Olympus objective, and show stimulated spines in basal conditions, 1 minute after glutamate uncaging stimulus and 30 minutes after stimulation. **(B)** Time-course of the structural plasticity experiment for the conditions specified in (A), as quantified by the spine volume change. Images were acquired every minute. Error bars are S.E.M. **(C)** Quantification of the stimulated spine volume during the transient phase of structural plasticity. The transient phase shown

tuned to 920nm to excite the GFP signal and, after that, an uncaging spot was defined on the top and center of one of the dendritic spines' head in the field. Thirty uncaging pulses of 6ms, 4-5mW, at 0.5Hz, were delivered to this spine through a Ti:Sapphire laser tuned to 720nm and, following that, image acquisitions restarted at the frequency of one per minute until about 30 minutes passed. The volume of the stimulated spine, as well as of the neighboring spines, was measured using the GFP signal. The measured volumes were normalized to the baseline volume, so as to indicate changes of volume. During this experiment, the control condition stimulated spines grew to 385 ± 69% times of their original volume immediately after uncaging (n = 13; **Figure 4.1.A-C**), and, at the end of the experiment, 30 minutes later, the spine volume was still 90 ± 9% bigger than the basal volume (**Figure 4.1.A-B,D**). In contrast, for neurons where neurofibromin was knockdown, the stimulated spine grew only 231 ± 36% times of the initial volume right after uncaging (n = 10; **Figure 4.1.A-C**) and, after 30 minutes, during the sustained phase of spine growth, the volume of the stimulated spine was only 34 ± 4% times bigger than the basal volume (**Figures 4.1.A-B,D**). Of note, the differences observed in the transient phase were not statistically significant, as denoted by the ANOVA test ($p = 0.07$, **Figure 4.1.C**). In contrast, the sustained volume of the imaged spines from neurons expressing NF1 shRNA was significantly smaller than that of spines from neurons expressing a scrambled control shRNA ($p < 0.05$, **Figure 4.1.D**). For both conditions, the neighboring spines' volume remained unchanged during the course of the experiment (data not shown). Hence, our data indicates that, under the conditions of our preparations, neurofibromin removal impairs spine growth during the sustained phase of dendritic spine structural plasticity, when compared to control neurons.

(Figure 4.1., continuation) here results of the subtraction of the sustained phase (average of the acquisitions taken between 25 and 30 minutes period) from the time point zero (right after glutamate uncaging). **(D)** Quantification of the stimulated spine volume during the sustained phase of structural plasticity, as normalized for the basal condition. The sustained phase was chosen to be the average of the data acquired 25 to 30 minutes after stimulation. Stars (*) denote statistically significant difference ($p < 0.05$) from the value in the stimulated spines in scrambled shRNA condition; # denote statistically significant difference ($p < 0.05$) from the value in the stimulated spines in NF1 shRNA condition.

Impaired Structural Plasticity by Neurofibromin Loss-of-Function is Ras-Dependent

Next, we hypothesized that the observed spine structural plasticity impairment, in neurons where neurofibromin was removed, is Ras-dependent. Ras signaling has previously been reported to be important for spine structural plasticity. As mentioned in the introduction of this chapter, Ras signaling inhibition by U0126 resulted in an impairment of the sustained phase of structural plasticity, leaving the early phase of structural plasticity unaffected (Harvey, Yasuda et al. 2008; Patterson, Szatmari et al. 2010), as seen here with removal of neurofibromin. It is possible that structural plasticity requires a tight regulation of Ras-MAPK signaling and that this biological phenomenon is affected by both hyper- and hypoactivation of Ras. If that is true, restoring the RasGAP function of neurofibromin should bring structural plasticity back to control levels. In order to test this hypothesis, we co-transfected organotypic slice cultures of the hippocampus with both NF1 shRNA and the GRD domain of neurofibromin (NF1-GRD), for 5-7 days. We stimulated single target spines with glutamate uncaging and acquired images of the stimulated spine for another 30 minutes, every minute. We observed that the GRD domain of neurofibromin was sufficient to rescue the spine structural plasticity of the stimulated spines to control levels during the sustained phase. Thirty minutes after uncaging, the stimulated spines had a volume that was 88 ± 5% times bigger than their respective basal volume and no statistical difference was observed between these spines and the spines of neurons expressing a scrambled control shRNA ($n = 13$ for sc-shRNA and $n = 9$ for sc-shRNA + NF1-GRD; $p > 0.05$; **Figures 4.1.A-B,D**). Surprisingly, the overexpression of the GRD domain of neurofibromin together with the scrambled control shRNA had no effect on the sustained volume of spines, which were 84 ± 8% times bigger than in the basal state ($n = 7$; $p > 0.05$; **Figures 4.1.A-B,D**). Also, there were no significant differences in the transient phase of spine growth between the conditions tested (385 ± 69% for sc-shRNA; 231 ± 36% for NF1 shRNA; 178 ± 40% for sc-shRNA + NF1-GRD; and 241 ± 31% for NF1 shRNA + NF1-GRD; $p = 0.07$; **Figure 4.1.C**). In conclusion, neurofibromin regulates spine growth during the sustained phase of structural plasticity in a Ras-dependent manner. Furthermore, this experiment indicates that a precise regulation of Ras activity is required for structural plasticity. Thus, hyperactive Ras impairs structural plasticity.

Impaired Structural Plasticity by Neurofibromin Loss-of-Function is Activity-Dependent

Another interesting question is whether the regulation of structural plasticity by neurofibromin is activity-dependent, especially since we demonstrated that neurofibromin is required for dendritic spine density maintenance in an activity-dependent way. In order to test this, we transfected organotypic hippocampal slice cultures with shRNA directed against neurofibromin or scrambled control shRNA and treated them with Mg^{2+} (8mM to a final concentration of 10mM), to block activity, for 6-7 days. Transfected neurons were imaged as before and spines were stimulated with glutamate uncaging. Measurements of the stimulated spine volume indicate that there were no differences between the control neurons and the neurons where neurofibromin was knockdown for structural plasticity during the transient phase (310% ± 51 for sc-shRNA, n = 12, and 201% ± 50 for NF1 shRNA, n = 11; p = 0.24 ANOVA; **Figures 4.2.A-B**). Equally, there were no differences for the transient phase among any other conditions (348% ± 62 for NF1-GRD, n = 11; 308% ± 57 for sc-shRNA + Mg^{2+}, n = 13; 350% ± 70 for NF1 shRNA + Mg^{2+}, n = 12; 359% ± 66 for NF1-GRD + Mg^{2+}, n = 16; p = 0.24 ANOVA; **Figures 4.2.A-B**).

In contrast, ANOVA indicates that there were significant differences in the sustained phases among the different conditions ($p = 7.32x10^{-6}$). As compared to the control condition of neurons expressing scrambled shRNA (61% ± 5), the sustained phase of structural plasticity was impaired in neurons with neurofibromin loss-of-function (23% ± 5 for NF1 shRNA; **Figures 4.2.A, C**), confirming the data presented on **Figure 4.1**. Also in line with the data from **Figure 4.1.**, there were no statistically significant differences between the sustained phases of the control neurons and the neurons expressing the NF1-GRD domain (77% ± 7 for NF1-GRD; **Figures 4.2.A, C**). Importantly, there were no differences between neurons expressing the scrambled control shRNA and those expressing the same construct and also treated with 10.33mM Mg^{2+} for 7 days (49% ± 5 for sc-shRNA + Mg^{2+}; **Figures 4.2.A,C**), which rules out a side effect of Mg^{2+} in structural plasticity. Interestingly, there were also no differences between the sustained phases of structural plasticity induced in neurons expressing the scrambled control shRNA and those expressing NF1 shRNA and incubated with Mg^{2+} for 7 days (61% ± 6 for NF1 shRNA + Mg^{2+}; **Figures 4.2.A, C**), indicating that the impairment in the sustained phase of structural plasticity in neurons where neurofibromin expression is reduced is activity-dependent. Incubation of neurons expressing NF1-

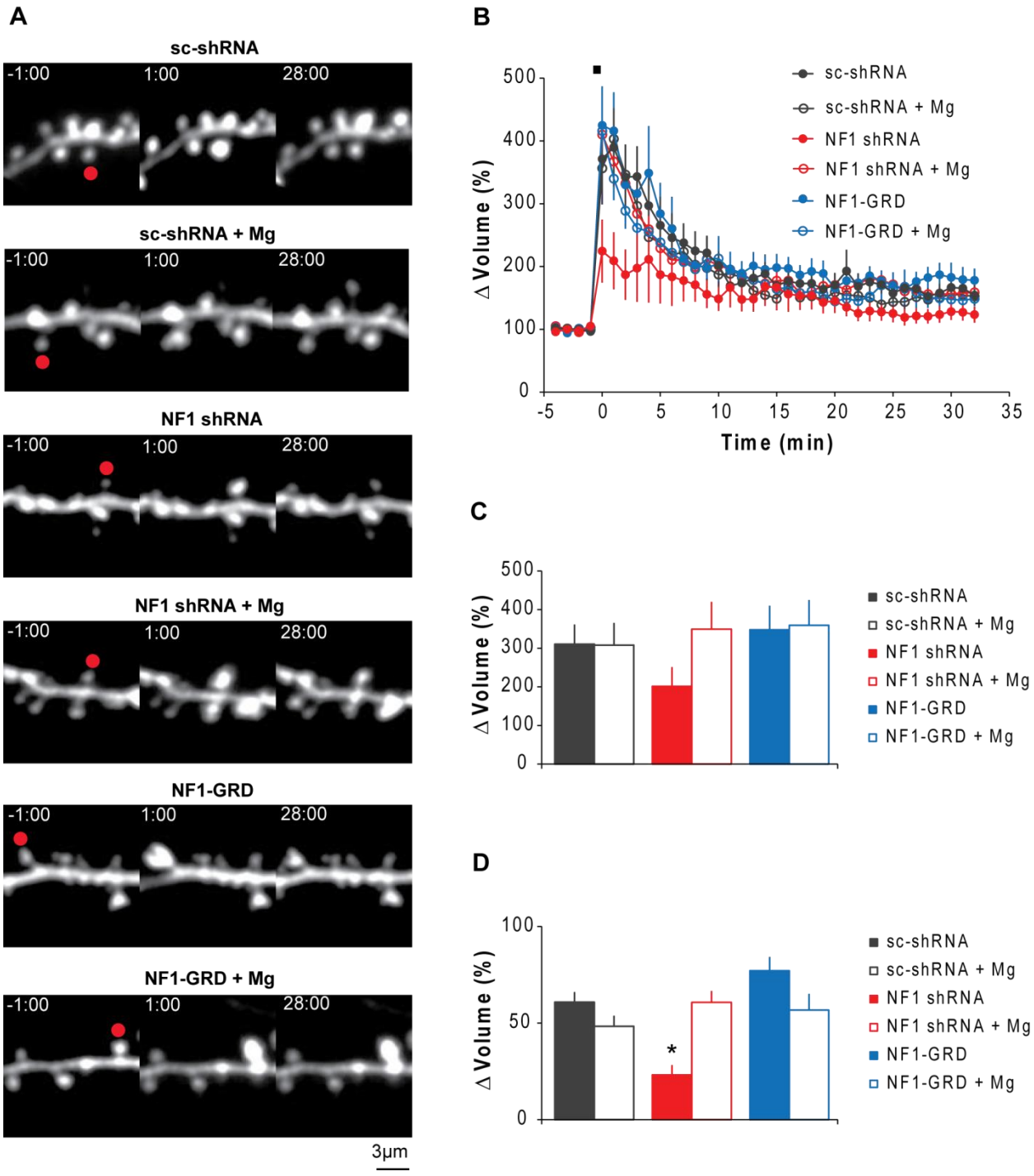

Figure 4.2. Neurofibromin impairs the sustained phase of the spine structural plasticity in CA1 pyramidal neurons of the hippocampus, in an activity-dependent manner. (A) Representative images of portions of secondary or tertiary dendrites of CA1 pyramidal neurons transfected with NF1 shRNA #2, scrambled shRNA, or NF1-GRD domain and treated with either 2mM or 10mM Mg^{2+}, for 6-7 days. The images were taken with a 60x, 0.9NA Olympus objective, and show stimulated spines in basal conditions, 1 minute after glutamate uncaging stimulus and 28 minutes after stimulation. **(B)** Time-course of the structural plasticity experiment for the conditions specified in (A), as quantified by the spine volume.

GRD with Mg^{2+} (57 ± 8%) did not lead to differences from the scrambled control shRNA neurons (61 ± 5%) during the sustained phase of structural plasticity (**Figures 4.2.A,C**). Also, when incubated with Mg^{2+} for 7 days, there were no differences between neurons expressing a scrambled control shRNA (49 ± 5%), NF1 shRNA (61 ± 6%) or NF1-GRD (57 ± 8%), which further supports the conclusion that the effect of neurofibromin on the sustained phase of structural plasticity is activity-dependent. In contrast, spine growth during the sustained phase of structural plasticity was significantly impaired for NF1 shRNA-transfected neurons (23 ± 5%), as compared with neurons expressing the NF1 shRNA and also incubated in elevated Mg^{2+} for 7 days (61 ± 6%), indicating that the effect of decreased levels of expression of neurofibromin in dendritic spine structural plasticity was abolished when neuronal activity was blocked. The GRD domain of neurofibromin, in either the presence (57 ± 8%) or absence (77 ± 7%) of elevated Mg^{2+}, had a significantly larger sustained phase than NF1 shRNA-expressing neurons (23 ± 5%). Lastly, there were no significant differences between the sustained phases in neurons expressing the NF1-GRD domain in control conditions (77 ± 7%) and the NF1-GRD domain (57 ± 8%) or NF1 shRNA (61 ± 6%) in the presence of extra Mg^{2+}. Taken together, these data demonstrate that neurofibromin impairs dendritic spine structural plasticity in an activity-dependent way.

Neurofibromin Does Not Regulate the NMDA Receptor Function

Husi and collaborators (2000) have shown that neurofibromin is in the complex that associates with the NMDAR via mass spectrometry (Husi, Ward et al. 2000). Hence, it is possible that the NMDAR is regulated by neurofibromin and/or vice-versa. Also, the data presented in this chapter (**Figure 4.2.**) and

---

(**Figure 4.2.**, **continuation**) Images were acquired every minute. Error bars are S.E.M. **(C)** Quantification of the stimulated spine volume during the transient phase of structural plasticity (average of volume at 0min subtracted by average of volume during the sustained phase (25-30min)). **(D)** Quantification of the stimulated spine volume during the sustained phase of structural plasticity, as normalized for the basal condition. The sustained phase was arbitrary chosen to be the average of the data acquired 25 to 30 minutes after stimulation. Stars (*) denote statistically significant difference ($p < 0.05$) from the value in the stimulated spines in scrambled shRNA condition (under 2mM Mg^{2+}); # denote statistically significant difference ($p < 0.05$) from the value in the stimulated spines in NF1 shRNA condition (under 2mM Mg^{2+}).

the previous chapter (**Figure 3.3.**) suggests a regulatory mechanism between these two molecules. Namely, the removal of neurofibromin affects the structural plasticity of dendritic spines downstream the NMDAR and blockade of the NMDAR activity abolishes the structural plasticity impairment caused by reduced expression of neurofibromin (**Figure 4.2.**). Furthermore, as seen in the previous chapter, the effect of neurofibromin removal in the spine number can be rescued when blocking the NMDAR with a strong antagonist, AP5 (**Figure 3.3.**). These data suggest that neurofibromin regulates NMDAR signaling and, most likely, the Ca^{2+} entry in the cell. In order to test this hypothesis, we performed Ca^{2+} imaging experiments and we measured the peak Ca^{2+} concentration in dendritic spines, as well as the NMDAR current (I_{NMDAR}) at the soma, following single uncaging pulses of 4-5mW of 6ms. Organotypic hippocampal slice cultures were transfected with shRNA directed against neurofibromin for 5-7 days. After that, the slices were incubated in ACSF containing 1μM TTX, 4mM $CaCl_2$, 0mM $MgCl_2$, 2mM MNI-L-glutamate and 20μM NBQX (to block the AMPARs). Whole-cell voltage-clamp recordings were performed with pipettes of 4-5mOhm resistance, containing a Cs-based internal solution and 500μM Oregon-Green BAPTA-5N (a green Ca^{2+}-sensitive dye) and 300μM Alexa-594 (a red Ca^{2+}-insensitive dye) and the neurons were held at 0mV in order to allow for NMDAR activation. Secondary and tertiary apical dendrites were selected and spines of interest were imaged with a 60x, 0.9NA Olympus objective. For stimulation, single pulses of 4-5mW were applied in a small region on the top and center of spine heads of interest to uncage MNI-L-glutamate and activate NMDARs. Glutamate uncaging has been accepted as a method fairly specific for NMDAR activation only, therefore it is possible to access the function of this receptor when such stimulation is used. The peak I_{NMDAR} at the soma and the Ca^{2+} concentration peak in the spine and neighboring dendrite were measured simultaneously before and upon stimulation. At the end of the day, a pipette was filled with the same internal solution mixed with a 10μM $CaCl_2$ solution and positioned on the top of the imaged slice. Two-photon scanning images were acquired and the Ca^{2+} concentrations observed during the experiments of that day were determined through normalization to the well-known Ca^{2+} concentration from the solution in the pipette.

Our data shows that immediately after stimulation there was Ca^{2+} influx in the stimulated dendritic spine, which was moderately restricted to the stimulated spine. A smaller increase in Ca^{2+} concentration

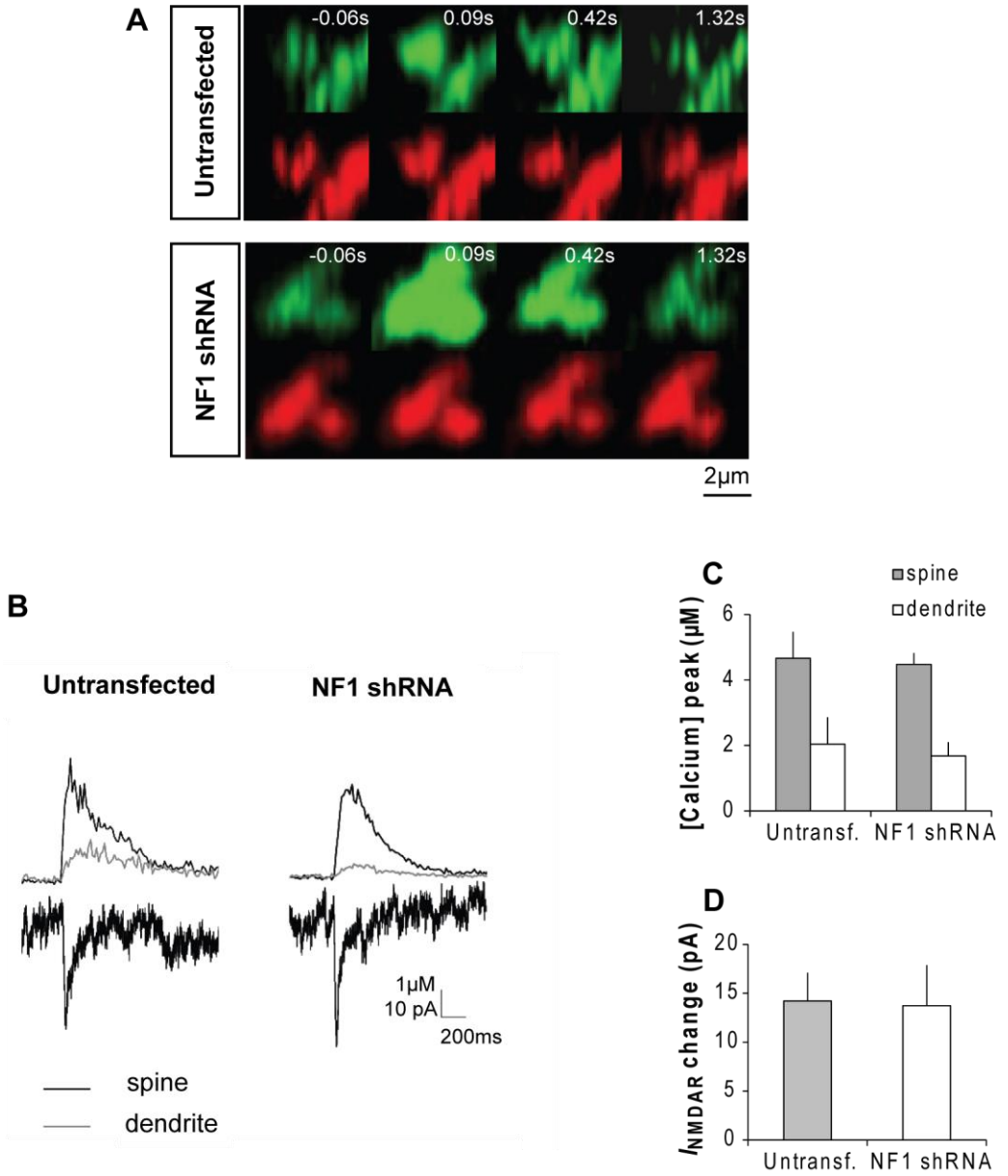

Figure 4.3. Neurofibromin does not regulate the I_{NMDAR} or its Ca^{2+} permeability. Organotypic slice cultures of the hippocampus were ballistically transfected with NF1 shRNA #2 or scrambled shRNA for 5-7 days. Whole-cell voltage-clamp recordings were made and the cells were held at 0mV, after being filled with a green Ca^{2+}-sensitive dye and a red Ca^{2+}-insensitive dye. Using a TPLSM, single dendritic spines were stimulated with MNI-L-glutamate uncaging and Ca^{2+} imaging was performed simultaneously to I_{NMDAR} recordings. **(A)** Representative images of the Ca^{2+} imaging experiment, showing the red channel for morphology and the green channel for Ca^{2+} imaging, before and upon stimulation. **(B)** Representative electrophysiological traces of the I_{NMDAR} measured at the soma upon uncaging stimulation, in pA, paired with the respective traces for Ca^{2+} entry in the spine and adjacent dendrite. **(C)** Quantification of the peak Ca^{2+} concentration in the stimulated dendritic spines and their adjacent dendrites, in µM, upon normalization to a defined pipette concentration of 10µM (n = 9 neurons for untransfected condition or n = 7 neurons for NF1 shRNA condition). Neurofibromin removal does not affect the Ca^{2+} entry through the NMDAR. **(D)** Quantification of the peak I_{NMDAR}, in pA, measured at the soma.

was also seen in the immediate adjacent dendrite (2.04 ± 0.34μM for untransfected neurons, n =9, and 1.68 ± 0.42μM for NF1 shRNA transfected neurons, n = 7; **Figures 4.3.A-C**). The Ca^{2+} was rapidly cleared from the spine and dendrite, returning to its basal concentration. This pattern was observed in both neurons transfected with NF1 shRNA and their neighboring untransfected neurons. Surprisingly, we observed no differences in the peak Ca^{2+} concentration in the stimulated dendritic spine between the two conditions (4.66 ± 0.81μM for untransfected neurons and 4.48 ± 0.82μM for neurons expressing a NF1-directed shRNA, p = 0.98, **Figures 4.3.A-C**), indicating that neurofibromin removal did not affect the NMDAR-mediated Ca^{2+} permeability. Equally, the I_{NMDAR} recorded at the soma was not different between the control condition and the case where neurofibromin was knockdown (14.22 ± 2.88pA for untransfected neurons and 13.73 ± 4.15pA for NF1 shRNA-expressing neurons, p = 0.84, **Figures 4.3.B-D**). Together, these data indicate that the NMDAR function is not affected by neurofibromin, despite the fact that these two proteins are present in the same protein complex.

Discussion

In this chapter, we asked whether neurofibromin plays a role in dendritic spine structural plasticity in the CA1 region of the hippocampus. We used shRNA constructs directed against *Nf1* to answer this question and stimulated single spines with two-photon glutamate uncaging. Under the conditions of our organotypic slice culture preparations, we observed that reduced levels of neurofibromin caused impairment in the late phase of dendritic spine plasticity compared to the control condition. In line with our observations, Costa and collaborators (2002) showed that a mouse model of NF1, consisting of a heterozygous mouse for the *Nf1* gene ($Nf1^{+/-}$) and therefore expressing reduced levels of neurofibromin, had impaired LTP in the Schaffer-collateral pathway of the hippocampus, following a standard physiological protocol of TBS to induce LTP (Costa, Fedorov et al. 2002).

Dendritic spines undergo functional and structural changes during synaptic plasticity. Several studies indicate a strong correlation between structural and functional plasticity (Engert and Bonhoeffer 1999; Maletic-Savatic, Malinow et al. 1999; Nagerl, Eberhorn et al. 2004; Zhou, Homma et al. 2004; Harvey, Yasuda et al. 2008; Lee, Escobedo-Lozoya et al. 2009; Patterson, Szatmari et al. 2010), being that a LTP-induced stimulus generally causes increases in the volume of spines undergoing LTP. Conversely, spines that undergo LTD often shrink or even disappear. As in functional LTP, where potentiated pathways remain potentiated for long periods, spine structural plasticity induced by a LTP stimulus lasts for at least 60 minutes (Matsuzaki, Ellis-Davies et al. 2001; Matsuzaki, Honkura et al. 2004). Using two-photon glutamate uncaging to induce LTP, we reported similar findings in our control condition to those observed by Matsuzaki and collaborators (2004). Like us, they delivered LTP-inducing stimuli in dendritic spines of GFP-expressing hippocampal pyramidal neurons in rat organotypic slices from 14-20 days old animals (Matsuzaki, Honkura et al. 2004), which increased the stimulated spine volume by about two-fold (stimulation of a single dendritic spine by 1-2Hz for 60s in 0mM Mg^{2+} extracellular solution). This increase persisted for more than 1h after stimulation (Matsuzaki, Honkura et al. 2004). In the current study, we used a different stimulation protocol, previously shown to induce LTP (Harvey and Svoboda 2007; Harvey, Yasuda et al. 2008; Lee, Escobedo-Lozoya et al. 2009; Patterson, Szatmari et al. 2010; Murakoshi, Wang et al. 2011), which induced a spine volume growth of similar magnitude that lasted for at least 30 minutes after stimulation. In contrast with control neurons, our data shows that neurons with low expression of neurofibromin had reduced volume changes 30 minutes upon receiving a LTP-inducing stimulus, supporting and extending previous findings that report impaired LTP in mice with reduced expression of neurofibromin (Costa, Fedorov et al. 2002; Li, Cui et al. 2005; Guilding, McNair et al. 2007).

The data presented in this chapter also establishes that Ras hyperactivation results in impaired structural plasticity, since overexpression of the GRD domain of neurofibromin (a manipulation that promotes Ras inactivation) abolishes the impairment of structural plasticity caused by reduced levels of neurofibromin. This further supports an important role of Ras in synaptic plasticity. Adding our data to the previous findings reporting that blocking a downstream effector of Ras (MEK) also impairs the sustained phase of spine structural plasticity (Harvey, Yasuda et al. 2008; Patterson, Szatmari et al. 2010), we

conclude that precise Ras activation is necessary for normal structural plasticity to occur. This idea was already suggested by others (Thomas and Huganir 2004; Stornetta and Zhu 2011) based on multiple reports that demonstrated that both hypo- and hyperactivation of Ras lead to impairments in synaptic plasticity. For example, on the side of blockade of LTP by Ras hyperactivation, another mutant heterozygous mouse for a different RasGAP (SynGAP) also exhibited impaired LTP in the hippocampus (Komiyama, Watabe et al. 2002). A HRas peptide impaired LTP in the CA1 region of the hippocampus (Thornton, Yaka et al. 2003). On the side of blockade of LTP by Ras hypoactivation, a RasGEF mutant ($RasGRF^{-/-}$), a situation that blocks Ras activation, displayed impaired LTP in the amygdala (Brambilla, Gnesutta et al. 1997). Inhibitors of Ras, such as FTase inhibitors, disrupt LTP in the CA1 region of the hippocampus (O'Kane, Stone et al. 2004). However, there are also studies that do not seem to support the theory that precise Ras regulation is required for optimal LTP magnitude. Namely, a study by Manabe and collaborators (2000) demonstrated that, in HRas deficient mice ($HRas^{-/-}$), the magnitude of the LTP (induced by tetanic stimulation) is almost the double of that of WT mice (Manabe, Aiba et al. 2000). In line with this study, we report that Ras hyperactivation decreased the magnitude of structural plasticity levels, which extends the information of Manabe's study showing that, conversely, HRas loss-of-function increases the magnitude of LTP. Manabe and collaborators (2000) also concluded that PPF was not significantly different between WT mice and HRas mutant mice, suggesting that presynaptic release probability is not affected by HRas proteins (Manabe, Aiba et al. 2000). Rather, their data suggests that the enhanced LTP in mutant mice results from postsynaptic mechanisms. Hence, our data is in line with the findings of this study, supporting a postsynaptic role of Ras signaling downstream neurofibromin in LTP.

We have also investigated whether the structural plasticity impairment by neurofibromin reduced levels is activity-dependent. In order to do so, we performed two-photon glutamate uncaging experiments, stimulating single dendritic spines from neurons previously treated with pharmacological agents that block the NMDAR and transfected with a control shRNA or a NF1-directed shRNA. We concluded that blockade of activity was sufficient to reverse the magnitude of structural plasticity in neurons expressing low levels of neurofibromin. Thus, the regulation of dendritic spine structural plasticity by neurofibromin is activity-dependent.

We speculate that this phenomenon might be related to a homeostatic mechanism to balance Ras activity and synaptic plasticity. In other words, we hypothesize that, under normal conditions, precise Ras regulation by neurofibromin and perhaps other RasGAPs is essential for the magnitude of structural plasticity, following NMDAR activation. When neurofibromin levels are reduced, Ras inactivation is inefficient due to the absence of the RasGAP, resulting in abnormally high or even persistent Ras activity upon NMDAR activation (and most likely other receptors, too, such as the TrkB receptor), which unbalances the precise signaling control required for maximal magnitude structural plasticity. It is possible that, under conditions of reduced inactivation by neurofibromin, permanent Ras hyperactivity leaves no space for further activation following NMDAR stimulation. In this case, the synapse would behave as insensitive to LTP-inducing stimulus, being unable to undergo potentiation, which would explain the reduced levels of structural plasticity seen here and LTP in general. In this case, when the NMDAR is chronically blocked (such as in our experiment, where we kept NMDAR inhibitors in the culture medium for 6-7 days), despite lack of inactivation by neurofibromin, Ras might remain under hyperactivation levels due to lack of NMDAR activation, which is upstream Ras (Yun, Gonzalez-Zulueta et al. 1998). As such, a single acute episode of NMDAR activation during the two-photon glutamate uncaging experiments (after removal of NMDAR inhibitors) would now activate a nearly basal level activity Ras (prone to be further activated) and follow the normal route of signaling-induced spine structural plasticity.

We also investigated if neurofibromin regulates the NMDAR by performing two-photon Ca^{2+} imaging and glutamate uncaging, which is one of the prime experiments to analyze Ca^{2+} entry through the NMDAR. The findings reported in this chapter indicate that neurofibromin does not regulate the NMDAR function, given that both the peak Ca^{2+} concentration and peak I_{NMDAR} were similar between neurons with reduced neurofibromin expression and control untransfected neurons. A study by Manabe and collaborators (2000) contradicts somewhat our conclusions, given that this other group concluded that HRas loss-of-function leads to an enhancement of the NMDA synaptic responses induced by an increase in the tyrosine phosphorylation of the NMDAR (Manabe, Aiba et al. 2000). NMDAR tyrosine phosphorylation is necessary to keep the NMDAR at the membrane. Hence, hypothetically, this study would predict that we would observe a decreased NMDAR current and Ca^{2+} permeability under conditions where neurofibromin levels were reduced and Ras activated. This discrepancy might be due to the

differences in the approach used in the two studies. Manabe et al. (2000) completely removed the *HRas* gene and, thus, it is expected that there is no residual activity of HRas. In our study, *HRas* was not removed, but simply it lacks complete regulation by neurofibromin, one among several RasGAPs present in dendritic spines of the hippocampus. It might be that other RasGAPs not removed, namely SynGAP (also present in dendritic spines of hippocampal neurons), can compensate for the reduced levels of neurofibromin. Also, it is possible that neurofibromin acts as a RasGAP over a different Ras isoform that not HRas. Another study by Thornton and collaborators (2003) is also in disagreement with our data. Thornton et al. (2003) provided evidence that HRas inactivates Src kinase, a tyrosine kinase that phosphorylates the GluN2A subunit of the NMDAR. This phosphorylation is necessary to keep the NMDAR at the membrane and incubation of rat hippocampal slices with a Tat-HRas depleted GluN2A from the synaptic membrane, causing a decrease in the magnitude of LTP in the Schaeffer-collateral pathway (Thornton, Yaka et al. 2003). Hence, in contrast with our results, this study reported that Ras hyperactivity decreases the NMDAR function.

Future Directions

Previous studies in NF1 patients and mouse models of NF1 have shown that a more intense learning paradigm is able to compensate the cognitive impairments observed in humans and mice afflicted with the disease (Costa, Fedorov et al. 2002). Hence, it will be interesting to test if a more intense input-specific glutamate uncaging stimulus is able to abolish the decreased sustained phase of structural plasticity in neurons expressing reduced expression of neurofibromin. Whether this experiment might not be conclusive under the cognitive view, since memory restoration by extended training has been shown to be independent of the hippocampus function, Costa and collaborators demonstrated that a strong, non-physiological stimulus (HFS), can abolish the impairment in LTP observed in *Nf1*$^{+/-}$ mice (Costa, Fedorov et al. 2002). It will also be interesting to pursue follow-up experiments to the Ca^{2+} imaging experiment in order to possibly identify a different receptor that could be regulated by neurofibromin.

CHAPTER V

Neurofibromin is a major RasGAP in the dendritic spines of CA1 pyramidal neurons of the hippocampus

Chapter V. Neurofibromin is a major RasGAP in the dendritic spines of CA1 pyramidal neurons of the hippocampus

Introduction

Many GAPs have been identified towards multiple members of the Ras family proteins (Bernards 2003) and it is likely that many more will be identified in the future. These proteins are fundamental for the regulation of Ras signaling, by inactivating Ras. Since the recent discovery that Ras is required for synaptic plasticity, learning and memory, several studies have tried to address the role of RasGAPs in proper memory formation, as well as disease (Silva, Frankland et al. 1997; Costa, Fedorov et al. 2002; Li, Cui et al. 2005; Guilding, McNair et al. 2007; Cui, Costa et al. 2008). Among these, a recent study demonstrated that neurofibromin regulates neurotransmission by inactivating Ras at the presynaptic terminals of interneurons, thereby preventing excessive GABA release and high inhibition in the hippocampus (Cui, Costa et al. 2008). SynGAP, another RasGAP, is present in dendritic spines, where it associates with the NMDAR at the PSD of hippocampal CA1 pyramidal neurons and regulates the numbers of synaptic AMPARs that are inserted at the postsynaptic sites during LTP (Kim, Lee et al. 2003; Krapivinsky, Medina et al. 2004; Kim, Dunah et al. 2005; Rumbaugh, Adams et al. 2006; Lee, Lee et al. 2011). However, it is yet unknown which RasGAP contributes to Ras inactivation in dendritic spines.

Given our findings in the previous chapters of this dissertation, namely the impact of neurofibromin removal in spine morphology (**chapter III**) and structural plasticity (**chapter IV**), as well as the involvement of Ras signaling dysregulation mechanisms, we hypothesize that neurofibromin may be an important RasGAP in dendritic spines, regulating Ras activity in this compartment during spine structural plasticity. A study from Hsueh and collaborators (2001) reporting that neurofibromin is present in dendritic spines of hippocampal cultured neurons and another study from Husi and collaborators (2000) reporting that neurofibromin associates with the NMDAR protein complex suggest that neurofibromin could be a RasGAP in dendritic spines (Husi, Ward et al. 2000; Hsueh, Roberts et al. 2001). In order to

study if neurofibromin regulates Ras activity in dendritic spines, we made use of advanced optical techniques that allow the visualization of interactions between molecules in small compartments, such as dendritic spines (Yasuda 2006; Yasuda, Harvey et al. 2006; Harvey, Yasuda et al. 2008; Lee, Escobedo-Lozoya et al. 2009; Murakoshi, Wang et al. 2011). Particularly, a previous study using TPFLIM and 2-photon glutamate uncaging revealed the spatiotemporal dynamics of HRas in single dendritic spines undergoing structural plasticity and LTP (Harvey, Yasuda et al. 2008). HRas is rapidly activated following single dendritic spine stimulation and its activity spreads from the stimulated spines along dendrites and into surrounding spines over ~ 10μm. Here, we used several neurofibromin manipulations, including neurofibromin removal by shRNA expression or overexpression of the GRD domain of neurofibromin, to identify whether neurofibromin acts as a RasGAP in dendritic spines, regulating Ras signaling in this compartment.

Results

An Improved Sensor to Detect Ras Activation

To measure the activity of HRas in dendritic spines, we developed a FRET-based sensor optimized for imaging under TPFLIM, using the previously described Ras sensor FRas-F (Yasuda, Harvey et al. 2006; Harvey, Yasuda et al. 2008) as a template. The HRas sensor consists of two components: HRas, tagged with one monomeric enhanced green fluorescent protein (mEGFP) in its N terminal (donor), and its binding partner Ras GTPase binding domain (RBD) of c-Raf, double-tagged with mRFP (mRFP-RBD-mRFP) in the N terminal and the C terminal (acceptor). When mEGFP-HRas is activated, mRFP-RBD-mRFP binds to mEGFP-HRas, causing FRET between mEGFP and mRFP (**Figure 5.1.A**). In the original sensor, RBD includes the R59A mutation, in order to decrease the binding affinity between RBD and HRas, allowing the inactivation of HRas following activation. The WT version of RBD as acceptor prevents the efficient sensor inactivation (Yasuda, Harvey et al. 2006).

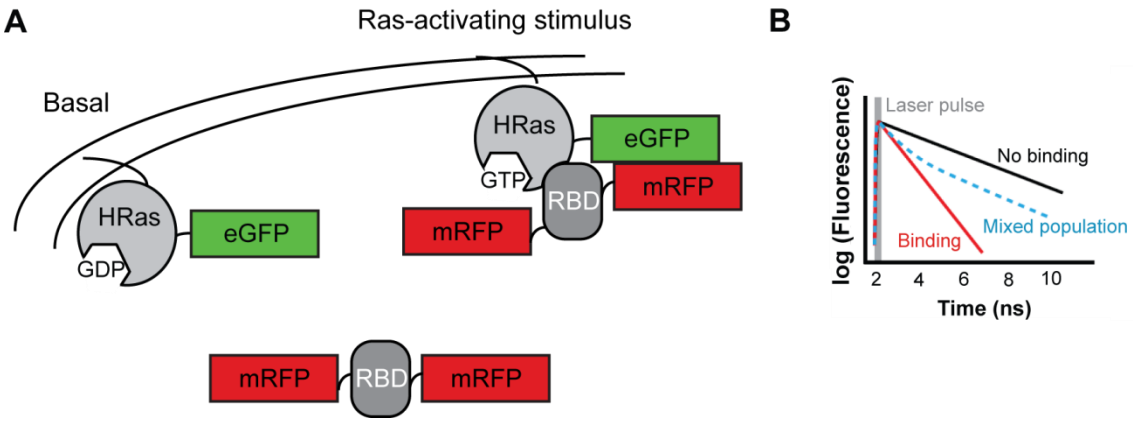

Figure 5.1. Design of the Ras sensor. (A) Schematic representation of the HRas sensor. The HRas sensor is composed of two molecules: the donor, which consists of HRas tagged with a mEGFP in its N terminal, and the acceptor, which consists of the Ras binding domain of c-Raf (RBD) with two mRFPs tagged to the N and C terminal of RBD. For the experiments presented in this dissertation, the acceptor was modified by the introduction of two mutations in RBD (K65E and K108A) and removal of a previous mutation (R59A; Yasuda, Harvey et al. 2006; Harvey, Yasuda et al. 2008). When HRas is activated, RBD is recruited to the membrane where it binds to HRas, producing FRET between mEGFP and mRFP. **(B)** Schematic of fluorescence decay curves after pulsed excitation. Slow and fast components correspond to the free donor and donor bound to acceptor, respectively. FRET decreases fluorescence lifetime. Fluorescence lifetime measurements can deconvolve the binding fraction. *Adapted from Yasuda, Harvey et al. 2006; Yasuda 2006; Harvey, Yasuda et al. 2008.*

At first, we decided to use the original sensor, but consistently observed the accumulation of RBD in the nucleus (**Figure 5.2.B**; **Figure 5.3.A-B**) and, therefore, the sensor did not activate in neurons upon a LTP-inducing stimulus similar to the one administered by Harvey and collaborators (2008). Having the acceptor in the nucleus makes it slow and difficult to move it to the plasma membrane upon Ras activation, which deteriorates the temporal resolution of Ras activation and likely the magnitude of the signal. Hence, we decided to start by performing experiments in cell lines (293T cells) to test the effect of a few new mutations on RBD in the localization and activation/inactivation of the Ras sensor. When testing for the localization of the sensor, we expect to find the GFP signal from mEGFP-HRas at the plasma membrane and possibly in other intracellular membranes, since HRas like other Ras forms undergoes prenylation and farnesylation to become a membrane protein (Hancock 2003; Wright and Philips 2006; Arozarena, Calvo et al. 2011). Conversely, we expect the RFP signal from mRFP-RBD-mRFP to be cytosolic like RBD. For all Ras sensors tested, we observed membrane localization for HRas,

A

Raf constructs	K_D (μM)
WT	0.13
K65E	0.67
K65M	0.41
T68A	1.3
R67A	2.1
R59A	3.8
Q66A	7.4
K84A	14

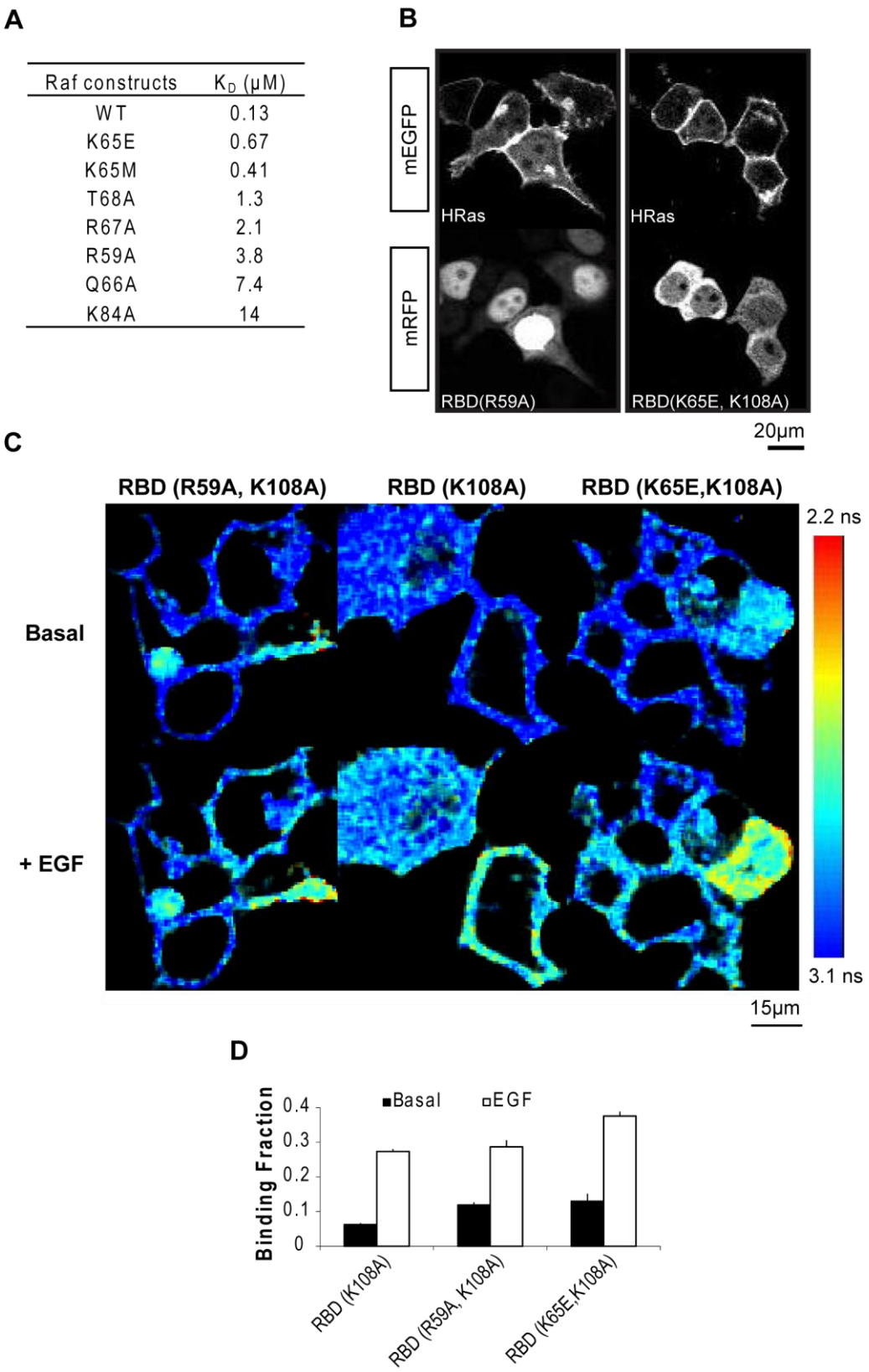

Figure 5.2. Characterization of the Ras sensor. (A) Table with the dissociation constants for the complexes between RafRBD WT and mutants and WT mant-Gpp(NH)p-Ras. *Adapted from Jaitner,*

as expected (**Figure 5.2.B**; **Figure 5.3.B-C**), but the RBD localization was rather diverse. We observed that the acceptor of the original sensor (mRFP-RBD^{59A}-mRFP) was concentrated in the nucleus of 293T cells (**Figure 5.2.B**), similarly to what was also observed in neurons (**Figure 5.3.A-B**). Thus, we analysed the sequence of RBD and, with the help of Dr. Hideji Murakoshi, we found a NLS in RBD. We introduced the mutation K108A, which disrupts the NLS. When RBD harbored both the R59A and the K108A mutations, the acceptor localized to the cytoplasm, being mostly excluded from the nucleus (data not shown), but this sensor was unable to activate in neurons (data not shown). Hence, we decided to replace the mutation R59A with the mutation K65E, which confers a higher affinity of RBD towards Ras, but still lower affinity than the WT version of RBD (**Figure 5.2.A**; (Jaitner, Becker et al. 1997)), therefore increasing the sensitivity of the HRas sensor. RBD harboring both K65E and K108A mutations is cytosolic (**Figure 5.2.B** and **Figure 5.3.A-C**) and activates well in neurons (**Figure 5.4.A-C**), to comparable levels as the sensor previously reported with similar stimulation (Yasuda, Harvey et al. 2006; Harvey, Yasuda et al. 2008).

Next we compared the efficiency of three sensors for Ras activity detection in HEK293T cells. We transfected HEK293T cells with the different Ras sensors and reduced the percentage of serum present in the culture medium from 10% to 0.5% sixteen hours after transfection. Eight hours later the cells were imaged in Hepes-buffered ACSF medium containing 1mM Ca^{2+} as previously described by Murakoshi et al. (2008). We acquired four basal FLIM images, followed by EGF (100ng/ml) stimulation. We promptly

---

(Figure 5.2., continuation) *Becker et al. 1997*. **(B)** Membrane localization of mEGFP-HRas as seen by the green and red fluorescence images of HEK293T cells transfected with mEGFP-HRas and the respective acceptor for each sensor. **(C)** Representative fluorescence lifetime images in HEK293T cells transfected with three different Ras sensors all consisting of the same donor, but different acceptors. The original acceptor (mRFP-RBD^{59A}- mRFP) described in Yasuda, Harvey et al. (2006) and Harvey, Yasuda et al. (2008), the acceptor with a disrupted NLS (mRFP-RBD^{108A}-mRFP) and the acceptor with the disrupted NLS plus a mutation that slightly decreases RBD affinity for Ras (mRFP-RBD^{65E,108A}-mRFP) were used. The top pseudocolored images show 293T cells expressing the different Ras sensors under basal conditions, whereas the bottom pseudocolored images show the same cells upon EGF (100ng/ml) stimulation. Warmer colors indicate shorter lifetimes and higher levels of Ras activity. Fluorescence lifetime imaging was performed 24 hours after transfection in a solution containing 30mM Na-HEPES (pH 7.3), 130mM NaCl, 2.5mM KCl, 1mM $CaCl_2$, 1mM $MgCl_2$, 2mM $NaHCO_3$, 1.25mM NaH_2PO_4 and 25mM glucose. **(F)** Fraction of donor bound to acceptor before and after the application of EGF (100ng/ml). Error bars indicate S.E.M. over 4 fields from one dish.

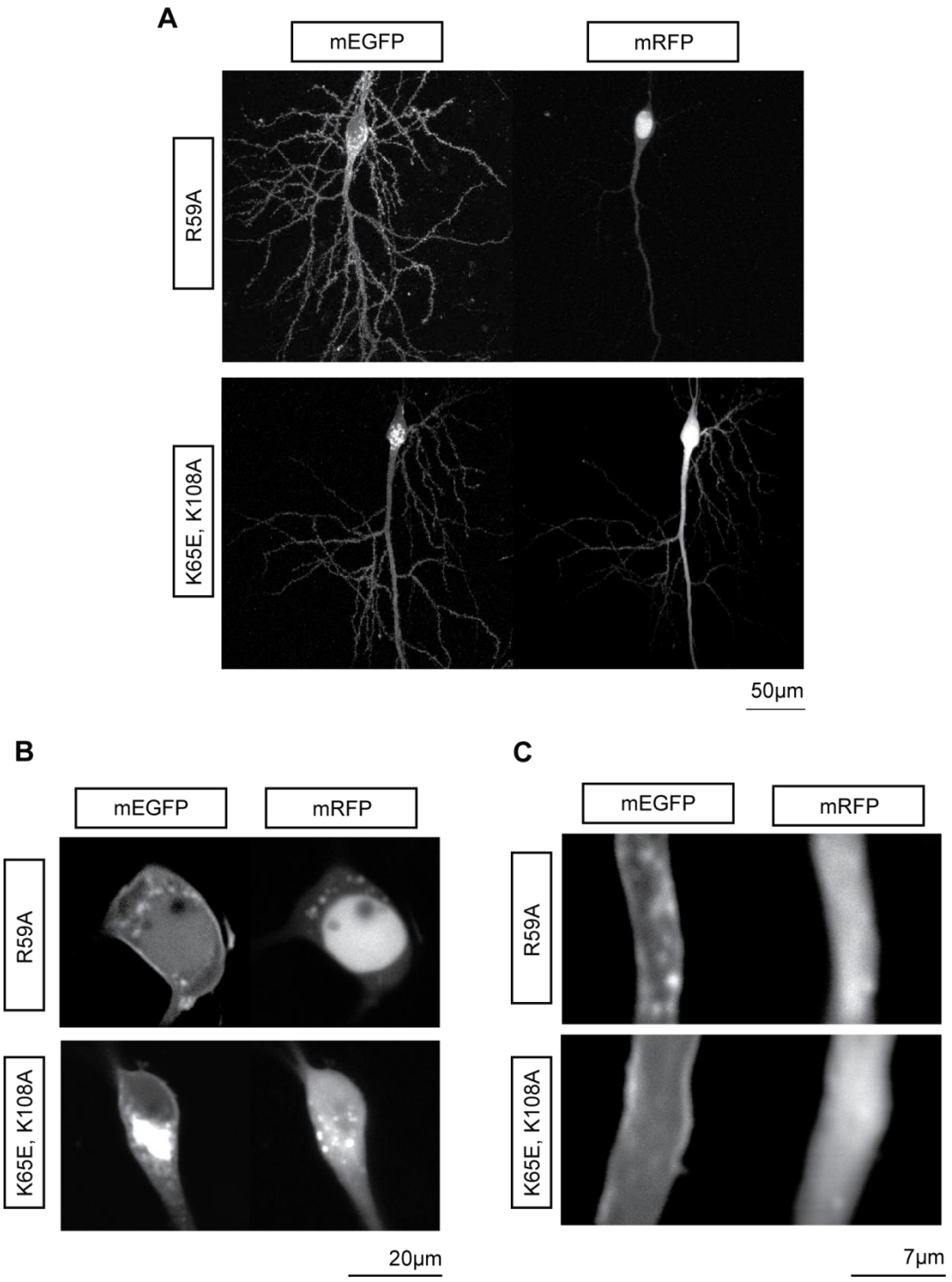

Figure 5.3. Localization of the Ras sensor in CA1 pyramidal neurons. (A) Images of neurons transfected with Ras sensors, showing the localization of the donor (mEGFP-HRas) and the localization of the acceptor (mRFP-RBD-mRFP). **(B)** Detail of cell soma showing membrane localization of mEGFP-HRas and the subcellular localization of the acceptor for each sensor. The acceptor accumulates in the nucleus if using mRFP-RBD^{59A}-mRFP, or is cytoplasmic if using mRFP-RBD^{65E,108A}-mRFP. **(C)** Detail of the localization of the Ras sensor in the primary apical dendrite of CA1 pyramidal neurons.

observed increased Ras activation upon EGF stimulation for all the sensors (**Figure 5.2.C-D**), as reported by the change from colder (higher lifetime, lower FRET between mEGFP and mRFP) to warmer colors (shorter lifetime, higher FRET between mEGFP and mRFP) in a pseudocolor code for lifetime (**Figure 5.1.B**). The basal binding fraction was slightly lower for the acceptor version mRFP-RBD^{108A}-mRFP (BF = 0.06 ± 0.004) as compared to the other two sensors tested, whereas no significant differences were seen between the acceptors mRFP-RBD^{59A,108A}-mRFP and mRFP-RBD^{65E,108A}-mRFP for the basal binding fraction (BF = 0.12 ± 0.008 for RBD^{59A,108A}; 0.13 ± 0.022 for RBD^{65E,108A}; **Figure 5.2.D**). However, the acceptor mRFP-RBD^{65E,108A}-mRFP allowed for a higher activation magnitude and, therefore, might be more sensitive than the acceptor mRFP-RBD^{59A,108A}-mRFP (peak BF = 0.29 ± 0.019 for RBD^{59A,108A}; peak BF = 0.38 ± 0.013; **Figure 5.2.D**). Moreover, testing experiments showed that the sensor using the acceptor mRFP-RBD^{59A,108A}-mRFP did not activate in neurons (data not shown). Therefore, given its cytosolic localization and higher sensitivity, we decided to use the sensor that includes the donor mRFP-RBD^{65E,108A}-mRFP for the following experiments in cultured hippocampal neurons.

Neurofibromin Acts as a RasGAP in Dendritic Spines of the Hippocampus

Using the optimized sensor, we measured the activity of HRas during dendritic spine structural plasticity. Pyramidal neurons of the CA1 region of cultured hippocampal slices were ballistically co-transfected with the HRas sensor and NF1 shRNA or scrambled control shRNA, or with the HRas sensor and the GRD domain of neurofibromin and treated with an elevated concentration of $MgCl_2$ (10mM) to prevent HRas activation following HRas overexpression. The FRET signal was measured under TPFLIM (Yasuda, Harvey et al. 2006; Harvey, Yasuda et al. 2008; Lee, Escobedo-Lozoya et al. 2009; Murakoshi, Wang et al. 2011). Simultaneously, the spine volume was monitored using the red fluorescence of mRFP-RBD^{65E,108A}-mRFP. To induce structural plasticity in a single dendritic spine, we applied a train of 30 two-photon glutamate uncaging pulses at 0.5Hz to the top center of the spine without extracellular $MgCl_2$. In control neurons, the spine volume increased rapidly by approximately 341 ± 8% following glutamate uncaging (transient phase) and relaxed to an elevated level of 56 ± 3% for more than 30 minutes later

(sustained phase) (**Figure 5.4.F-H**). In neurons where neurofibromin was knockdown, the spine volume increased to approximately 370 ± 7% during the transient phase and relaxed to an elevated level of 66 ± 5% during the sustained phase (**Figure 5.4.F-H**). There was no statistically significant difference between the scrambled control shRNA and the NF1 shRNA during both the transient and sustained phases of spine structural plasticity. In the neurons expressing the NF1-GRD domain, we observed a spine volume increase of up to 472 ± 11% during the transient phase, followed by an elevated maintenance of up to 96 ± 7% during the sustained phase (**Figure 5.4.G-H**). Statistical analysis proved that the structural plasticity observed in neurons expressing both the Ras sensor and the NF1-GRD domain was increased compared to the control condition (ANOVA, $p = 5.43x10^{-5}$, followed by post-hoc tests; **Figure 5.4.H**). Hence, in line with the data from **chapter IV** (**Figure 4.2.**), the blockade of activity with $MgCl_2$ removed the structural plasticity impairment seen in neurons expressing reduced levels of neurofibromin, suggesting that the HRas sensor does not interfere with structural plasticity. However, in contrast with the results obtained in **chapter IV** (**Figure 4.2.**), we observed an enhanced structural plasticity in neurons overexpressing the GRD domain of neurofibromin.

When dendritic spine structural plasticity was induced, HRas activity was rapidly activated, within approximately 0.5 - 1 minute, in the stimulated spines of neurons transfected with a scrambled control shRNA. Examples of Ras activation upon single dendritic spine activation can be appreciated in **Figure 5.3.A**. Ras activity remained elevated for a few minutes (approximately 2 minutes, **Figure 5.4.A-C**) and, then, gradually decreased until close to basal levels (**Figure 5.4.A-C,E**). Despite the higher binding affinity of RBD for HRas with the mutation K65E instead of R59A, we did not observe obvious effects on Ras^{GTP} inactivation during our control experiments (**Figures 5.4.A-C**). However, further binding affinity experiments will be required to rule out possible issues with the sensor inactivation. As previously reported by Harvey et al. (2008), the time course of HRas activation was similar to that of dendritic spine volume change (**Figure 5.4.C,F**). Equally, the time course of Ras activation was similar to that one reported by Harvey and collaborators (2008) when using FRas-F and a similar stimulation protocol, with a gradual decrease of Ras activity to basal levels in about 10 minutes.

We also measured Ras activation in neurons where neurofibromin was knockdown (NF1 shRNA) and in neurons expressing NF1-GRD. In neurons expressing NF1 shRNA, the basal Ras activity was,

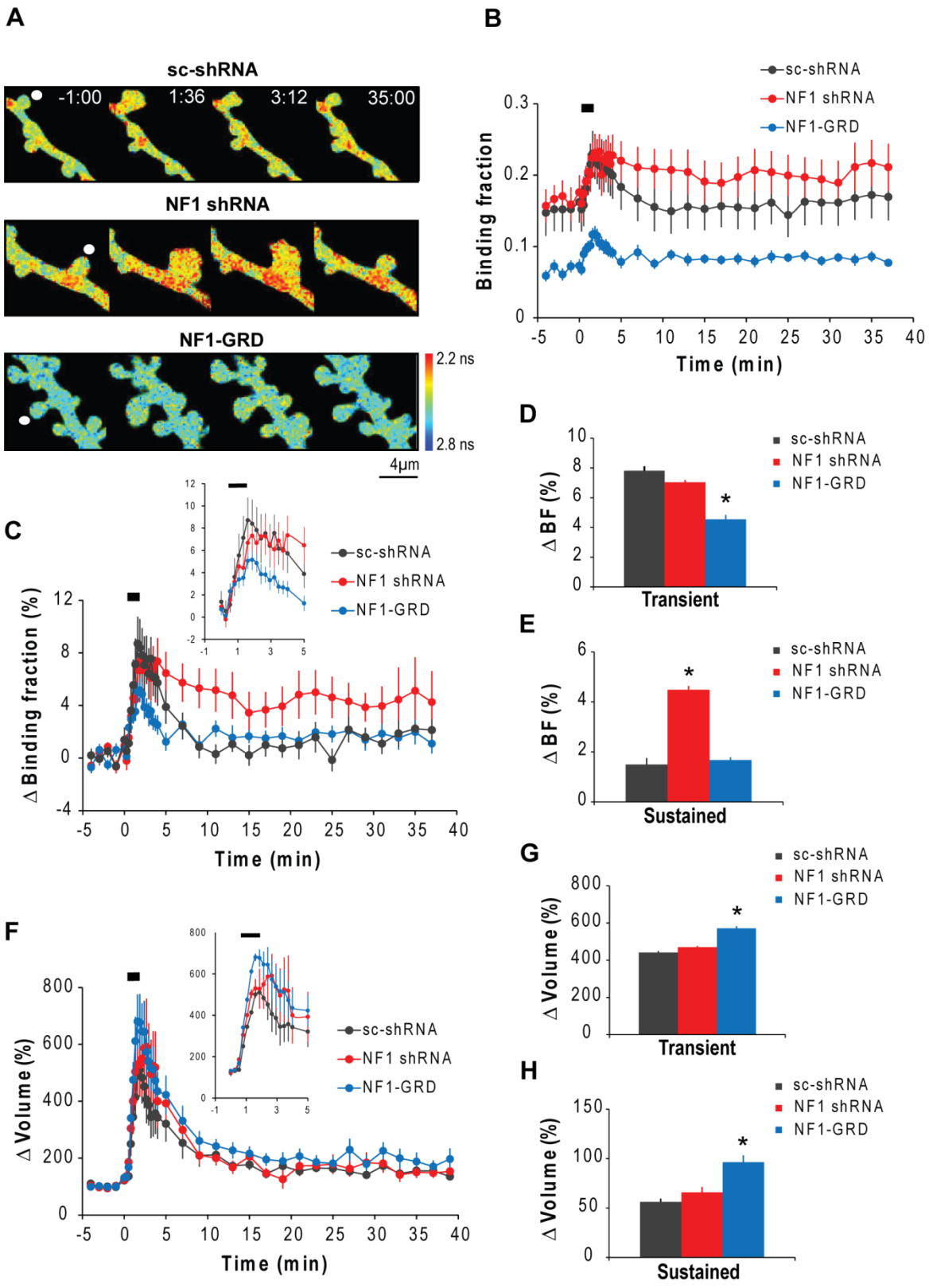
A
sc-shRNA
-1:00
1:36
3:12
35:00
NF1 shRNA
NF1-GRD
2.2 ns
2.8 ns
4μm
B
sc-shRNA
NF1 shRNA
NF1-GRD
Binding fraction
Time (min)
C
sc-shRNA
NF1 shRNA
NF1-GRD
Δ Binding fraction (%)
Time (min)
D
sc-shRNA
NF1 shRNA
NF1-GRD
Δ BF (%)
Transient
E
sc-shRNA
NF1 shRNA
NF1-GRD
Δ BF (%)
Sustained
F
sc-shRNA
NF1 shRNA
NF1-GRD
Δ Volume (%)
Time (min)
G
sc-shRNA
NF1 shRNA
NF1-GRD
Δ Volume (%)
Transient
H
sc-shRNA
NF1 shRNA
NF1-GRD
Δ Volume (%)
Sustained

overall, similar to that of neurons expressing a scrambled control shRNA (**Figure 5.4.B**). Also, Ras activation upon glutamate uncaging reached a similar level (7.82 ± 0.29% for sc-shRNA against 7.04 ± 0.15% for NF1 shRNA). However, the inactivation of Ras^{GTP} was much more inefficient in NF1 shRNA expressing neurons. The Ras activation signal decayed slowly and incompletely, being that, 30 minutes after stimulation, Ras activity was still moderately elevated (4.48 ± 0.15% for NF1 shRNA against 1.50 ± 0.25% for sc-shRNA). Statistical analysis proved that the Ras activity observed for neurons where neurofibromin was knockdown was significantly higher during the sustained phase of structural plasticity, when compared to control neurons (ANOVA, $p = 1.3x10^{-11}$; **Figure 5.4.A-C,E**). Thus, neurofibromin regulates the inactivation of HRas in dendritic spines and, therefore, has RasGAP activity in dendritic spines.

Figure 5.4. Neurofibromin is a major RasGAP in the dendritic spines of CA1 pyramidal neurons of the hippocampus. (A) Representative fluorescence lifetime images of Ras activity in CA1 pyramidal neurons, in the presence of scrambled shRNA (top panel), NF1 shRNA (middle panel) or the GRD domain of neurofibromin (bottom panel). At time zero, 30 uncaging pulses were applied to the spine marked by the white circle in 0mM extracellular Mg^{2+}. Warmer colors indicate shorter lifetimes and higher levels of Ras activation. **(B)** Time course of Ras activation in the stimulated spine in neurons expressing a scrambled shRNA, NF1 shRNA or NF1-GRD domain, upon MNI-L-glutamate uncaging. Black bar, time of stimulus. **(C)** Time course of Ras activation in the stimulated spine normalized to the baseline. This data shows that Ras activity increases by approximately 10% at its peak and decreases to baseline levels in 10min, under the control condition, as measured by changes in binding fraction normalized to the baseline. For neurons where neurofibromin was knockdown, Ras activity increases to approximately the same level during the transient phase, with a much weaker inactivation 30 minutes after stimulation and with a slow decay. Expression of the NF1-GRD domain had the opposite effect, leading to a much more modest Ras activation level right after uncaging stimulation (about 5% activation), which decays quickly (in approximately 5min) compared to the control. The inset to (C) shows a closer view of the first 5 minutes. **(D)** Transient (averaged over 64s - 128s) Ras activation. Stars (*) denote statistically significant difference ($p < 0.05$) from the value in the stimulated spines of the scrambled control shRNA. Ras activation immediately following uncaging is significantly smaller when the NF1-GRD domain is overexpressed. **(E)** Sustained (averaged over 21min - 37min) Ras activation. Stars (*) denote statistically significant difference ($p < 0.05$) from the value in the stimulated spines of the scrambled control shRNA. Ras activity decreases 21 – 37 minutes after stimulation to levels close to basal activity in both the scrambled control shRNA and the NF1-GRD conditions. In contrast, Ras activity remains elevated in the stimulated spines of neurons expressing NF1 shRNA, compared to the scrambled control shRNA condition, indicating that removal of neurofibromin impairs Ras inactivation. **(F)** Averaged time course of spine volume change in the same experiments as in **(B)** and **(C)**. The inset to (F) shows a closer view of the first 5 minutes. **(G)** Transient (volume change averaged over 1 - 1.5min subtracted by that over 21 - 37min) volume change. **(H)** Sustained volume change (volume change averaged over 21 - 37min). The sustained volume is significantly higher in neurons expressing the NF1-GRD domain.

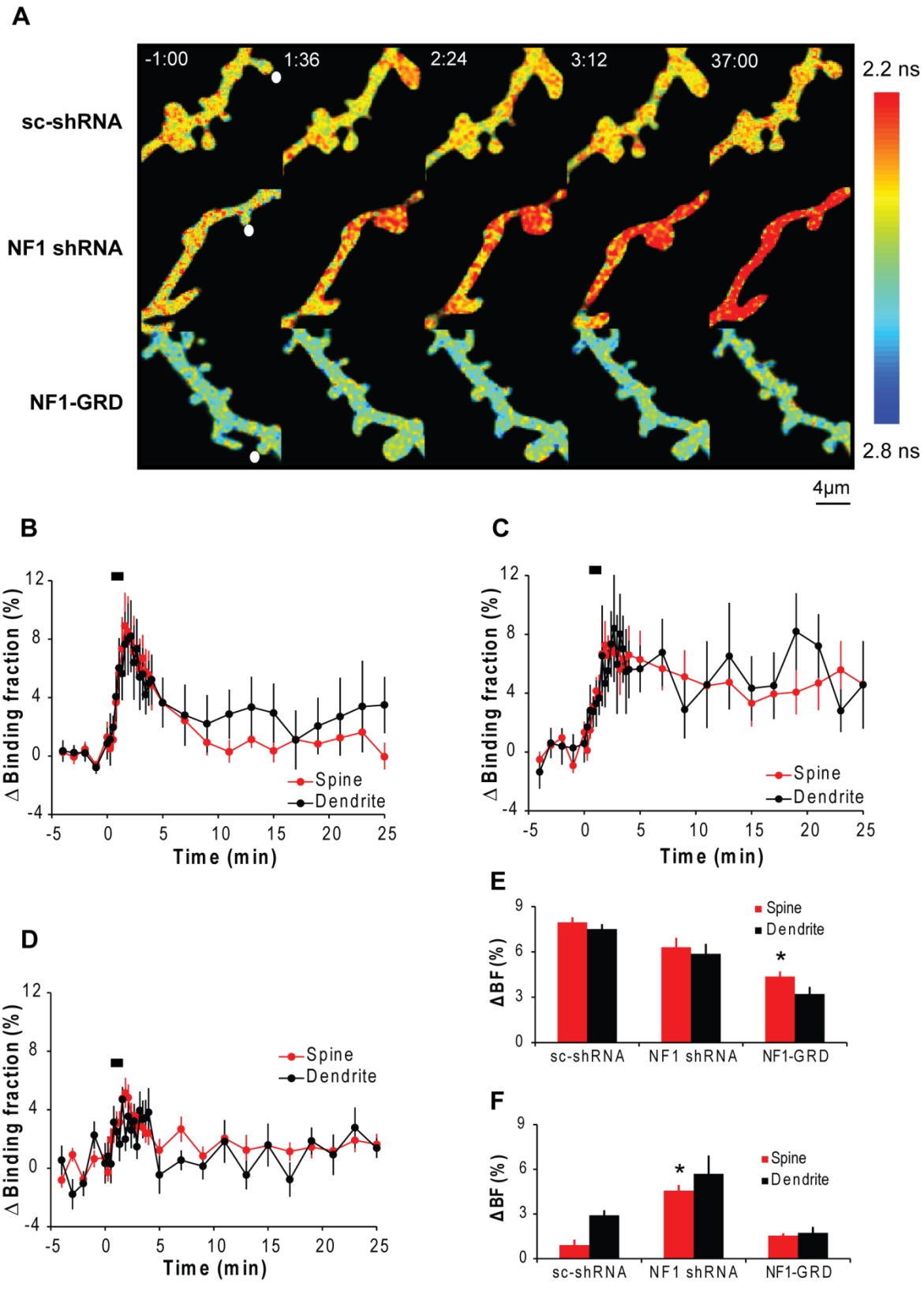
A
-1:00
1:36
2:24
3:12
37:00
2.2 ns
2.8 ns
sc-shRNA
NF1 shRNA
NF1-GRD
4μm
B
C
D
E
F
Δ Binding fraction (%)
Time (min)
Spine
Dendrite
ΔBF (%)
sc-shRNA
NF1 shRNA
NF1-GRD
*

In neurons expressing the NF1-GRD domain, the basal binding fraction was lower than that observed in control neurons, indicating lower basal Ras activity (ANOVA, $p = 2.15x10^{-6}$; **Figure 5.4.A-B, D**) and showing that the GRD domain of neurofibromin is able to inactivate HRas in dendritic spines, under basal conditions. Furthermore, following glutamate uncaging stimulation, Ras activity increased to 4.55 ± 0.29%, which was significantly lower than the transient increase in Ras activity observed in control neurons (7.82 ± 0.29%) and neurons expressing NF1 shRNA (7.04 ± 0.15%; **Figure 5.4.C-D**).

Additionally, Ras^{GTP} inactivation in neurons expressing the NF1-GRD domain occurred much faster than in control neurons. In other words, Ras activity was already close to basal levels 5 minutes after single spine stimulation and it remained low for at least another 30 minutes (**Figure 5.4.C-D**). Therefore, the GRD domain of neurofibromin is effective at restricting the full range of HRas activation to lower levels in dendritic spines and it also accelerates the inactivation of HRas, further supporting the conclusion that neurofibromin has major RasGAP activity in dendritic spines and is likely to be one of the major negative regulators of HRas signaling in these subcellular compartments.

Figure 5.5. Neurofibromin is a RasGAP in the dendritic spines and adjacent dendrites of CA1 pyramidal neurons of the hippocampus. (A) Representative fluorescence lifetime images of Ras activity in CA1 pyramidal neurons, in the presence of scrambled shRNA (top panel), NF1 shRNA (middle panel) or the NF1-GRD domain (bottom panel). The black bar indicates the time at which a train of 30 uncaging pulses were applied to the spine marked by the white circle in 0mM extracellular Mg^{2+}. Warmer colors indicate shorter lifetimes and higher levels of Ras activation. **(B)** Time course of Ras activation in the stimulated spine and nearby dendrite in neurons expressing scrambled shRNA, upon MNI-L-glutamate uncaging. This data shows that Ras activation occurs also outside the stimulated spine, in the nearby dendrite. Ras activity increases by approximately 10% at its peak and decreases to baseline levels within 10 minutes. **(C)** Time course of Ras activation in the stimulated spine and nearby dendrite in neurons expressing NF1 shRNA, upon MNI-L-glutamate uncaging. Ras activity increases by approximately 8% at its peak, but does not quickly decrease to baseline levels. Instead, it remains elevated at least for 25 minutes after stimulation. Simultaneous Ras activation in the adjacent dendrite remains elevated by approximately 6.5% of the baseline for, at least, 25 minutes after stimulation. **(D)** Time course of Ras activation in the stimulated spine and nearby dendrite in neurons expressing the NF1-GRD domain, upon MNI-L-glutamate uncaging. Ras activity only increases by approximately 4.5% at its peak and decreases to baseline levels in only 5 minutes. **(E)** Transient (averaged over 64 - 128s) Ras activation. Ras is activated in both the stimulated spines and adjacent dendrite in all conditions. Stars (*) denote significantly different values compared to those from sc-shRNA measure at the spine. **(F)** Sustained (averaged over 19 - 25min) Ras activation. For all the conditions tested, Ras activity is similar between the stimulated dendritic spines and their adjacent dendrites.

Ras activity was also monitored in the adjacent dendrite to the stimulated spine. Harvey et al. (2008) previously reported the spreading of Ras activity to the adjacent dendrite and neighboring dendritic spines following single dendritic spine stimulation with a LTP-inducing stimulus similar to the one administered here (Harvey, Yasuda et al. 2008). We compared the HRas activity in the stimulated spine and in the dendrite, during the transient and sustained phases of structural plasticity, in scrambled control shRNA neurons, neurons where neurofibromin was knockdown, and neurons expressing the GRD domain of neurofibromin. HRas activity displayed a relatively small gradient between the stimulated spines and adjacent dendrite, rather showing activation in both compartments that was close to simultaneous.

Hence, in control neurons, Ras activated to similar levels in the stimulated spine (7.95 ± 0.33%) and in the adjacent dendrite (7.51± 0.32%) during the transient phase of structural plasticity ($p = 0.36$; **Figure 5.5.A-B,E**). The same similar level of Ras activation between the stimulated spine (6.31 ± 0.61% for NF1 shRNA and 4.37 ± 0.34% for NF1-GRD) and the adjacent dendrite (6.50 ± 0.66% for NF1 shRNA and 3.22 ± 0.46% for NF1-GRD) was observed for neurons expressing NF1 shRNA and neurons overexpressing the GRD domain of neurofibromin ($p = 0.39$ for NF1 shRNA and $p = 0.06$ for NF1-GRD; **Figure 5.5.C-E**). During the sustained phase of structural plasticity (19-25 minutes after stimulation), the situation was quite similar. In other words, Ras activity was not statistically different between the stimulated dendritic spine and the adjacent dendrite for any of the conditions tested (2.91 ± 0.33% in dendrite against 0.91 ± 0.36% in the stimulated spine, $p = 0.13$, for sc-shRNA; 5.70 ± 1.23% in dendrite against 4.57 ± 0.37% in the stimulated spine, $p = 0.85$, for NF1-shRNA; 1.74 ± 0.40% in the dendrite and 1.54 ± 0.15% in the stimulated spine, $p = 0.78$, for NF1-GRD; **Figure 5.5.D,F**). This data suggests that HRas activation is not restricted to the stimulated dendritic spine, but rather occurs also in the adjacent dendrite or spreads to the adjacent dendrite.

Discussion

In this chapter, we investigated whether neurofibromin has a RasGAP function in the dendritic spines of CA1 pyramidal neurons, using a newly modified Ras sensor and a combination of TPFLIM and two-photon glutamate uncaging. We show that neurofibromin is a major RasGAP in the dendritic spines of CA1 pyramidal neurons, as evidenced by the FLIM experiments. More specifically, when compared to control neurons, those expressing low levels of neurofibromin showed deficient Ras inactivation after single dendritic spine stimulation with a LTP-inducing stimulus. Also, enhanced neurofibromin GAP activity, by overexpression of the GRD domain of neurofibromin, resulted in lower peak activation response and faster inactivation.

First, we modified the previously described Ras sensor FRas-F, used by Yasuda and collaborators (2006) and by Harvey and collaborators (2008), because the original acceptor of the sensor FRas-F (mRFP-RBD^{59A}-mRFP) would accumulate in the nucleus of CA1 pyramidal neurons, as reported by its red fluorescence **(Figure 5.3.)**. Hence, the acceptor was not readily available to bind the donor (mEGFP-HRas) at the time of stimulation and Ras activation was never observed in neurons (data not shown). We introduced two new mutations (K65E and K108A), which resulted in an HRas sensor capable of reporting Ras activation in 293T cells, to the same level as the original sensor FRas-F (Yasuda, Harvey et al. 2006). Furthermore, it was also able to report Ras activation in CA1 pyramidal neurons to levels similar to those reported by Harvey and collaborators (2008) when using the original FRas-F and a similar protocol of stimulation to ours (Harvey, Yasuda et al. 2008). Lastly, the newly modified Ras sensor was able to inactivate in pyramidal neurons, indicating that it is a valuable tool for imaging Ras activity in small neuronal compartments, such as dendritic spines. However, further experiments will be required to completely rule out the possibility of deficient inactivation by the modified sensor.

Under our preparation conditions, when using the newly modified sensor, a LTP stimulus capable of inducing structural plasticity in single dendritic spines (Lee, Escobedo-Lozoya et al. 2009; Patterson, Szatmari et al. 2010; Murakoshi, Wang et al. 2011) was sufficient to cause HRas activation in dendritic spines. Ras activation was not confined to the stimulated spine as in the case of CaMKII activation (Lee,

Escobedo-Lozoya et al. 2009), but was also observed in the adjacent dendrite under control conditions. This data supports findings by Yasuda et al. (2006) and Harvey et al. (2008), who previously reported that Ras activation spreads along the adjacent dendrite and neighboring spines over a length of at least 10µm (Yasuda, Harvey et al. 2006; Harvey, Yasuda et al. 2008). However, we did not investigate the spreading of Ras activation to the neighboring dendritic spines in the present study. Also in line with Harvey et al. (2008), our sensor reported a transient peak of activation of about 8% and Ras^{GTP} inactivated in approximately 10 minutes to nearly basal level. Hence, the new sensor is a reliable reporter of Ras activity.

After verifying that the new sensor is a good reporter of Ras activity in dendritic spines of CA1 pyramidal neurons, we imaged Ras activation under conditions where neurofibromin activity was manipulated. Our data suggests that neurofibromin inactivates Ras in dendritic spines and their adjacent dendrites upon single spine stimulation. Neurofibromin knockdown does not seem to have a significant effect in the basal levels of Ras activity (**Figure 5.2.B.**) nor during the transient phase of structural plasticity, since Ras activation is similar to that one of the control condition during these stages. However, neurofibromin removal by shRNA results in persistent Ras activation in dendritic spines and their adjacent dendrites, during the sustained phase of structural plasticity (19-25 minutes upon stimulation), suggesting an inefficient Ras^{GTP} inactivation under reduced levels of neurofibromin expression, as compared to control neurons. In contrast, overexpression of the GRD domain of neurofibromin blocks full Ras activation, as compared to control neurons, and accelerates the inactivation of Ras^{GTP}, which happens in only 5 minutes. Thus, our data is in agreement with a role of neurofibromin as a RasGAP in the dendritic spines of CA1 neurons and this is the first study identifying a RasGAP in dendritic spines by direct visualization of Ras activation.

We were surprised to observe that Ras activation in the adjacent dendrites was always similar to that seen in the stimulated spines, even during the transient phase of structural plasticity. This suggests that Ras activation might occur in dendrites, rather than spreading from the stimulated spine to the adjacent dendrites, in contrast with the findings reported by Yasuda et al. (2006) and Harvey et al. (2008). This would be a rather new idea and requires additional experiments in order to be confirmed. Also during

the sustained phase of structural plasticity, Ras activation in the adjacent dendrite was always similar to Ras activation in the stimulated spine for all conditions tested. The experiments performed here are not clear on how neurofibromin might affect the hypothetical spreading of Ras activity. Further experiments will be required to answer this question, namely the analysis of the spatial profile of Ras activation along at least 10μm of dendrite and neighboring spines (Harvey, Yasuda et al. 2008). If this analysis is carefully performed, it will be possible to understand if Ras activation occurs primarily in the stimulated dendritic spine, then spreading to the adjacent dendrite, or if conversely it occurs simultaneously in the stimulated dendritic spine and adjacent dendrite. If spreading occurs, then the spatial profiling of Ras activity in multiple sites along the 10μm of dendrite and neighboring dendritic spines will allow us to understand whether neurofibromin controls the Ras activation spreading upon single dendritic spine stimulation.

Regarding the spine volume changes during Ras activation experiments, our data is mostly consistent with the major findings shown in **chapter IV** of this dissertation. Therefore, as shown in the previous chapter (**Figure 4.2.**), when activity is blocked with 10mM of $MgCl_2$, the spine structural plasticity abnormalities observed under neurofibromin manipulations are no longer seen. All facts taken together, this data was expected. However, we observed an unexpected discrepancy between the structural plasticity experiments performed in **chapter IV** and the FLIM experiments performed in **chapter V**: when co-expressing the HRas sensor and the GRD domain of neurofibromin, we observed that the spine enlargement was bigger than the control condition for both the transient and sustained phases of structural plasticity, in contrast with the data collected in **chapter IV** for NF1-GRD with 10mM $MgCl_2$, where we observed no differences between the structural plasticity of control neurons and those overexpressing the NF1-GRD domain in the presence of high $MgCl_2$ concentration. Despite the fact that Harvey et al. (2008) demonstrated that there are no differences between the structural plasticity in neurons overexpressing GFP and neurons expressing the FRas-F sensor, it is possible that the newly modified HRas sensor has an effect in structural plasticity of dendritic spines, though the control condition experiments, which show similar values both in the presence (156% ± 3; **Figure 5.2.**) and absence (161% ± 2; **Figure 4.2.**) of HRas sensor, appear to rule out that possibility. It is also possible that the enhanced structural plasticity during the co-expression of both the HRas sensor and the GRD domain of neurofibromin results from a compensatory effect of simultaneously overexpressing a protein and its

inactivator, therefore maintaining the optimal balance of Ras activity required to maximal structural plasticity.

Future Directions

The data presented in **chapter V** suggests that neurofibromin is a major RasGAP in dendritic spines of CA1 pyramidal neurons. Therefore, it will be very interesting to unravel new details in this field and expand the knowledge on the mechanisms controlled by neurofibromin. Namely, it will be interesting to analyze the spatial profile of Ras activation along the dendrites of CA1 pyramidal neurons upon single spine stimulation under conditions of neurofibromin manipulation. Harvey and Svoboda (2007) reported that after input-specific LTP induction by two-photon glutamate uncaging or synaptic stimulation, subthreshold stimuli, which by themselves were too weak to trigger LTP, caused robust LTP and spine enlargement at neighboring spines, provided that these ones would be no more than 10 μm away from the stimulated spine and that the subthreshold stimulus was applied within 10 minutes of input-specific LTP induction (Harvey and Svoboda 2007). This form of plasticity spans a similar length with the spread of Ras activity (Harvey, Yasuda et al. 2008). In order to test the involvement of Ras in this form of plasticity, Harvey and collaborators (2008) applied a MEK inhibitor (U0126) between the first suprathreshold and the second subthreshold stimuli and observed a reduction of structural plasticity in response to subthreshold stimuli, but not in response to suprathreshold stimuli. Furthermore, the subthreshold stimuli did not produce any additional Ras activation, suggesting that spreading of Ras is essential to produce the facilitation of plasticity (Harvey, Yasuda et al. 2008; Lee and Yasuda 2009). Hence, if neurofibromin regulates the spatial spreading of Ras activation, it will most likely interfere with this form of plasticity. Taken into account the data presented in this chapter, we hypothesize that overexpression of the NF1-GRD domain blocks the spatial spreading of Ras activation and abolishes the plasticity form described by Harvey and Svoboda (2007). Future experiments will be required to answer these questions and unveil the details of neurofibromin RasGAP function in dendritic spines.

CHAPTER VI

General discussion and future directions

Chapter VI. General discussion and future directions

The ability of synapses to change their strength in response to neuronal activity is commonly referred as synaptic plasticity. Synaptic plasticity is the central cellular mechanism that underlies memory formation. Understanding the molecular mechanisms controlling the morphological plasticity of dendritic spines may be important in determining the cellular processes that underlie long-lasting neuronal plasticity and memory storage. In the hippocampus, numerous signaling systems have been implicated in synaptic plasticity and memory formation. There is a substantial interplay between these signaling pathways, increasing the level of complexity and implying a great degree of integration and coordination for signal transduction in hippocampal LTP induction. Among the multiple pathways, a wide variety of studies in the past 15 years denote a clear importance of the Ras pathway in synaptic plasticity and memory formation in general, across many species, brain areas and types of synapses. Specifically at the dendritic spine level, the Ras signaling pathway has been shown to participate in morphological stability and structural plasticity.

Neurofibromin is Required for Dendritic Spine Maintenance

In this work, we demonstrate that neurofibromin, a RasGAP, plays an important role in the dendritic spines of CA1 pyramidal neurons by regulating the Ras signaling pathway (**chapter III**). This finding brings new insights to a recent report that demonstrated that reduced neurofibromin levels in hippocampal interneurons led to a deregulation of the Ras pathway (Cui, Costa et al. 2008). In contrast with our study, Cui and collaborators refute a role of neurofibromin in the regulation of the Ras pathway in pyramidal neurons of the hippocampus.

A recent study by Lin et al. (2007) also contrasts Cui and collaborators (2008) observations by demonstrating that neurofibromin is required to maintain the normal dendritic spine density in mature

hippocampal cultured neurons (DIV16-17), but via the PKA-Ena/VASP pathway. In that study, the authors reported that removal of neurofibromin by shRNA (the same approach that we used in the present work) significantly decreased the spine density. Additionally, Lin et al. (2007) demonstrated that neurofibromin plays a role at the postsynaptic sites of hippocampal neurons. However, they did not analyze the role of the Ras pathway in the phenotype (Lin, Lei et al. 2007). The same study also demonstrated that neurofibromin has a function in young neurons (DIV4-5), by regulating filopodia formation via de PKA-Ena/VASP pathway (Lin, Lei et al. 2007). Furthermore, an older study by Hsueh et al. (2001) demonstrated that neurofibromin is present in the dendritic spines of cultured hippocampal neurons by immunostaining techniques. Using subcellular fractionation and co-immunoprecipitation experiments, Hsueh et al. (2001) demonstrated that neurofibromin is present in the PSD of hippocampal neurons, where it interacts with the complex of Syndecan2/CASK (Hsueh, Roberts et al. 2001).

In line with Lin et al. (2007) findings, we report that neurofibromin regulates the dendritic spine density of mature CA1 pyramidal neurons in the hippocampus, in organotypic slice cultures (DIV17-22). However, in contrast with that study, we demonstrate that the loss of dendritic spines by neurofibromin removal is mediated by the Ras pathway, as manipulations that decreased Ras activity could rescue the phenotype and restore the normal dendritic spine density. On the other hand, our study does not necessarily disagree with that study, since we did not investigate the role of PKA signaling in this phenotype. Equally, they did not investigate whether Ras signaling could rescue the spine density loss. Our studies might, therefore, be complementary. Perhaps in line with this possibility, our data indicates that the effect of neurofibromin in dendritic spine density is not only mediated by a dysregulation of the Ras pathway, but also by different signaling pathways, since overexpression of a constitutively active form of HRas ($HRas^{12V}$) was not sufficient to mimic the dendritic spine morphology phenotype observed upon removal of neurofibromin. Given the findings by Lin et al. (2007) demonstrating that reduced levels of neurofibromin expression cause a decrease in the dendritic spine density through the PKA-Ena/VASP pathway, we speculate that this pathway, in conjunction with the Ras pathway, is involved in the phenotype. It is also possible that additional signaling pathways, eventually related to regulation by the Sec14-PH domain of neurofibromin, might be involved in this phenotype. Alternatively, this might be explained by the possibility that neurofibromin is a RasGAP specific towards a different Ras isoform, such

as KRas or NRas. However, these hypotheses were not explored in the present work. In the future it will be interesting to dissect whether neurofibromin is a general GAP for all Ras isoforms or whether it is specific towards one or more Ras isoforms.

We have also shown that the regulation of the dendritic spine density by neurofibromin observed in our preparations is activity-dependent, as demonstrated by the rescue of the phenotype under conditions where the NMDAR was pharmacologically and chronically blocked.

In line with the morphology data, spontaneous activity recordings in this study demonstrated a decreased frequency in mEPSCs in neurons with reduced levels of expression of neurofibromin. This result also supports the hypothesis that the number of functional excitatory synapses is reduced upon neurofibromin removal. As approximately 90% of the excitatory synapses are made onto dendritic spines (Sweatt 2004; Bhatt, Zhang et al. 2009), this finding is not surprising. Hence, neurofibromin not only regulates the dendritic spine number in pyramidal neurons of the CA1 region of the hippocampus, but it also maintains the normal number of excitatory synapses. We also show that neurofibromin does not affect the AMPAR content of excitatory synapses, since the amplitude of mEPSCs is similar between control neurons and neurons with reduced levels of neurofibromin. In line with our findings, Arendt et al. (2004) showed that the synRas mouse, which overexpresses a CA-HRas, does not have different mEPSCs amplitudes from their control littermates (Arendt, Gärtner et al. 2004).

Neurofibromin is Required for the Structural Plasticity of Dendritic Spines

In this work we showed that neurofibromin is required for normal dendritic spine structural plasticity in excitatory neurons. To date, the effects of neurofibromin loss-of-function in synaptic plasticity had only been explained by presynaptic Ras signaling hyperactivation in inhibitory interneurons (Cui, Costa et al. 2008). Therefore, we have unveiled additional cellular correlates of impaired synaptic plasticity in the hippocampus by reporting impairment in dendritic spine structural plasticity in a situation

of low expression levels of neurofibromin. Also for the plasticity studies, our data supports that the hyperactivation of Ras, caused by neurofibromin inactivation, is responsible for the reduced magnitude of structural plasticity in neurons where neurofibromin has been knockdown, since overexpression of the GRD domain of neurofibromin is sufficient to restore the long lasting phase of dendritic spine structural plasticity.

Spines are important compartments for information storage and synaptic plasticity is currently accepted to be the basis for learning and memory. Furthermore, structural plasticity has recently emerged as the morphological correlate of synaptic plasticity. Hence, it is likely that the cognitive impairments observed in NF1 patients and mouse model can be explained by the reduced magnitude of structural plasticity upon manipulations that decrease neurofibromin expression levels. Moreover, our study emphasizes once more the important function of precise Ras signaling regulation in synaptic plasticity. Interestingly, we also show that the effect of neurofibromin removal in structural plasticity is activity-dependent under the condition of our preparations. As hypothesized in **chapter IV**, it is possible that this is due to a homeostatic mechanism to maintain a balance of Ras activity and synaptic plasticity under conditions of low expression levels of neurofibromin (**Figure 6.1.**).

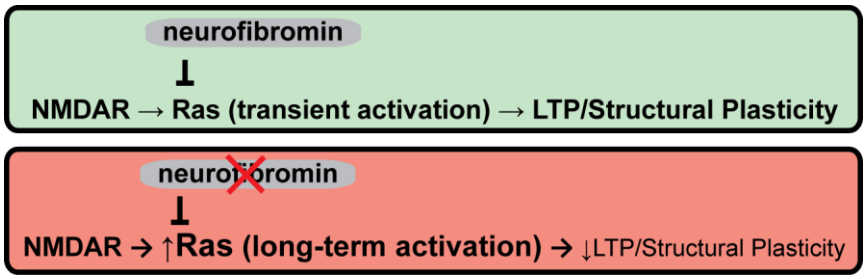

Figure 6.1. Model of Ras regulation by neurofibromin in dendritic spines. Under normal conditions, neurofibromin is a RasGAP in dendritic spines, inactivating Ras. This is essential for the perfect balance of Ras activation, which is transient following NMDAR activation, leading to LTP/structural plasticity. Under conditions of neurofibromin loss-of-function, Ras is hyperactivated following NMDAR opening. This results in unbalanced Ras signaling, ultimately leading to LTP/structural plasticity deficits.

Investigation of a possible regulatory effect of neurofibromin over the NMDAR by calcium imaging and two-photon glutamate uncaging led to the conclusion that the NMDAR function is not regulated by neurofibromin. It is possible that neurofibromin acts on a different channel, instead. For example, in capsaicin-sensitive sensory neurons, it has been shown that the *Nf1*$^{+/-}$ mouse has enhanced sodium currents (Wang, Duan et al. 2010). Alternatively, neurofibromin could regulate the TrkB receptor, a well-known path to activate Ras signaling, or even a different type of receptor still to be unraveled.

In summary, the spine structural plasticity experiments performed here suggest that deficits in learning and memory observed in NF1 patients and in the mouse model of the disease might be explained, at least in part, by the reduction of the magnitude of structural plasticity that we observed under low levels of neurofibromin expression. Similarly, the reduction of the dendritic spine and synapse number in the CA1 region of the hippocampus in our experiments might explain the cognitive deficits reported in NF1. Indeed, neurological and neurodegenerative disorders are frequently associated with aberrant spine structure and plasticity in critical brain regions; a number of psychiatric and neurological disorders are associated with substantial alterations in either spine density or morphology.

Neurofibromin is a RasGAP in the Dendritic Spines of CA1 Neurons

To study whether neurofibromin regulates Ras activity in dendritic spines during spine structural plasticity, Ras activity was monitored in single dendritic spines undergoing structural plasticity in neurons in which neurofibromin activity was manipulated, using a combination FLIM and two-photon glutamate uncaging (**chapter V**). Our data suggest that neurofibromin acts as a major RasGAP in dendritic spines of CA1 pyramidal neurons. We found that, under downregulation of neurofibromin, Ras activation in dendritic spines decays much more slowly than that measured in control neurons: following LTP induction, Ras activity decays over 10 min under the control condition, while in neurons with reduced expression levels of neurofibromin Ras activity inactivation lasts more than 30 minutes. In other words,

neurofibromin knockdown resulted in a slower and incomplete inactivation of Ras in dendritic spines. Conversely, overexpression of the GRD domain of neurofibromin blocks full Ras activation, as compared to control neurons, and accelerates the inactivation of Ras^{GTP}.

Similar to our protocol, Harvey et al. (2008) monitored Ras activation following the delivery of a LTP-inducing stimulus to single dendritic spines and showed Ras activation and inactivation exhibited the same timecourse as the one that we report for the control condition in our own experiments. Besides, they reported the spreading of Ras activity from the stimulated spine to the adjacent dendrite and, then, to adjacent spines, too, over a range of at least 10μm (Harvey, Yasuda et al. 2008). In the present study, spreading of Ras activation was not quantified, due to the small sample available. However, careful inspection of the FLIM images suggests that also in our preparations there was Ras activity spreading and that this phenomenon might be, at least in part, regulated by the RasGAP function of neurofibromin. On the other hand, our data suggests that Ras activation might occur at the level of dendrites themselves, since a simultaneous activation of Ras in both the stimulated spine and the adjacent dendrite was observed in the course of our experiments. Further experiments will be crucial to confirm this hypothesis. Like in Murakoshi and collaborators recent report, it will be necessary to characterize the spatial profile of Ras activation along at least 10μm of dendrite as a function of the distance from the stimulated spine (Murakoshi, Wang et al. 2011). If confirmed that Ras activation occurs in dendrites, there will be a small or no gradient of Ras activity between stimulated spines and adjacent dendrites, with indistinguishable activity levels between the two compartments. If Ras activity spreads rapidly from the stimulated spine into the adjacent dendrite, the high spatiotemporal resolution of TPFLIM combined with the analysis of the spatial profile of Ras activation will detect a small gradient of Ras activity between the stimulated spine and the adjacent dendrite. While this is still ongoing investigation, our results suggest that neurofibromin is one of the main GAPs regulating the Ras signaling pathway in dendritic spines of CA1 pyramidal neurons. In addition to this, by characterizing the spatial profile of Ras activation under neurofibromin activity manipulations, we are currently examining the effects of neurofibromin in Ras activation spreading along dendrites upon single spine stimulation with a LTP-inducing stimulus similar to the one delivered in the current work.

Another exciting question would be whether neurofibromin is a RasGAP for all Ras isoforms or if it shows specificity towards a particular isoform or isoforms. The different Ras isoforms localize to different subcellular compartments and different subdomains of the plasma membrane and, perhaps, even to specific subdomains of intracellular membranes (Arozarena, Calvo et al. 2011). It is possible that neurofibromin particularly activates specific isoforms depending on their subcellular localization. Accordingly, a previous report indicated that neurofibromin activity can be inhibited by some lipids, whereas other lipids are unable to affect its activity. The same report also demonstrated that neurofibromin binds H-Ras with 4 times higher affinity than N-Ras (Bollag and McCormick 1991). Site-specific regulatory effects have been described for other Ras regulators. For example, whereas some GEFs preferentially activate Ras at the plasma membrane, others act on endomembrane systems (Arozarena, Calvo et al. 2011). Even higher degree of specificity could be determined by the fact that the same Ras regulator can act at distinct locations depending on different stimuli (Arozarena, Calvo et al. 2011).

It would be equally interesting to identify if neurofibromin regulates specific signaling pathways downstream Ras or if its RasGAP effects generalize to all pathways downstream Ras. Ras subcellular localization can mobilize different Ras scaffolds, which could determine which pathway is activated downstream of Ras. Moreover, if neurofibromin specifically inactivates one or other Ras isoform, it is likely that it affects signaling pathways downstream Ras differently, since different Ras isoforms activate different downstream signaling pathways with different intensities. For example, whereas KRas is the most potent activator of c-Raf, HRas is the most potent activator of PI3K (Yan, Roy et al. 1998). To date, the reports on the topic are contradictory, given that some of them have only identified the Ras-MAPK signaling pathway as the target of neurofibromin regulation, leaving the Ras-PI3K/Akt signaling pathway unaffected (Guilding, McNair et al. 2007); whereas others show that the Ras-PI3K/Akt pathway is also affected (Boyanapalli, Lahoud et al. 2006). Hence, the identity of the signaling pathways downstream Ras that are affected by neurofibromin regulation remains an open question.

References

Adams, J. P. and J. D. Sweatt (2002). "Molecular psychology: roles for the ERK MAP kinase cascade in memory." Annu Rev Pharmacol Toxicol **42**: 135-163.

Agrawal, A. G. and R. R. Somani (2009). "Farnesyltransferase inhibitor as anticancer agent." Mini-Reviews in Medicinal Chemistry **9**(6): 638-652.

Ahmed, M. S. and S. A. Siegelbaum (2009). "Recruitment of N-Type Ca(2+) channels during LTP enhances low release efficacy of hippocampal CA1 perforant path synapses." Neuron **63**(3): 372-385.

Albers, A. C. and D. H. Gutmann (2009). "Gliomas in patients with neurofibromatosis type 1." Expert Review of Neurotherapeutics **9**(4): 535-539.

Alpár, A., K. Palm, et al. (2003). "Expression of constitutively active p21H-rasval12 in postmitotic pyramidal neurons results in increased dendritic size and complexity." Journal of Comparative Neurology **467**(1): 119-133.

Arai, J. A., S. Li, et al. (2009). "Sos2 is dispensable for NMDA-induced Erk activation and LTP induction." Neuroscience Letters **455**(1): 22-25.

Arendt, T., U. Gärtner, et al. (2004). "Neuronal activation of Ras regulates synaptic connectivity." European Journal of Neuroscience **19**(11): 2953-2966.

Arozarena, I., F. Calvo, et al. (2011). "Ras, an actor on many stages: posttranslational modifications, localization, and site-specified events." Genes & Cancer **2**(3): 182-194.

Atkins, C. M., J. C. Selcher, et al. (1998). "The MAPK cascade is required for mammalian associative learning." Nature Neuroscience **1**(7): 602-609.

Baba, H., B. Fuss, et al. (1995). "GapIII, a new brain-enriched member of the GTPase-activating protein family." Journal of Neuroscience Research **41**(6): 846-858.

Bailey, C. H. and M. Chen (1988). "Long-term memory in Aplysia modulates the total number of varicosities of single identified sensory neurons." Proceedings of the National Academy of Sciences of the United States of America **85**(7): 2373-2377.

Bannerman, D. M., B. Niewoehner, et al. (2008). "NMDA receptor subunit NR2A is required for rapidly acquired spatial working memory but not incremental spatial reference memory." The Journal of Neuroscience **28**(14): 3623-3630.

Barria, A., V. Derkach, et al. (1997). "Identification of the Ca2+/calmodulin-dependent protein kinase II regulatory phosphorylation site in the alpha-amino-3-hydroxyl-5-methyl-4-isoxazole-propionate-type glutamate receptor." Journal of Biological Chemistry **272**(52): 32727-32730.

Bernards, A. (2003). "GAPs galore! A survey of putative Ras superfamily GTPase activating proteins in man and Drosophila." Biochimica et Biophysica Acta (BBA) **1603**(2): 47-82.

Bernards, A. and J. Settleman (2005). "GAPs in growth factor signalling." Growth Factors **23**(2): 143-149.

Bhatt, D. H., S. Zhang, et al. (2009). "Dendritic spine dynamics." Annual Review of Physiology **71**: 261-282.

Bi, G. Q. and M. M. Poo (1998). "Synaptic modifications in cultured hippocampal neurons: dependence on spike timing, synaptic strength, and postsynaptic cell type." The Journal of Neuroscience **18**(24): 10464-10472.

Biou, V., H. Brinkhaus, et al. (2008). "Interactions between drebrin and Ras regulate dendritic spine plasticity." European Journal of Neuroscience **27**(11): 2847-2859.

Bliss, T. V. and G. L. Collingridge (1993). "A synaptic model of memory: long-term potentiation in the hippocampus." Nature **361**(6407): 31-39.

Bliss, T. V., G. L. Collingridge, et al. (2003). "Introduction. Long-term potentiation and structure of the issue." Philosophical Transactions of the Royal Society of London. Series B, Biological sciences **358**(1432): 607-611.

Bliss, T. V. and T. Lomo (1973). "Long-lasting potentiation of synaptic transmission in the dentate area of the anaesthetized rabbit following stimulation of the perforant path." Journal of Physiology **232**(2): 331-356.

Bloodgood, B. L. and B. L. Sabatini (2005). "Neuronal activity regulates diffusion across the neck of dendritic spines." Science **310**(5749): 866-869.

Bollag, G. and F. McCormick (1991). "Differential regulation of rasGAP and neurofibromatosis gene product activities." Nature **351**(6327): 576-579.

Bonhoeffer, T. and R. Yuste (2002). "Spine motility. Phenomenology, mechanisms, and function." Neuron **35**(6): 1019-1027.

Borasio, G. D., J. John, et al. (1989). "ras p21 protein promotes survival and fiber outgrowth of cultured embryonic neurons." Neuron **2**(1): 1087-1096.

Bortolotto, Z. A. and G. L. Collingridge (1993). "Characterisation of LTP induced by the activation of glutamate metabotropic receptors in area CA1 of the hippocampus." Neuropharmacology **32**(1): 1-9.

Bourne, J. N. and K. M. Harris (2008). "Balancing structure and function at hippocampal dendritic spines." Annual Review of Neuroscience **31**: 47-67.

Bowtell, D., P. Fu, et al. (1992). "Identification of murine homologues of the Drosophila son of sevenless gene: potential activators of ras." Proceedings of the National Academy of Sciences of the United States of America **89**: 6511-6515.

Boyanapalli, M., O. B. Lahoud, et al. (2006). "Neurofibromin binds to caveolin-1 and regulates ras, FAK, and Akt." Biochemical and Biophysical Research Communications **340**(4): 1200-1208.

Brambilla, R., N. Gnesutta, et al. (1997). "A role for the Ras signalling pathway in synaptic transmission and long-term memory." Nature **390**(6657): 281-286.

Bredt, D. S. and R. A. Nicoll (2003). "AMPA receptor trafficking at excitatory synapses." Neuron **40**(2): 361-379.

Brown, J. A., K. A. Diggs-Andrews, et al. (2011). "Neurofibromatosis-1 heterozygosity impairs CNS neuronal morphology in a cAMP/PKA/ROCK-dependent manner." Molecular and Cellular Neuroscience.

Brown, M. D. and D. B. Sacks (2009). "Protein scaffolds in MAP kinase signalling." Cellular Signalling **21**(4): 462-469.

Carter, A. G. and B. L. Sabatini (2004). "State-dependent calcium signaling in dendritic spines of striatal medium spiny neurons." Neuron **44**(3): 483-493.

Chen, H. J., M. Rojas-Soto, et al. (1998). "A synaptic Ras-GTPase activating protein (p135 SynGAP) inhibited by CaM kinase II." Neuron **20**(5): 895-904.

Cichowski, K., S. Santiago, et al. (2003). "Dynamic regulation of the Ras pathway via proteolysis of the NF1 tumor suppressor." Genes & Development **17**(4): 449-454.

Cichowski, K., T. S. Shih, et al. (1999). "Mouse models of tumor development in neurofibromatosis type 1." Science **286**(5447): 2172-2176.

Costa, R. M., N. B. Fedorov, et al. (2002). "Mechanism for the learning deficits in a mouse model of neurofibromatosis type 1." Nature **415**(6871): 526-530.

Costa, R. M. and A. J. Silva (2002). "Molecular and cellular mechanisms underlying the cognitive deficits associated with neurofibromatosis 1." Journal of Child Neurology **17**(8): 622-626.

Costa, R. M. and A. J. Silva (2003). "Mouse models of neurofibromatosis type I: bridging the GAP." Trends in Molecular Medicine **9**(1): 19-23.

Costa, R. M., T. Yang, et al. (2001). "Learning deficits, but normal development and tumor predisposition, in mice lacking exon 23a of Nf1." Nature Genetics **27**(4): 399-405.

Crittenden, J. R., I. Cantuti-Castelvetri, et al. (2009). "Dysregulation of CalDAG-GEFI and CalDAG-GEFII predicts the severity of motor side-effects induced by anti-parkinsonian therapy." Proceedings of the National Academy of Sciences of the United States of America **106**(8): 2892-2896.

Cui, Y., R. M. Costa, et al. (2008). "Neurofibromin Regulation of ERK Signaling Modulates GABA Release and Learning." Cell **135**(3): 549-560.

Cullen, P. J. and P. J. Lockyer (2002). "Integration of calcium and Ras signalling." Nature Reviews. Molecular Cell Biology **3**(5): 339-348.

Danglot, G., V. Régnier, et al. (1995). "Neurofibromatosis 1 (NF1) mRNAs expressed in the central nervous system are differentially spliced in the 5' part of the gene." Human Molecular Genetics **4**(5): 915-920.

Dasgupta, B., L. L. Dugan, et al. (2003). "The neurofibromatosis 1 gene product neurofibromin regulates pituitary adenylate cyclase-activating polypeptide-mediated signaling in astrocytes." The Journal of Neuroscience **23**(26): 8949-8954.

Dasgupta, B., Y. Yi, et al. (2005). "Proteomic analysis reveals hyperactivation of the mammalian target of rapamycin pathway in neurofibromatosis 1-associated human and mouse brain tumors." Cancer Research **65**(7): 2755-2760.

Daston, M. M. and N. Ratner (1992). "Neurofibromin, a predominantly neuronal GTPase activating protein in the adult, is ubiquitously expressed during development." Developmental Dynamics **195**(3): 216-226.

Daston, M. M., H. Scrable, et al. (1992). "The protein product of the neurofibromatosis type 1 gene is expressed at highest abundance in neurons, Schwann cells, and oligodendrocytes." Neuron **8**(3): 415-428.

De Roo, M., P. Klauser, et al. (2008). "LTP promotes a selective long-term stabilization and clustering of dendritic spines." Plos Biology **6**(9): 1850-1860.

Denayer, E., T. Ahmed, et al. (2008). "Spred1 is required for synaptic plasticity and hippocampus-dependent learning." The Journal of Neuroscience **28**(53): 14443-14449.

Derkach, V., A. Barria, et al. (1999). "Ca2+/calmodulin-kinase II enhances channel conductance of alpha-amino-3-hydroxy-5-methyl-4-isoxazolepropionate type glutamate receptors." Proceedings of the National Academy of Sciences of the United States of America **96**(6): 3269-3274.

Douglas, R. M. and G. V. Goddard (1975). "Long-term potentiation of the perforant path-granule cell synapse in the rat hippocampus." Brain Research **86**(2): 205-215.

Ehlers, M. D. (2000). "Reinsertion or degradation of AMPA receptors determined by activity-dependent endocytic sorting." Neuron **28**(2): 511-525.

Ehrhardt, A., G. R. Ehrhardt, et al. (2002). "Ras and relatives--job sharing and networking keep an old family together." Experimental Hematology **30**(10): 1089-1106.

Eichenbaum, H., C. Stewart, et al. (1990). "Hippocampal representation in place learning." The Journal of Neuroscience **10**(11): 3531-3542.

Elowe, S., S. J. Holland, et al. (2001). "Downregulation of the Ras-mitogen-activated protein kinase pathway by the EphB2 receptor tyrosine kinase is required for ephrin-induced neurite retraction." Molecular and Cellular Biology **21**(21): 7429-7441.

Endo, M. and T. Yamashita (2009). "Inactivation of Ras by p120GAP via focal adhesion kinase dephosphorylation mediates RGMa-induced growth cone collapse." The Journal of Neuroscience **29**(20): 6649-6662.

Engert, F. and T. Bonhoeffer (1999). "Dendritic spine changes associated with hippocampal long-term synaptic plasticity." Nature **399**(6731): 66-70.

English, J. D. and J. D. Sweatt (1997). "A requirement for the mitogen-activated protein kinase cascade in hippocampal long term potentiation." Journal of Biological Chemistry **272**(31): 19103-19106.

Enoki, R., Y. L. Hu, et al. (2009). "Expression of long-term plasticity at individual synapses in hippocampus is graded, bidirectional, and mainly presynaptic: optical quantal analysis." Neuron **62**(2): 242-253.

Ethell, I. M. and Y. Yamaguchi (1999). "Cell surface heparan sulfate proteoglycan syndecan-2 induces the maturation of dendritic spines in rat hippocampal neurons." Journal of Cell Biology **144**(3): 575-586.

Feig, L. A. (1999). "Tools of the trade: use of dominant-inhibitory mutants of Ras-family GTPases." Nature Cell Biology **1**(2): E25-27.

Feig, L. A. and G. M. Cooper (1988). "Inhibition of NIH 3T3 cell proliferation by a mutant ras protein with preferential affinity for GDP." Molecular Cell Biology **8**(8): 3235-3243.

Ferrer, I. and F. Gullotta (1990). "Down's syndrome and Alzheimer's disease: dendritic spine counts in the hippocampus." Acta Neuropathologica **79**(6): 680-685.

Fiala, J. C., M. Feinberg, et al. (1998). "Synaptogenesis via dendritic filopodia in developing hippocampal area CA1." The Journal of Neuroscience **18**(21): 8900-8911.

Fiala, J. C., J. Spacek, et al. (2002). "Dendritic spine pathology: cause or consequence of neurological disorders?" Brain Research Reviews **39**(1): 29-54.

Fivaz, M. and T. Meyer (2005). "Reversible intracellular translocation of KRas but not HRas in hippocampal neurons regulated by Ca2+/calmodulin." The Journal of Cell Biology **170**(3): 429-441.

Gaarskjaer, F. B. (1978). "Organization of the mossy fiber system of the rat studied in extended hippocampi. II. Experimental analysis of fiber distribution with silver impregnation methods." The Journal of Comparative Neurology **178**(1): 73-88.

Garey, L. J., W. Y. Ong, et al. (1998). "Reduced dendritic spine density on cerebral cortical pyramidal neurons in schizophrenia." Journal of Neurology, Neurosurgery and Psychiatry **65**(4): 446-453.

Gärtner, U., A. Alpár, et al. (2005). "Enhanced Ras activity promotes spine formation in synRas mice neocortex." Neuroreport **16**(2): 149-152.

Gärtner, U., A. Alpár, et al. (2004). "Constitutive Ras activity induces hippocampal hypertrophy and remodeling of pyramidal neurons in synRas mice." Journal of Neuroscience Research **77**(5): 630-641.

Giese, K. P., E. Friedman, et al. (2001). "Hippocampus-dependent learning and memory is impaired in mice lacking the Ras-guanine-nucleotide releasing factor 1 (Ras-GRF1)." Neuropharmacology **41**(6): 791-800.

Goldin, M. and M. Segal (2003). "Protein kinase C and ERK involvement in dendritic spine plasticity in cultured rodent hippocampal neurons." European Journal of Neuroscience **17**(12): 2529-2539.

Grewal, S. S., R. D. York, et al. (1999). "Extracellular-signal-regulated kinase signalling in neurons." Current Opnion in Neurobiology **9**(5): 544-553.

Grossman, A. W., N. M. Elisseou, et al. (2006). "Hippocampal pyramidal cells in adult Fmr1 knockout mice exhibit an immature-appearing profile of dendritic spines." Brain Research **1084**(1): 158-164.

Grutzendler, J., N. Kasthuri, et al. (2002). "Long-term dendritic spine stability in the adult cortex." Nature **420**(6917): 812-816.

Guilding, C., K. McNair, et al. (2007). "Restored plasticity in a mouse model of neurofibromatosis type 1 via inhibition of hyperactive ERK and CREB." European Journal of Neuroscience **25**(1): 99-105.

Guo, H. F., I. The, et al. (1997). "Requirement of Drosophila NF1 for activation of adenylyl cyclase by PACAP38-like neuropeptides." Science **276**(5313).

Guo, H. F., J. Tong, et al. (2000). "A neurofibromatosis-1-regulated pathway is required for learning in Drosophila." Nature **403**(6772): 895-898.

Gutmann, D. H., M. Boguski, et al. (1993). "Analysis of the neurofibromatosis type 1 (NF1) GAP-related domain by site-directed mutagenesis." Oncogene **8**(3): 761-769.

Gutmann, D. H. and F. S. Collins (1993). "The neurofibromatosis type 1 gene and its protein product, neurofibromin." Neuron **10**(3): 335-343.

Gutmann, D. H., R. T. Geist, et al. (1995). "Expression of the neurofibromatosis 1 (NF1) isoforms in developing and adult rat tissues." Cell Growth and Differentiation **6**(3): 315-323.

Hancock, J. F. (2003). "Ras proteins: different signals from different locations." Nature Reviews Molecular Cell Biology **4**(5): 373-385.

Hannan, F., I. Ho, et al. (2006). "Effect of neurofibromatosis type I mutations on a novel pathway for adenylyl cyclase activation requiring neurofibromin and Ras." Human Molecular Genetics **15**(7).

Harding, A. and J. F. Hancock (2008). "Ras nanoclusters: combining digital and analog signaling." Cell Cycle **7**(2): 127-134.

Harms, K. J., M. S. Rioult-Pedotti, et al. (2008). "Transient spine expansion and learning-induced plasticity in layer 1 primary motor cortex." The Journal of Neuroscience **28**(22): 5686-5690.

Harris, K. M. (1999). "Structure, development, and plasticity of dendritic spines." Current Opinion in Neurobiology **9**(3): 343-348.

Harris, K. M., F. E. Jensen, et al. (1992). "Three-dimensional structure of dendritic spines and synapses in rat hippocampus (CA1) at postnatal day 15 and adult ages: implications for the maturation of synaptic physiology and long-term potentiation." The Journal of Neuroscience **12**(7): 2685-2705.

Harris, K. M. and J. K. Stevens (1989). "Dendritic spines of CA 1 pyramidal cells in the rat hippocampus: serial electron microscopy with reference to their biophysical characteristics." The Journal of Neuroscience **9**(8): 2982-2997.

Harvey, C. D. and K. Svoboda (2007). "Locally dynamic synaptic learning rules in pyramidal neuron dendrites." Nature **450**(7173): 1195-1200.

Harvey, C. D., R. Yasuda, et al. (2008). "The Spread of Ras Activity Triggered by Activation of a Single Dendritic Spine." Science **321**(5885): 136-140.

Harvey, J. and G. L. Collingridge (1992). "Thapsigargin blocks the induction of long-term potentiation in rat hippocampal slices." Neuroscience Letters **139**(2): 197-200.

Hawes, J. J., R. G. Tuskan, et al. (2007). "Nf1 expression is dependent on strain background: implications for tumor suppressor haploinsufficiency studies." Neurogenetics **8**(2): 121-130.

Hayashi, Y., S. H. Shi, et al. (2000). "Driving AMPA receptors into synapses by LTP and CaMKII: requirement for GluR1 and PDZ domain interaction." Science **287**(5461): 2262-2267.

Heasman, S. J. and A. J. Ridley (2008). "Mammalian Rho GTPases: new insights into their functions from in vivo studies." Nature Reviews Molecular Cell Biology **9**(9): 690-701.

Heinemann, U., D. Schmitz, et al. (2000). "Properties of entorhinal cortex projection cells to the hippocampal formation." Annals of the New York Academy of Sciences **911**: 112-126.

Herron, C. E., R. A. Lester, et al. (1985). "Intracellular demonstration of an N-methyl-D-aspartate receptor mediated component of synaptic transmission in the rat hippocampus." Neuroscience Letters **60**(1): 19-23.

Heumann, R., C. Goemans, et al. (2000). "Transgenic activation of Ras in neurons promotes hypertrophy and protects from lesion-induced degeneration." Journal of Cell Biology **151**(7): 1537-1548.

Hinton, V. J., W. T. Brown, et al. (1991). "Analysis of neocortex in three males with the fragile X syndrome." American Journal of Medical Genetics **41**(3): 289-294.

Hjorth-Simonsen, A. (1972). "Projection of the lateral part of the entorhinal area to the hippocampus and fascia dentata." Journal of Comparative Neurology **146**(2): 219-232.

Hjorth-Simonsen, A. and B. Jeune (1972). "Origin and termination of the hippocampal perforant path in the rat studied by silver impregnation." Journal of Comparative Neurology **144**(2): 215-232.

Ho, I. S., F. Hannan, et al. (2007). "Distinct functional domains of neurofibromatosis type 1 regulate immediate versus long-term memory formation." The Journal Neuroscience **27**(25): 6852-6857.

Hofman, K. J., E. L. Harris, et al. (1994). "Neurofibromatosis type 1: the cognitive phenotype." Journal of Pediatrics **124**(4): S1-8.

Holtmaat, A. and K. Svoboda (2009). "Experience-dependent structural synaptic plasticity in the mammalian brain." Nature Reviews Neuroscience **10**(9): 647-658.

Horne, E. A. and M. L. Dell'Acqua (2007). "Phospholipase C is required for changes in postsynaptic structure and function associated with NMDA receptor-dependent long-term depression." The Journal of Neuroscience **27**(13): 3523-3534.

Hsueh, Y. P., A. M. Roberts, et al. (2001). "Bipartite interaction between neurofibromatosis type I protein (neurofibromin) and syndecan transmembrane heparan sulfate proteoglycans." The Journal of Neuroscience **21**(11): 3764-3770.

Hu, G. Y., O. Hvalby, et al. (1987). "Protein kinase C injection into hippocampal pyramidal cells elicits features of long term potentiation." Nature **328**(6129): 426-429.

Huang, E. J. and L. F. Reichardt (2003). "Trk receptors: roles in neuronal signal transduction." Annual Review of Biochemistry **72**: 609-642.

Huang, J., A. Furuya, et al. (2007). "Very-KIND, a KIND domain containing RasGEF, controls dendrite growth by linking Ras small GTPases and MAP2." The Journal of Cell Biology **179**(3): 539-552.

Husi, H., M. A. Ward, et al. (2000). "Proteomic analysis of NMDA receptor-adhesion protein signaling complexes." Nature Neuroscience **3**(7): 661-669.

Huttenlocher, P. R. and P. T. Heydemann (1984). "Fine structure of cortical tubers in tuberous sclerosis: a Golgi study." Annals of Neurology **16**(5): 595-602.

Hyman, S. L., A. Shores, et al. (2005). "The nature and frequency of cognitive deficits in children with neurofibromatosis type 1." Neurology **65**(7): 1037-1044.

Irwin, S. A., B. Patel, et al. (2001). "Abnormal dendritic spine characteristics in the temporal and visual cortices of patients with fragile-X syndrome: a quantitative examination." American Journal of Medical Genetics **98**(2): 161-167.

Iwashita, S. and S. Y. Song (2008). "RasGAPs: a crucial regulator of extracellular stimuli for homeostasis of cellular functions." Molecular bioSystems **4**(3): 213-222.

Jacks, T., T. S. Shih, et al. (1994). "Tumour predisposition in mice heterozygous for a targeted mutation in Nf1." Nature Genetics **7**(3): 353-361.

Jaitner, B. K., J. Becker, et al. (1997). "Discrimination of amino acids mediating Ras binding from noninteracting residues affecting raf activation by double mutant analysis." Journal of Biological Chemistry **272**(47): 29927-29933.

Jett, K. and J. M. Friedman (2010). "Clinical and genetic aspects of neurofibromatosis 1." Genetics in Medicine **12**(1): 1-11.

Johannessen, C. M., E. E. Reczek, et al. (2005). "The NF1 tumor suppressor critically regulates TSC2 and mTOR." Proceedings of the National Academy of Sciences of the United States of America **102**(24): 8573-8578.

Kasai, H., M. Fukuda, et al. (2010). "Structural dynamics of dendritic spines in memory and cognition." Trends in Neurosciences **33**(3): 121-129.

Kasai, H., M. Matsuzaki, et al. (2003). "Structure–stability–function relationships of dendritic spines." Trends in Neurosciences **26**(7): 360-368.

Kayl, A. E. and B. D. r. Moore (2000). "Behavioral phenotype of neurofibromatosis, type 1." Mental Retardation and Developmental Disabilities Research Reviews **6**(2): 117-124.

Kennedy, M. B., H. C. Beale, et al. (2005). "Integration of biochemical signalling in spines." Nature Reviews Neuroscience **6**(6): 423-434.

Kerchner, G. A. and R. A. Nicoll (2008). "Silent synapses and the emergence of a postsynaptic mechanism for LTP." Nature Reviews Neuroscience **9**(11): 813-825.

Kessels, H. W. and R. Malinow (2009). "Synaptic AMPA receptor plasticity and behavior." Neuron **61**(3): 340-350.

Kim, J. H., H. K. Lee, et al. (2003). "The role of synaptic GTPase-activating protein in neuronal development and synaptic plasticity." The Journal of Neuroscience **23**(4): 1119-1124.

Kim, J. H., D. Liao, et al. (1998). "SynGAP: a synaptic RasGAP that associates with the PSD-95/SAP90 protein family." Neuron **20**(4): 683-691.

Kim, M. J., A. W. Dunah, et al. (2005). "Differential roles of NR2A- and NR2B-containing NMDA receptors in Ras-ERK signaling and AMPA receptor trafficking." Neuron **46**(5): 745-760.

Klose, A., M. R. Ahmadian, et al. (1998). "Selective disactivation of neurofibromin GAP activity in neurofibromatosis type 1." Human Molecular Genetics **7**(8): 1261-1268.

Komiyama, N. H., A. M. Watabe, et al. (2002). "SynGAP regulates ERK/MAPK signaling, synaptic plasticity, and learning in the complex with postsynaptic density 95 and NMDA receptor." The Journal of Neuroscience **22**(22): 9721-9732.

Koth, C. W., L. E. Cutting, et al. (2000). "The association of neurofibromatosis type 1 and attention deficit hyperactivity disorder." Child Neuropsychology **6**(3): 185-194.

Krab, L. C., S. M. Goorden, et al. (2008). "Oncogenes on my mind: ERK and MTOR signaling in cognitive diseases." Trends in Genetics **24**(10): 498-510.

Krapivinsky, G., I. Medina, et al. (2004). "SynGAP-MUPP1-CaMKII synaptic complexes regulate p38 MAP kinase activity and NMDA receptor-dependent synaptic AMPA receptor potentiation." Neuron **43**(4): 563-574.

Kumar, V., M. X. Zhang, et al. (2005). "Regulation of dendritic morphogenesis by Ras-PI3K-Akt-mTOR and Ras-MAPK signaling pathways." The Journal of Neuroscience **25**(49): 11288-11299.

Kushner, S. A., Y. Elgersma, et al. (2005). "Modulation of presynaptic plasticity and learning by the H-ras/extracellular signal-regulated kinase/synapsin I signaling pathway." The Journal of Neuroscience **25**(42): 9721-9734.

Kwon, H. B. and B. L. Sabatini (2011). "Glutamate induces de novo growth of functional spines in developing cortex." Nature **474**(7349): 100-104.

Larizza, L., C. Gervasini, et al. (2009). "Developmental abnormalities and cancer predisposition in neurofibromatosis type 1." Current Molecular Medicine **9**(5): 634-653.

Larson, J., D. Wong, et al. (1986). "Patterned stimulation at the theta frequency is optimal for the induction of hippocampal long-term potentiation." Brain Research **368**(2): 347-350.

Lauri, S. E., M. Palmer, et al. (2007). "Presynaptic mechanisms involved in the expression of STP and LTP at CA1 synapses in the hippocampus." Neuropharmacology **52**(1): 1-11.

Lee, H. K., M. Barbarosie, et al. (2000). "Regulation of distinct AMPA receptor phosphorylation sites during bidirectional synaptic plasticity." Nature **405**(6789): 955-959.

Lee, H. K., K. Takamiya, et al. (2003). "Phosphorylation of the AMPA receptor GluR1 subunit is required for synaptic plasticity and retention of spatial memory." Cell **112**(5): 631-643.

Lee, K. J., Y. Lee, et al. (2011). "Requirement for Plk2 in orchestrated ras and rap signaling, homeostatic structural plasticity, and memory." Neuron **69**(5): 957-973.

Lee, S. J., Y. Escobedo-Lozoya, et al. (2009). "Activation of CaMKII in single dendritic spines during long-term potentiation." Nature **458**(7236): 299-304.

Lee, S. J. and R. Yasuda (2009). "Spatiotemporal Regulation of Signaling in and out of Dendritic Spines: CaMKII and Ras." The Open Neuroscience Journal **3**: 117-127.

Leondaritis, G., L. Petrikkos, et al. (2009). "Regulation of the Ras-GTPase activating protein neurofibromin by C-tail phosphorylation: implications for protein kinase C/Ras/extracellular signal-regulated kinase 1/2 pathway signaling and neuronal differentiation." Journal of Neurochemistry **109**(2): 573-583.

Lewis, D. A. and G. Gonzalez-Burgos (2008). "Neuroplasticity of neocortical circuits in schizophrenia." Neuropsychopharmacology **33**(1): 141-165.

Li, C., Y. Cheng, et al. (2001). "Differential localization of the neurofibromatosis 1 (NF1) gene product, neurofibromin, with the F-actin or microtubule cytoskeleton during differentiation of telencephalic neurons." Brain Rsearch. Developmental Brain Research **130**(2): 231-248.

Li, W., Y. Cui, et al. (2005). "The HMG-CoA reductase inhibitor lovastatin reverses the learning and attention deficits in a mouse model of neurofibromatosis type 1." Current Biology **15**(21): 1961-1967.

Liao, D., X. Zhang, et al. (1999). "Regulation of morphological postsynaptic silent synapses in developing hippocampal neurons." Nature Neuroscience **2**(1): 37-43.

Lin, Y. L., Y. T. Lei, et al. (2007). "Syndecan-2 induces filopodia and dendritic spine formation via the neurofibromin-PKA-Ena/VASP pathway." Journal of Cell Biology **177**(5): 829-841.

Ling, D. S., L. S. Bernardo, et al. (2002). "Protein kinase Mzeta is necessary and sufficient for LTP maintenance." Nature Neuroscience **5**(4): 295-296.

Lisman, J. E. (2009). "The pre/post LTP debate." Neuron **63**(3): 281-284.

Lockyer, P. J., S. Kupzig, et al. (2001). "CAPRI regulates Ca(2+)-dependent inactivation of the Ras-MAPK pathway." Current Biology **11**(12): 981-986.

Lopes da Silva, F. H. and D. E. Arnolds (1978). "Physiology of the hippocampus and related structures." Annual Review of Physiology **40**: 185-216.

Lovinger, D. M., K. L. Wong, et al. (1987). "Protein kinase C inhibitors eliminate hippocampal long-term potentiation." Brain Research **436**(1): 177-183.

Lu, W., H. Man, et al. (2001). "Activation of synaptic NMDA receptors induces membrane insertion of new AMPA receptors and LTP in cultured hippocampal neurons." Neuron **29**(1): 243-254.

Lynch, G., J. Larson, et al. (1983). "Intracellular injections of EGTA block induction of hippocampal long-term potentiation." Nature **305**(5936): 719-721.

Maekawa, M., S. Li, et al. (1994). "A novel mammalian Ras GTPase-activating protein which has phospholipid-binding and Btk homology regions." Molecular and Cellular Biology **14**(10): 6879-6885.

Mainen, Z. F., M. Maletic-Savatic, et al. (1999). "Two-photon imaging in living brain slices." Methods **18**(2): 231-239.

Makino, H. and R. Malinow (2009). "AMPA receptor incorporation into synapses during LTP: the role of lateral movement and exocytosis." Neuron **64**(3): 381-390.

Malenka, R. C. and M. F. Bear (2004). "LTP and LTD: an embarrassment of riches." Neuron **44**(1): 5-21.

Malenka, R. C., J. A. Kauer, et al. (1988). "Postsynaptic calcium is sufficient for potentiation of hippocampal synaptic transmission." Science **242**(4875): 81-84.

Malenka, R. C. and R. A. Nicoll (1998). "Long-term depression with a flash." Nature Neuroscience **1**(2): 89-90.

Malenka, R. C. and R. A. Nicoll (1999). "Long-term potentiation--a decade of progress." Science **285**(5435): 1870-1874.

Maletic-Savatic, M., R. Malinow, et al. (1999). "Rapid dendritic morphogenesis in CA1 hippocampal dendrites induced by synaptic activity." Science **283**(5409): 1923-1927.

Malinow, R. and R. C. Malenka (2002). "AMPA receptor trafficking and synaptic plasticity." Annual Review of Neuroscience **25**: 103-126.

Malinow, R., H. Schulman, et al. (1989). "Inhibition of postsynaptic PKC or CaMKII blocks induction but not expression of LTP." Science **245**(4920): 862-866.

Man, H. Y., Q. Wang, et al. (2003). "Activation of PI3-kinase is required for AMPA receptor insertion during LTP of mEPSCs in cultured hippocampal neurons." Neuron **38**(4): 611-624.

Manabe, T., A. Aiba, et al. (2000). "Regulation of long-term potentiation by H-Ras through NMDA receptor phosphorylation." Journal of Neuroscience **20**(7): 2504-2511.

Mangoura, D., Y. Sun, et al. (2006). "Phosphorylation of neurofibromin by PKC is a possible molecular switch in EGF receptor signaling in neural cells." Oncogene **25**(5): 735-745.

Marchuk, D. A., A. M. Saulino, et al. (1991). "cDNA cloning of the type 1 neurofibromatosis gene: complete sequence of the NF1 gene product." Genomics **11**(4): 931-940.

Marin-Padilla, M. (1972). "Structural abnormalities of the cerebral cortex in human chromosomal aberrations: a Golgi study." Brain Research **44**(2): 625-629.

Markman, B., R. Dienstmann, et al. (2010). "Targeting the PI3K/Akt/mTOR pathway--beyond rapalogs." Oncotarget **1**(7): 530-543.

Markram, H., J. Lubke, et al. (1997). "Regulation of synaptic efficacy by coincidence of postsynaptic APs and EPSPs." Science **275**(5297): 213-215.

Matias, C., J. C. Dionísio, et al. (2002). "Thapsigargin blocks STP and LTP related calcium enhancements in hippocampal CA1 area." Neuroreport **13**(18): 2577-2580.

Matsuzaki, M., G. C. Ellis-Davies, et al. (2001). "Dendritic spine geometry is critical for AMPA receptor expression in hippocampal CA1 pyramidal neurons." Nature Neuroscience **4**(11): 1086-1092.

Matsuzaki, M., N. Honkura, et al. (2004). "Structural basis of long-term potentiation in single dendritic spines." Nature **429**(6993): 761-766.

Mazzucchelli, C. and R. Brambilla (2000). "Ras-related and MAPK signalling in neuronal plasticity and memory formation." Cellular and Molecular Life Sciences. **57**(4): 604-611.

McAllister, A. K. (2000). "Biolistic transfection of neurons." Science STKE **51**: pl1.

McClatchey, A. I. (2007). "Neurofibromatosis." Annual Review of Pathology **2**: 191-216.

McKinney, B. C., A. W. Grossman, et al. (2005). "Dendritic spine abnormalities in the occipital cortex of C57BL/6 Fmr1 knockout mice." American Journal of Medical Genetics. Part B, Neuropsychiatric Genetics **136B**(1): 98-102.

Merino, S. M. and S. Maren (2006). "Hitting Ras where it counts: Ras antagonism in the basolateral amygdala inhibits long-term fear memory." European Journal of Neuroscience **23**(1): 196-204.

Milburn, M. V., L. Tong, et al. (1990). "Molecular switch for signal transduction: structural differences between active and inactive forms of protooncogenic ras proteins." Science **247**(4945): 939-945.

Mitin, N., K. L. Rossman, et al. (2005). "Signaling interplay in Ras superfamily function." Current Biology **15**(14): R563-574.

Moressis, A., A. R. Friedrich, et al. (2009). "A dual role for the adaptor protein DRK in Drosophila olfactory learning and memory." The Journal of Neuroscience **29**(8): 2611-2625.

Morris, R. G., S. Davis, et al. (1990). "Hippocampal Synaptic Plasticity and NMDA Receptors: A Role in Information Storage?" Philosophical Transactions of the Royal Society of London. Biological Sciences **329**(1253).

Morris, R. G., R. F. Halliwell, et al. (1989). "Synaptic plasticity and learning. II: Do different kinds of plasticity underlie different kinds of learning?" Neuropsychologia **27**(1): 41-59.

Moser, M. B., M. Trommald, et al. (1997). "Spatial training in a complex environment and isolation alter the spine distribution differently in rat CA1 pyramidal cells." Journal of Comparative Neurology **380**(3): 373-381.

Muhia, M., B. K. Yee, et al. (2010). "Disruption of hippocampus-regulated behavioural and cognitive processes by heterozygous constitutive deletion of SynGAP." European journal of Neuroscience **31**(3): 529-543.

Mulkey, R. M., S. Endo, et al. (1994). "Involvement of a calcineurin/inhibitor-1 phosphatase cascade in hippocampal long-term depression." Nature **369**(6480): 486-488.

Muller, D. and G. Lynch (1989). "Evidence that changes in presynaptic calcium currents are not responsible for long-term potentiation in hippocampus." Brain Research **479**(2): 290-299.

Müller, W. and J. A. Connor (1991). "Dendritic spines as individual neuronal compartments for synaptic Ca2+ responses." Nature **354**(6348): 73-76.

Murakoshi, H., S.-J. Lee, et al. (2008). "Highly sensitive and quantitative FRET–FLIM imaging in single dendritic spines using improved non-radiative YFP." Brain Cell Biology **36**(1-4): 31-42.

Murakoshi, H., H. Wang, et al. (2011). "Local, persistent activation of Rho GTPases during plasticity of single dendritic spines." Nature **472**(7341): 100-104.

Murray, H. J. and J. J. O'Connor (2004). "A role for monomeric G-proteins in synaptic plasticity in the rat dentate gyrus in vitro." Brain Research **1000**(1-2): 85-91.

Nagerl, U. V., N. Eberhorn, et al. (2004). "Bidirectional activity-dependent morphological plasticity in hippocampal neurons." Neuron **44**(5): 759-767.

Newey, S. E., V. Velamoor, et al. (2005). "Rho GTPases, dendritic structure, and mental retardation." Journal of Neurobiology **64**(1): 58-74.

Newpher, T. M. and M. D. Ehlers (2008). "Glutamate receptor dynamics in dendritic microdomains." Neuron **58**(4): 472-497.

Nicoll, R. A. (2003). "Expression mechanisms underlying long-term potentiation: a postsynaptic view." Philosophical Transactions of the Royal Society of London. Series B, Biological sciences **358**(1432): 721-726.

Nimchinsky, E. A., A. M. Oberlander, et al. (2001). "Abnormal development of dendritic spines in FMR1 knock-out mice." The Journal of Neuroscience **21**(14): 5139-5146.

Nimchinsky, E. A., B. L. Sabatini, et al. (2002). "Structure and function of dendritic spines." Annual Review of Physiology **64**: 313-353.

Noguchi, J., M. Matsuzaki, et al. (2005). "Spine-neck geometry determines NMDA receptor-dependent Ca2+ signaling in dendrites." Neuron **46**(4): 609-622.

Nordlund, M. L., T. A. Rizvi, et al. (1995). "Neurofibromin expression and astrogliosis in neurofibromatosis (type 1) brains." Journal of Neuropathology and Experimental Neurology **54**(4): 588-600.

North, K. (2000). "Neurofibromatosis type 1." American Journal of Medical Genetics **97**(2): 119-127.

Nusser, Z., R. Lujan, et al. (1998). "Cell type and pathway dependence of synaptic AMPA receptor number and variability in the hippocampus." Neuron **21**(3): 545-559.

O'Kane, E. M., T. W. Stone, et al. (2004). "Increased long-term potentiation in the CA1 region of rat hippocampus via modulation of GTPase signalling or inhibition of Rho kinase." Neuropharmacology **46**(6): 879-887.

Obenaus, A., I. Mody, et al. (1989). "Dantrolene-Na (Dantrium) blocks induction of long-term potentiation in hippocampal slices." Neuroscience Letters **98**(2): 172-178.

Ohno, M., P. W. Frankland, et al. (2001). "Inducible, pharmacogenetic approaches to the study of learning and memory." Nature Neuroscience **4**(12): 1238-1243.

Otmakhova, N. A., N. Otmakhov, et al. (2000). "Inhibition of the cAMP pathway decreases early long-term potentiation at CA1 hippocampal synapses." The Journal of Neuroscience **20**(12): 4446-4451.

Packard, M. G. and J. L. McGaugh (1996). "Inactivation of hippocampus or caudate nucleus with lidocaine differentially affects expression of place and response learning." Neurobiology of Learning and Memory **65**(1): 65-72.

Papa, M., M. C. Bundman, et al. (1995). "Morphological analysis of dendritic spine development in primary cultures of hippocampal neurons." The Journal of Neuroscience **15**: 1-11.

Park, M., E. C. Penick, et al. (2004). "Recycling endosomes supply AMPA receptors for LTP." Science **305**(5692): 1972-1975.

Patterson, M. A., E. M. Szatmari, et al. (2010). "AMPA receptors are exocytosed in stimulated spines and adjacent dendrites in a Ras-ERK-dependent manner during long-term potentiation." Proceedings of the National Academy of Sciences of the United States of America **107**(36): 15951-15956.

Pena, V., M. Hothorn, et al. (2008). "The C2 domain of SynGAP is essential for stimulation of the Rap GTPase reaction." EMBO Reports **9**(4): 350-355.

Pettit, D. L., S. Perlman, et al. (1994). "Potentiated transmission and prevention of further LTP by increased CaMKII activity in postsynaptic hippocampal slice neurons." Science **266**(5192): 1881-1885.

Pologruto, T. A., B. L. Sabatini, et al. (2003). "ScanImage: flexible software for operating laser scanning microscopes." BioMedical Engineering OnLine **2**(13).

Poo, M. M. (2001). "Neurotrophins as synaptic modulators." Nature Reviews Neuroscience **2**(1): 24-32.

Pouzet, B., W. N. Zhang, et al. (2002). "Hippocampal lesioned rats are able to learn a spatial position using non-spatial strategies." Behavioural Brain Research **133**(2): 279-291.

Purpura, D. P. (1975). "Normal and aberrant neuronal development in the cerebral cortex of human fetus and young infant." UCLA Forum of Medical Sciences(18): 141-169.

Qian, X., L. Esteban, et al. (2000). "The Sos1 and Sos2 Ras-specific exchange factors: differences in placental expression and signaling properties." EMBO Journal **19**(4): 642-654.

Qin, Y., Y. Zhu, et al. (2005). "State-dependent Ras signaling and AMPA receptor trafficking." Genes & Development **19**(17): 2000-2015.

Quilliam, L. A., J. F. Rebhun, et al. (2002). "A Growing Family of Guanine Nucleotide Exchange Factors Is Responsible for Activation of Ras-Family GTPases." Progress in Nucleic Acid Research and Molecular Biology **71**: 391-444.

Raaijmakers, J. H. and J. L. Bos (2009). "Specificity in Ras and Rap signaling." The Journal of Biological Chemistry **284**(17): 10995-10999.

Rauen, K. A. (2007). "HRAS and the Costello syndrome." Clinical Genetics **71**(2): 101-108.

Regehr, W. G. and D. W. Tank (1990). "Postsynaptic NMDA receptor-mediated calcium accumulation in hippocampal CA1 pyramidal cell dendrites." Nature Neuroscience **345**(6278).

Rizvi, T. A., S. Akunuru, et al. (1999). "Region-specific astrogliosis in brains of mice heterozygous for mutations in the neurofibromatosis type 1 (Nf1) tumor suppressor." Brain Research **816**(1): 111-123.

Roche, K. W., R. J. O'Brien, et al. (1996). "Characterization of multiple phosphorylation sites on the AMPA receptor GluR1 subunit." Neuron **16**(6): 1179-1188.

Rosen, L. B., D. D. Ginty, et al. (1994). "Membrane depolarization and calcium influx stimulate MEK and MAP kinase via activation of Ras." Neuron **12**(6): 1207-1221.

Rowbotham, I., I. M. Pit-ten Cate, et al. (2009). "Cognitive control in adolescents with neurofibromatosis type 1." Neuropsychology **23**(1): 50-60.

Rudelli, R. D., W. T. Brown, et al. (1985). "Adult fragile X syndrome. Clinico-neuropathologic findings." Acta Neuropathologica **67**(3-4): 289-295.

Rumbaugh, G., J. P. Adams, et al. (2006). "SynGAP regulates synaptic strength and mitogen-activated protein kinases in cultured neurons." Proceedings of the National Academy of Sciences of the United States of America **103**(12): 4344-4351.

Sacktor, T. C., P. Osten, et al. (1993). "Persistent activation of the zeta isoform of protein kinase C in the maintenance of long-term potentiation." Proceedings of the National Academy of Sciences of the United States of America **90**(18): 8342-8346.

Seeger, G., U. Gärtner, et al. (2005). "Transgenic activation of Ras in neurons increases synapse formation in mouse neocortex." Journal of Neural Transmission **112**(6): 751-761.

Shalin, S. C., C. M. Hernandez, et al. (2006). "Kinase suppressor of Ras1 compartmentalizes hippocampal signal transduction and subserves synaptic plasticity and memory formation." Neuron **50**(5): 765-779.

Shankar, G. M., B. L. Bloodgood, et al. (2007). "Natural oligomers of the Alzheimer amyloid-beta protein induce reversible synapse loss by modulating an NMDA-type glutamate receptor-dependent signaling pathway." The Journal Neuroscience **27**(11): 2866-2875.

Sheng, M. and C. C. Hoogenraad (2007). "The postsynaptic architecture of excitatory synapses: a more quantitative view." Annual Review of Biochemistry **76**: 823-847.

Sheng, M. and M. J. Kim (2002). "Postsynaptic signaling and plasticity mechanisms." Science **298**(5594): 776-780.

Shilyansky, C., Y. S. Lee, et al. (2010). "Molecular and Cellular Mechanisms of Learning Disabilities: A Focus on NF1." Annual Review of Neuroscience **33**(1): 221-243.

Silva, A. J., Y. Elgersma, et al. (2000). "Molecular and cellular mechanisms of cognitive function: implications for psychiatric disorders." Biological Psychiatry **47**(3): 200-209.

Silva, A. J., P. W. Frankland, et al. (1997). "A mouse model for the learning and memory deficits associated with neurofibromatosis type I." Nature Genetics **15**(3): 281-284.

Silva, A. J., C. F. Stevens, et al. (1992). "Deficient hippocampal long-term potentiation in alpha-calcium-calmodulin kinase II mutant mice. Science **257**(5067): 201-206.

Sobczyk, A., V. Scheuss, et al. (2005). "NMDA receptor subunit-dependent [Ca2+] signaling in individual hippocampal dendritic spines." The Journal of Neuroscience **25**(26): 6037-6046.

Sousa, S. F., P. A. Fernandes, et al. (2008). "Farnesyltransferase inhibitors: a detailed chemical view on an elusive biological problem." Current Medicinal Chemistry **15**(15): 1478-1492.

Spruston N. (2008). "Pyramidal neurons: dendritic structure and synaptic integration." Nature Reviews Neuroscience **9**(3):206-21.

Stoppini, L., P. A. Buchs, et al. (1991). "A simple method for organotypic cultures of nervous tissue." Journal of Neuroscience Methods **37**(2): 173-182.

Stornetta, R. L. and J. J. Zhu (2011). "Ras and Rap signaling in synaptic plasticity and mental disorders." The Neuroscientist **17**(1): 54-78.

Stubley-Weatherly, L., J. W. Harding, et al. (1996). "Effects of discrete kainic acid-induced hippocampal lesions on spatial and contextual learning and memory in rats." Brain Research **716**(1-2): 29-38.

Suetsugu, M. and P. Mehraein (1980). "Spine distribution along the apical dendrites of the pyramidal neurons in Down's syndrome. A quantitative Golgi study." Acta Neuropathologica **50**(3): 207-210.

Sung, P. J., A. B. Rodrigues, et al. (2010). "Cytosolic Ras supports eye development in Drosophila." Molecular and Cellular Biology **30**(24): 5649-5657.

Svoboda, K. and D. W. Tank (1996). "Direct measurement of coupling between dendritic spines and shafts." Science **272**(5262).

Svoboda, K. and R. Yasuda (2006). "Principles of two-photon excitation microscopy and its applications to neuroscience." Neuron **50**(6): 823-839.

Sweatt, J. D. (2004). "Mitogen-activated protein kinases in synaptic plasticity and memory." Current Opinion in Neurobiology **14**(3): 311-317.

Sziklas, V., S. Lebel, et al. (1998). " Conditional associative learning and the hippocampal system." Hippocampus **8**(2): 131-137.

Tada, T. and M. Sheng (2006). "Molecular mechanisms of dendritic spine morphogenesis." Current Opinion in Neurobiology **16**(1): 95-101.

Takai, Y., T. Sasaki, et al. (2001). "Small GTP-binding proteins." Physiology Reviews **81**(1): 153-208.

Tan, S. E. and S. S. Chen (1997). "The activation of calcium/calmodulin-dependent protein kinase II after glutamate or potassium stimulation in hippocampal slices." Brain Research Bulletin **43**(3): 269-273.

Tanaka, J., Y. Horiike, et al. (2008). "Protein synthesis and neurotrophin-dependent structural plasticity of single dendritic spines." Science **319**(5870): 1683-1687.

Tavazoie, S. F., V. A. Alvarez, et al. (2005). "Regulation of neuronal morphology and function by the tumor suppressors Tsc1 and Tsc2." Nature Neuroscience **8**(12): 1727-1734.

The, I., G. E. Hannigan, et al. (1997). "Rescue of a Drosophila NF1 mutant phenotype by protein kinase A." Science **276**(5313): 791-794.

Thomas, G. M. and R. L. Huganir (2004). "MAPK cascade signalling and synaptic plasticity." Nature Reviews. Neuroscience **5**(3): 173-183.

Thornton, C., R. Yaka, et al. (2003). "H-Ras modulates N-methyl-D-aspartate receptor function via inhibition of Src tyrosine kinase activity." The Journal of Biological Chemistry **278**(26): 23823-23829.

Tidyman, W. E. and K. A. Rauen (2009). "The RASopathies: developmental syndromes of Ras/MAPK pathway dysregulation." Current Opinion in Genetics & Development **19**(3): 230-236.

Toki, S., H. Kawasaki, et al. (2001). "Guanine nucleotide exchange factors CalDAG-GEFI and CalDAG-GEFII are colocalized in striatal projection neurons." Journal of Comparative Neurology **437**(4): 398-407.

Tong, J., F. Hannan, et al. (2002). "Neurofibromin regulates G protein-stimulated adenylyl cyclase activity." Nature Neuroscience **5**(2): 95-96.

Tonini, R., S. Franceschetti, et al. (2001). "Involvement of CDC25Mm/Ras-GRF1-dependent signaling in the control of neuronal excitability." Molecular and Cellular Neuroscience **18**(6): 691-701.

Trachtenberg, J. T., B. E. Chen, et al. (2002). "Long-term in vivo imaging of experience-dependent synaptic plasticity in adult cortex." Nature **420**(6917): 788-794.

Vandenbroucke, I. (2004). "Neurofibromin is actively transported to the nucleus." FEBS Letters **560**(1-3): 98-102.

Vazquez, L. E., H. J. Chen, et al. (2004). "SynGAP regulates spine formation." The Journal of Neuroscience **24**(40): 8862-8872.

Vigil, D., J. Cherfils, et al. (2010). "Ras superfamily GEFs and GAPs: validated and tractable targets for cancer therapy?" Nature Reviews. Cancer **10**(12): 842-857.

Wang, Y., J. H. Duan, et al. (2010). "Augmented sodium currents contribute to the enhanced excitability of small diameter capsaicin-sensitive sensory neurons isolated from Nf1+/ mice." Journal of Neurophysiology **103**(4): 2085-2094.

Wang, Z., J. G. Edwards, et al. (2008). "Myosin Vb mobilizes recycling endosomes and AMPA receptors for postsynaptic plasticity." Cell **135**(3): 535-548.

Ward, B. A. and D. H. Gutmann (2005). "Neurofibromatosis 1: from lab bench to clinic." Pediatric Neurology **32**(4): 221-228.

Williams, J. A., H. S. Su, et al. (2001). "A circadian output in Drosophila mediated by neurofibromatosis-1 and Ras/MAPK." Science **293**(5538): 2251-2256.

Wimmer, R. and M. Baccarini (2010). "Partner exchange: protein-protein interactions in the Raf pathway." Trends in Biochemical Sciences **35**(12): 660-668.

Wright, L. P. and M. R. Philips (2006). "Thematic review series: lipid posttranslational modifications. CAAX modification and membrane targeting of Ras." Journal of lipid research **47**(5): 883-891.

Wu, G. Y., K. Deisseroth, et al. (2001). "Spaced stimuli stabilize MAPK pathway activation and its effects on dendritic morphology." Nature Neuroscience **4**(2).

Xu, G. F., B. Lin, et al. (1990). "The catalytic domain of the neurofibromatosis type 1 gene product stimulates ras GTPase and complements ira mutants of S. cerevisiae." Cell **63**(4): 835-841.

Xu, T., X. Yu, et al. (2009). "Rapid formation and selective stabilization of synapses for enduring motor memories." Nature **462**(7275): 915-919.

Yan, J., S. Roy, et al. (1998). "Ras isoforms vary in their ability to activate Raf-1 and phosphoinositide 3-kinase." The Journal of Biological Chemistry **273**(37): 24052-24056.

Yasuda, R. (2006). "Imaging spatiotemporal dynamics of neuronal signaling using fluorescence resonance energy transfer and fluorescence lifetime imaging microscopy." Current Opinion in Neurobiology **16**(5): 551-561.

Yasuda, R., C. D. Harvey, et al. (2006). "Supersensitive Ras activation in dendrites and spines revealed by two-photon fluorescence lifetime imaging." Nature Neuroscience **9**(2): 283-291.

Yasuda, R. and H. Murakoshi (2011). "The mechanisms underlying the spatial spreading of signaling activity." Current Opinion in Neurobiology **21**(2): 313-321.

Yasuda, R., E. A. Nimchinsky, et al. (2004). "Imaging calcium concentration dynamics in small neuronal compartments." Science STKE **2004**(219): pl5.

Yasumatsu, N., M. Matsuzaki, et al. (2008). "Principles of long-term dynamics of dendritic spines." The Journal of Neuroscience **28**(50): 13592-13608.

Ye, X. and T. J. Carew (2010). "Small G protein signaling in neuronal plasticity and memory formation: the specific role of ras family proteins." Neuron **68**(3): 340-361.

Yun, H. Y., M. Gonzalez-Zulueta, et al. (1998). "Nitric oxide mediates N-methyl-D-aspartate receptor-induced activation of p21ras." Proceedings of the National Academy of Sciences of the United States of America **95**(10): 5773-5778.

Yunoue, S., H. Tokuo, et al. (2003). "Neurofibromatosis type I tumor suppressor neurofibromin regulates neuronal differentiation via its GTPase-activating protein function toward Ras." The Journal of Biological Chemistry **278**(29): 26958-26969.

Yuste, R. and T. Bonhoeffer (2001). "Morphological changes in dendritic spines associated with long-term synaptic plasticity." Annual Review of Neuroscience **24**: 1071-1089.

Yuste, R. and T. Bonhoeffer (2004). "Genesis of dendritic spines: insights from ultrastructural and imaging studies." Nature Reviews. Neuroscience **5**(1): 24-34.

Yuste, R. and A. Majewska (2001). "Book Review: On the Function of Dendritic Spines." The Neuroscientist **7**(5): 387-395.

Yuste, R., A. Majewska, et al. (2000). "From form to function: calcium compartmentalization in dendritic spines." Nature Neuroscience **3**(7): 653-659.

Zhou, Q., K. J. Homma, et al. (2004). "Shrinkage of dendritic spines associated with long-term depression of hippocampal synapses." Neuron **44**(5): 749-757.

Zhu, J. J., Y. Qin, et al. (2002). "Ras and Rap control AMPA receptor trafficking during synaptic plasticity." Cell **110**(4): 443-455.

Zhu, Y., T. Harada, et al. (2005). "Inactivation of NF1 in CNS causes increased glial progenitor proliferation and optic glioma formation." Development **132**(24): 5577-5588.

Zhu, Y., M. I. Romero, et al. (2001). "Ablation of NF1 function in neurons induces abnormal development of cerebral cortex and reactive gliosis in the brain." Genes & Development **15**(7): 859-876.

Zito, K., V. Scheuss, et al. (2009). "Rapid functional maturation of nascent dendritic spines." Neuron **61**(2): 247-258.

Zuo, Y., A. Lin, et al. (2005). "Development of long-term dendritic spine stability in diverse regions of cerebral cortex." Neuron **46**(2): 181-189.